

# Coupled electro-elastic deformation and instabilities of a toroidal membrane

Zhaowei Liu<sup>a</sup>, Andrew McBride<sup>a</sup>, Basant Lal Sharma<sup>b</sup>, Paul Steinmann<sup>a,c</sup>, Prashant Saxena<sup>a,\*</sup>

<sup>a</sup>*Glasgow Computational Engineering Centre, James Watt School of Engineering, University of Glasgow, Glasgow, G12 8LT, United Kingdom*

<sup>b</sup>*Department of Mechanical Engineering, Indian Institute of Technology Kanpur, Kanpur, Uttar Pradesh-208016, India*

<sup>c</sup>*Chair of Applied Mechanics, University of Erlangen–Nuremberg, Paul-Gordan-Str. 3, D-91052, Erlangen, Germany*

---

## Abstract

We analyse here the problem of large deformation of dielectric elastomeric membranes under coupled electromechanical loading. Extremely large deformations (enclosed volume changes of 100 times and greater) of a toroidal membrane are studied by the use of a variational formulation that accounts for the total energy due to mechanical and electrical fields. A modified shooting method is adopted to solve the resulting system of coupled and highly nonlinear ordinary differential equations. We demonstrate the occurrence of limit point, wrinkling, and symmetry-breaking buckling instabilities in the solution of this problem. Onset of each of these “reversible” instabilities depends significantly on the ratio of the mechanical load to the electric load, thereby providing a control mechanism for state switching.

*Keywords:* Electroelastic membrane, Limit point, Wrinkling, Buckling, Stability analysis

---

## 1. Introduction

Thin electroelastic structures made from electroactive polymers [56] find wide use in engineering applications including artificial muscles [5], soft grippers [3, 31, 34], and energy generators [50]. In this work we use the theory of nonlinear electroelasticity [18] to analyse the large deformation of a toroidal electroelastic membrane inflated by a mechanical pressure and actuated by an electric potential difference applied across its thickness. Extreme deformations induce limit point, wrinkling, and symmetry-breaking buckling instabilities in the membrane. These are systematically studied in this contribution.

### 1.1. Nonlinear electroelasticity

Developments in the theory of electroelasticity date back to the classic work of Toupin [75]. By combining the theory of continuum mechanics and electrostatics, a framework was established for

---

\*Corresponding author

*Email address:* prashant.saxena@glasgow.ac.uk (Prashant Saxena)

12 analysing the nonlinear response of isotropic dielectric materials. Toupin [76] extended his seminal  
13 work by deriving the governing equations for the dynamics of elastic dielectrics. Eringen [25] followed  
14 by formulating the governing equations in an alternative way and applied his method to the problem  
15 of an incompressible thick-walled cylindrical tube subjected to a radial electric field. Tiersten [73]  
16 simplified the formulations proposed by Toupin [75] and Eringen [25], thereby making a fundamental  
17 contribution to nonlinear electroelastic material modelling. He also made significant contributions to  
18 the theory of piezoelectricity [73, 74].

19 Interest in the development of nonlinear theories of electroelasticity was renewed owing to the de-  
20 velopment and industry adoption of dielectric elastomers that can undergo large deformations and  
21 nonlinear electroelastic coupling. McMeeking and Landis [44] used the principle of virtual work to  
22 derive simpler governing equations for quasi-electrostatics in Eulerian form. Concurrently, Dorfmann  
23 and Ogden [18, 19] developed a general Lagrangian formulation and constitutive relations within the  
24 framework of continuum mechanics to simulate the finite deformation of electroelastic materials cou-  
25 pled to electric fields. Rate-dependent theories to account for dissipation owing to viscoelasticity in  
26 dielectric elastomers were developed by Ask et al. [4] and Saxena et al. [65]. Variational formulations  
27 of electroelasticity to enable the development of computational methods were presented by Vu et al.  
28 [78], Liu [39], and have been applied to analyse stability by computation of higher variations by Bus-  
29 tamante et al. [9], and Saxena and Sharma [64]. A comprehensive review of the theory of nonlinear  
30 electroelasticity and its applications is presented in [23].

### 31 *1.2. Dielectric elastomers*

32 Electroactive polymers are materials that can undergo deformation due to an applied electric field.  
33 Dielectric elastomers are one of the most commonly used electroactive polymers. They are composed  
34 of a soft elastomer sandwiched between two compliant electrodes. Application of a potential difference  
35 between the two electrodes results in a large deformation in the elastomer due to the electrostatic forces  
36 generated by the opposite electric charges [56].

37 This principle has been widely used in the design of sensing and actuating systems. For example,  
38 Bar-Cohen et al. [5] explored their use as artificial muscles. Moretti et al. [50] developed wave energy  
39 generators based on the inflation of dielectric elastomers. Kofod et al. [30] presented the principle of  
40 self-organized dielectric elastomer minimum energy structures (DEMESs) and developed a gripper [31].  
41 Araromi et al. [3] applied DEMESs as a gripper to capture debris in space. Lau et al. [34] developed a  
42 dielectric elastomer finger for grasping and pinching highly deformable objects. For a detailed review  
43 on grippers made of dielectric elastomers, see Shintake et al. [66]. Ozsecen et al. [55] developed haptic

44 interfaces, Michel et al. [47] performed a feasibility study for a bionic propulsion system, and O'Halloran  
45 et al. [54] explored sensing systems based on dielectric elastomers. We refer to the review papers by  
46 Suo [68] and Lu et al. [41] for further detailed discussion on dielectric elastomers.

### 47 *1.3. Biological and engineering applications with toroidal membranes*

48 Biological membranes with a toroidal shape also naturally exist in human body. One of the most  
49 important cells in the human body, Erythrocyte (red blood cell), is a small dielectrophoretic (DEP)  
50 electromagnetic field (EMF) driven cell [58]. It has a unique toroidal shape in order to increase the  
51 surface area-to-volume ratio which increases the diffusion of oxygen and carbon dioxide through their  
52 cell membrane. Toroidal structures are common in DNA-binding enzymes [27] and bacteriophages [35].  
53 Further discussion on natural biological toroidal structures can be found in [17]. Topologically, a  
54 torus can be considered as the simplest example of a genus 1 orientable surface which appeals to  
55 mathematicians and engineers. Toroidal membranes and shells are widely applied in engineering such  
56 as tyres, air springs [13], soft grippers and inflatable actuators. Zang et al. [81] designed a bionic toroidal  
57 soft gripper in order to catch objects with arbitrary shapes and sizes. Adams et al. [1] designed an  
58 electro-pneumatic device using a string of inflatable toroidal membranes for water pipe inspection. Thus,  
59 analysing the mechanics of large deformation in toroidal membranes can not only aid the engineering  
60 design of such devices but also develop a better understanding of certain biological processes at the  
61 cellular level.

### 62 *1.4. Instabilities in nonlinear membranes*

63 Nonlinear membranes are widely applied in engineering structures and naturally appear in the form  
64 of biological tissues. Air bags, diaphragm valves, balloons, skin tissue, and cell walls are examples of  
65 nonlinear membranes.

66 Inflation can cause large deformation in the membranes resulting in instabilities. A well-known  
67 instability phenomenon of inflating membranes is the limit point. This is a critical point after which the  
68 membrane appears to lose stiffness to inflation and undergoes very large inflation with a small increase  
69 in pressure. This phenomenon is also called snap-through bifurcation and has been well studied [see  
70 e.g. 7, 10, 29, 52, 70]. Computation of accurate pressure-volume characteristics in this case require a  
71 path-following scheme due to the non-uniqueness of solution [59].

72 In-plane deformation of membrane can also result in wrinkling which is a form of localised buckling.  
73 An ideal membrane is a structure with negligible bending stiffness and can only sustain tensile load-  
74 ing. If any part of the membrane structure experiences compression, it undergoes local out-of-plane

75 deformation to avoid the in-plane compressive stresses. Tension field theory developed by Pipkin [57]  
76 and Steigmann [67] is a widely used tool to model wrinkles in nonlinear elastic membranes. It assumes  
77 zero bending stiffness and an infinitely continuous distribution of wrinkles orientated in the direction  
78 of the positive principal stress. To avoid a contribution to the energy by compressive stresses, a relaxed  
79 energy function is used that constrains the stress tensor to be positive semi-definite. As a result the  
80 amplitude and wavelength of wrinkles cannot be computed by using this theory. This theory has been  
81 applied to study wrinkles in axisymmetric hyperelastic membranes [37, 38] and to model wrinkles in skin  
82 during wound closure [69], to name a few applications. A generalisation of the tension field theory has  
83 been attempted (although without a rigorous mathematical proof) for the case of electroelasticity by  
84 De Tommasi et al. [14], De Tommasi et al. [15], Greaney et al. [26], and for the case of magnetoelasticity  
85 by Reddy and Saxena [59, 60], Saxena et al. [63]. Wong and Pellegrino [79] developed an analytical  
86 method to quantify the location, amplitude, and wavelengths of linear elastic membranes. Nayyar  
87 et al. [53] and Barsotti [6] developed a nonlinear finite element method for simulating stretch-induced  
88 wrinkling of hyperelastic thin sheets.

89 While wrinkling is a localised buckling, the membrane structure can also experience a global buckling  
90 on account of large deformations. In structures with a geometrical symmetry, this instability manifests  
91 as a bifurcation from the symmetric principal solution and leads to a loss of symmetry. The theory  
92 of elastic buckling, developed by Koiter [32] and Budiansky [8], provides methods to evaluate the  
93 critical point of such instability. This typically requires checking the sign of the second variation of  
94 the total potential energy to determine the stability state. Chaudhuri and Dasgupta [11] studied the  
95 perturbed deformations of inflated hyperelastic circular membranes, Venkata and Saxena [77] analysed  
96 buckling of hyperelastic toroidal membranes, Xie et al. [80] analysed the shape bifurcations of a dielectric  
97 elastomeric sphere through a direct perturbation approach, and Reddy and Saxena [59, 60], Saxena et al.  
98 [63] analysed shape bifurcations of magnetoelastic membranes.

### 99 *1.5. Electroelastic instability*

100 Experimental investigation of dielectric elastomeric membranes have revealed all the three instabil-  
101 ities discussed in Section 1.4. An experimental investigation of electroelastic membranes by Kollosche  
102 et al. [33] demonstrates an interplay between the limit point and wrinkling instabilities due to coupling  
103 effects. Li et al. [36] studied large voltage-induced deformation of dielectric elastomers. In addition  
104 to wrinkling and limit point, they also demonstrate symmetry-breaking and bulge formation in the  
105 inflation of a circular membrane. Careful experimental investigations on the rate-dependent behaviour  
106 of dielectric elastomers have shown a relation between the viscoelastic reponse and the breakdown limit

107 [2, 28, 45]. Zhang et al. [82] and Mao et al. [42] presented a controlled experimental procedure to  
108 produce wrinkles in dielectric elastomer membranes.

109 Theoretical and computational procedures to model these electroelastic instabilities have been de-  
110 veloped largely for bulk media with some recent works towards the analysis of membranes. Zhao and  
111 Suo [83] analysed the instability of dielectric elastomers to guide the design of actuator configurations  
112 and materials. Rudykh et al. [62] presented a method to use snap-through instability of thick-wall  
113 electroactive balloons to design actuators. Miehe et al. [48] developed an algorithm for finite element  
114 computations of both structural and material stability analysis in electroelasticity. Dorfmann and Og-  
115 den [20] studied the critical stretch corresponding to loss of stability of a thick electroelastic plate by  
116 perturbation of the equilibrium equations. Dorfmann and Ogden [21] also investigated radial deforma-  
117 tions of a thick-walled spherical shell using the nonlinear electroelastic theory. Melnikov and Ogden [46]  
118 presented a mathematical approach to study bifurcation of a finitely deformed thick-walled cylindrical  
119 tube. A more complete set of references can be found in the comprehensive review on the instability of  
120 soft dielectrics by Dorfmann and Ogden [24].

121 Xie et al. [80] undertook a bifurcation analysis of a spherical dielectric membrane under inflation and  
122 also derived post-buckling solutions. Greaney et al. [26] used a modified tension field theory to analyse  
123 wrinkling and pull-in instabilities in dielectric membranes. For the related problem of magnetoelastic  
124 membranes, Reddy and Saxena [59] recently demonstrated new instability phenomena of an additional  
125 limit point and reversal of wrinkling location in an inflating toroidal magnetoelastic membrane. In  
126 addition to the engineering and biological applications discussed in Section 1.3, these results provided a  
127 partial motivation to study instabilities in a toroidal electroelastic membranes. In this contribution we,  
128 for the first time, present a novel analysis of the interaction between limit point, wrinkling, and buckling  
129 instabilities in a toroidal membrane. For the wrinkling analysis we apply the tension field theory of  
130 Steigmann [67] generalised to electroelasticity by De Tommasi et al. [14] and Greaney et al. [26]. We  
131 extend the aforementioned theoretical works by providing the numerical details to apply the tension  
132 field theory and thereby deliver physically meaningful predictions of wrinkled solutions post-instability.  
133 These predictions are compared to primary solutions that ignore the inability of a membrane to sustain  
134 compressive states.

### 135 *1.6. Organisation of the manuscript*

136 This contribution is organised as follows: Section 2 introduces the kinematics of the deformation.  
137 Section 3 formulates the equilibrium equations using the first variation of the total potential energy func-  
138 tional that is composed of mechanical and electrical contributions. The Mooney-Rivlin model [49, 61]

139 is adopted for the hyperelastic energy density and the electrical contribution is accounted for via the  
140 energy density function by coupling the electric displacement to the deformation tensor. Three instabili-  
141 ties (snap-through, wrinkling and loss of symmetry) are analysed and discussed in detail. Computations  
142 of wrinkling using the energy relaxation method are presented in Section 4. Section 5 describes the  
143 second variation analysis of the energy function to consider the loss of symmetry in the circumfer-  
144 ential direction of the torus. Section 6 presents several numerical examples to elucidate the theory.  
145 Conclusions are presented in Section 7.

## 146 1.7. Notation

147 *Brackets.* Three types of brackets are used. Square brackets [ ] are used to clarify the order of  
148 operations in an algebraic expression. Curly brackets { } define a set and circular brackets ( ) are  
149 used to define the parameters of a function. If brackets are used to denote an interval then ( ) stands  
150 for an open interval and [ ] a closed interval.

*Symbols.* A variable typeset in a normal weight font represents a scalar. A bold weight font denotes a  
vector or a second-order tensor. An upper-case bold letter denotes a vector or tensor in the reference  
configuration and a lowercase bold letter denotes a vector or tensor in the current (deformed) configura-  
tion. A tensor directly enclosed by square brackets, for example [A], denotes the matrix representation  
of the tensor in a selected coordinate system. A subscript denotes the partial derivative with respect  
to the field. For example, consider a function  $A(a, b(a), c(a))$ .  $A_b$  denotes the partial derivative of  $A$   
with respect to  $b$ , which is equivalent to  $\frac{\partial A}{\partial b}$ .  $\frac{dA}{da}$  is the full derivative with respect to  $a$ , given by

$$\frac{dA}{da} = \frac{\partial A}{\partial a} + \frac{\partial A}{\partial b} \frac{\partial b}{\partial a} + \frac{\partial A}{\partial c} \frac{\partial c}{\partial a}.$$

151 *Functions.*  $\det(\mathbf{A})$  denotes the determinant of the second-order tensor  $\mathbf{A}$ .  $\text{diag}(a, b, c)$  denotes a second-  
152 order tensor with only diagonal entries  $a, b$  and  $c$ .

## 153 2. Kinematics

154 Consider the toroidal membrane in Figure 1 with major and minor radii  $R_b$  and  $R_s (< R_b)$ , respec-  
155 tively. The initial thickness of the membrane  $H$  is assumed constant, where  $H/R_s \ll 1$ . The geometry  
156 and kinematics of this system are similar to previously studied problems [59, 77]. The torus is inflated  
157 by an internal pressure  $\tilde{P}$  and an electric potential difference  $\Phi_0$  is applied across its thickness. The  
158 membrane is assumed to be incompressible.

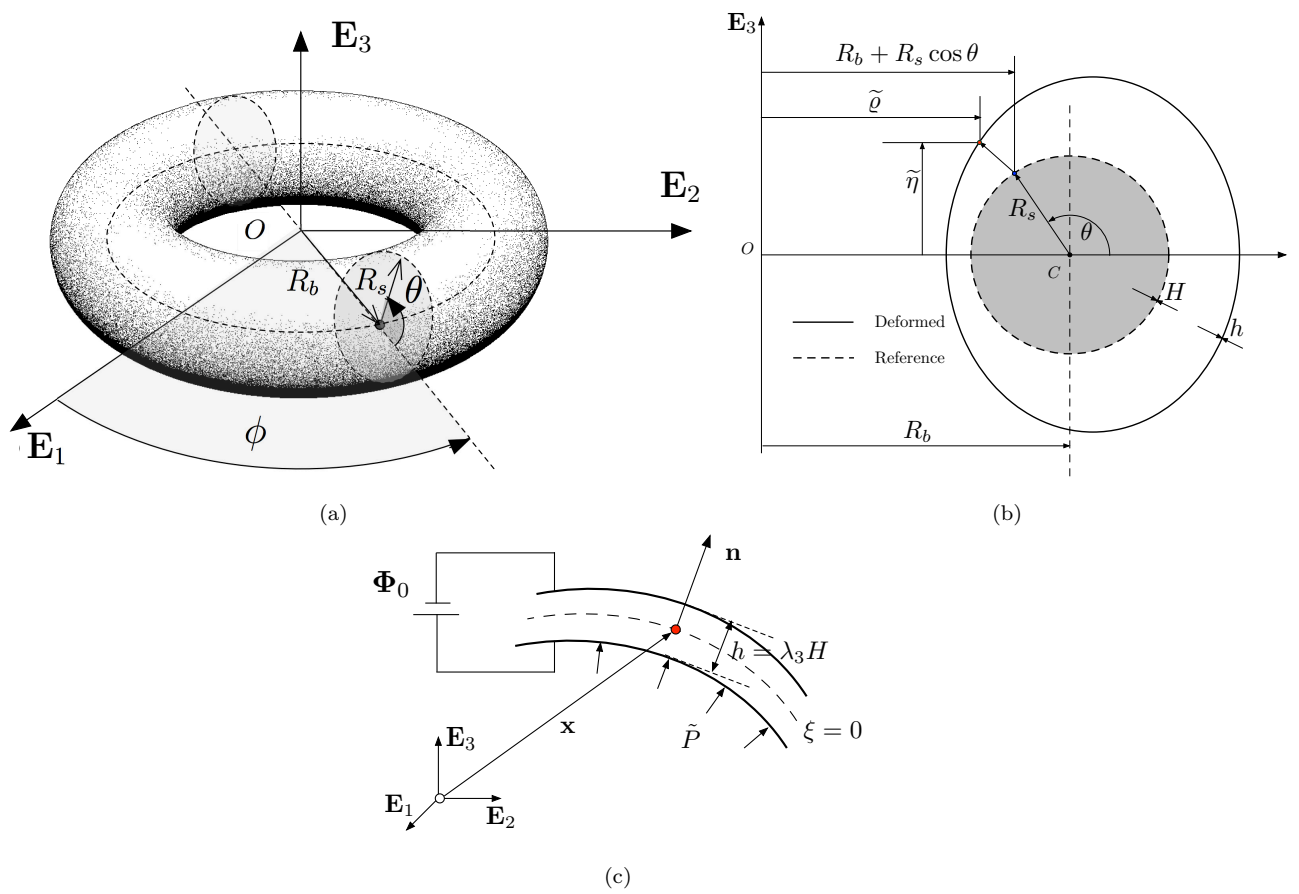


Figure 1: (a) The reference configuration of a toroidal membrane with circular cross-section highlighted. (b) The reference and deformed configurations of a cross section of the toroidal membrane. (c) Close-up of part of the deformed membrane.

The position vector  $\mathbf{X}$  of a point in the undeformed toroidal membrane is given by

$$\begin{aligned} \mathbf{X}(\theta, \phi, \xi) = & [R_b + [R_s + \xi] \cos \theta] \cos \phi \mathbf{E}_1 + [R_b + [R_s + \xi] \cos \theta] \sin \phi \mathbf{E}_2 \\ & + [R_s + \xi] \sin \theta \mathbf{E}_3, \end{aligned} \quad (1)$$

where  $\xi$  is the distance of the point from the mid-surface (defined by  $\xi = 0$ ) of the membrane along the radius. The set  $\{\mathbf{E}_i\}$  of orthonormal vectors is the basis corresponding to the  $(Y^1, Y^2, Y^3)$  coordinate system with origin  $O$ . The components of the covariant metric tensor with respect to the local (curvilinear) system  $(\theta, \phi, \xi)$  (see Figure 1) for the membrane in its reference (perfect torus) configuration, are given by

$$[\mathbf{G}] = \begin{bmatrix} R_s^2 & 0 & 0 \\ 0 & [R_b + R_s \cos \theta]^2 & 0 \\ 0 & 0 & 1 \end{bmatrix}, \quad (2)$$

with determinant  $G = \det \mathbf{G} = R_s^2 [R_b + R_s \cos \theta]^2$ . Here, we have used the small thickness assumption ( $H \ll R_s < R_b$ ).

## 2.2. Deformed configuration

Let the position vector of the deformed mid-surface be given by  $\mathbf{x}$  (corresponding to  $\mathbf{X}$  in the reference configuration) with the unit outward normal vector  $\mathbf{n}$ . It can be shown that

$$\mathbf{x} = \tilde{\varrho} \cos \phi \mathbf{E}_1 + \tilde{\varrho} \sin \phi \mathbf{E}_2 + \tilde{\eta} \mathbf{E}_3, \quad (3)$$

where  $\tilde{\varrho} : [0, 2\pi) \times [0, 2\pi) \rightarrow \mathbb{R}$  and  $\tilde{\eta} : [0, 2\pi) \times [0, 2\pi) \rightarrow \mathbb{R}$  are functions depending on  $\theta$  and  $\phi$  that describe the position of points on the mid-surface as shown in Figure 1c. Components of the three-dimensional covariant metric tensor for the deformed configuration are given by

$$[\tilde{\mathbf{g}}] = \begin{bmatrix} \tilde{\varrho}_\theta^2 + \tilde{\eta}_\theta^2 & \tilde{\varrho}_\theta \tilde{\varrho}_\phi + \tilde{\eta}_\theta \tilde{\eta}_\phi & 0 \\ \tilde{\varrho}_\theta \tilde{\varrho}_\phi + \tilde{\eta}_\theta \tilde{\eta}_\phi & \tilde{\varrho}_\phi^2 + \tilde{\varrho}^2 + \tilde{\eta}_\phi^2 & 0 \\ 0 & 0 & \lambda_3^2 \end{bmatrix}, \quad (4)$$

where  $\lambda_3 = h/H$  with  $h$  being the thickness of the torus in the deformed configuration. We further introduce the dimensionless quantities

$$\gamma = \frac{R_s}{R_b}, \quad \varrho = \frac{\tilde{\varrho}}{R_b}, \quad \eta = \frac{\tilde{\eta}}{R_b}, \quad (5)$$



where the parameter  $\gamma$  describes the aspect ratio of the undeformed torus. The two principle stretches  $\lambda_1$  and  $\lambda_2$  can be expressed using the reference and deformed covariant metric tensors as

$$\begin{aligned}\lambda_1^2 &= \mathcal{P} + \mathcal{Q}, \\ \lambda_2^2 &= \mathcal{P} - \mathcal{Q},\end{aligned}\tag{6}$$

where

$$\begin{aligned}\mathcal{P} &= \frac{1}{2} \left[ \frac{\varrho_\theta^2 + \eta_\theta^2}{\gamma^2} + \frac{\varrho_\phi^2 + \eta_\phi^2 + \varrho^2}{[1 + \gamma \cos \theta]^2} \right], \\ \mathcal{Q} &= \frac{1}{2} \sqrt{\left[ \frac{\varrho_\theta^2 + \eta_\theta^2}{\gamma^2} - \frac{\varrho_\phi^2 + \eta_\phi^2 + \varrho^2}{[1 + \gamma \cos \theta]^2} \right]^2 + 4 \left[ \frac{\varrho_\theta \varrho_\phi + \eta_\theta \eta_\phi}{\gamma[1 + \gamma \cos \theta]} \right]^2}.\end{aligned}$$

The deformation map  $\mathbf{X}$ , from the undeformed configuration to the deformed configuration, is defined via

$$\mathbf{x} = \mathbf{X}(\mathbf{X}),$$

and the corresponding deformation gradient is defined by

$$\mathbf{F}(\mathbf{X}) := \text{Grad } \mathbf{X}(\mathbf{X}).$$

Henceforth, for notational convenience, it is assumed that  $\mathbf{X}$  and  $\mathbf{x}$  are related as above to map the evaluation at  $\mathbf{x}$  of quantities defined on the deformed configuration to their counterparts at  $\mathbf{X}$  on the undeformed configuration. The incompressibility constraint is given by

$$J = \det(\mathbf{F}) = 1,$$

as a consequence of which, the third principle stretch follows as

$$\lambda_3^2 = \frac{1}{\lambda_1^2 \lambda_2^2} = \frac{\gamma^2 [1 + \gamma \cos \theta]^2}{[\varrho_\theta \eta_\phi - \varrho_\phi \eta_\theta]^2 + \varrho^2 [\varrho_\theta^2 + \eta_\theta^2]}.\tag{7}$$

The right Cauchy–Green deformation tensor  $\mathbf{C} = \mathbf{F}^\top \mathbf{F}$  is given in the local coordinate system of the torus by

$$[\mathbf{C}] = \text{diag} (\lambda_1^2, \lambda_2^2, \lambda_3^2).\tag{8}$$

**Remark 1.** *If the solution is symmetric with respect to  $\mathbf{E}_3$  along the  $\phi$  (azimuthal) direction (which happens to be the case for the principal solution as shown in Section 3.3.), the first two principle stretches can be simplified as*

$$\lambda_1 = \frac{1}{\gamma} [\varrho_\theta^2 + \eta_\theta^2]^{1/2}, \quad \lambda_2 = \frac{\varrho}{1 + \gamma \cos \theta}.\tag{9}$$

### 163 3. Electroelastic energy based variational formulation and equations of equilibrium

164 This section formulates the equations of electroelastic equilibrium using the first variation of the total  
 165 potential energy functional. Section 3.1 briefly presents the equations for electrostatics. Thereafter the  
 166 total potential energy of the system under an applied pressure and an electric field is given. Section 3.3  
 167 considers the first variation of the total potential energy and the resulting three governing equations.  
 168 Section 3.4 decomposes the energy density function into an elastic energy density function and an  
 169 electric contribution. A Mooney–Rivlin constitutive model is employed for the elastic energy density.  
 170 This yields the governing equations presented in Section 3.5. A numerical method is proposed in  
 171 Section 3.6 to solve the resulting system of nonlinear ordinary differential equations (ODEs).

#### 172 3.1. Electrostatics

Maxwell’s equations for electrostatics are given by

$$\text{Curl } \mathbf{E} = \mathbf{0}, \quad \text{and} \quad \text{Div } \mathbf{D} = 0, \quad (10)$$

where  $\mathbf{E}$  is the electric field in the reference configuration and  $\mathbf{D}$  is the electric displacement in the reference configuration assuming the free charge density in the volume is zero. Equation (10)<sub>2</sub> motivates the introduction of an electric vector potential  $\mathbf{A}$  defined as

$$\mathbf{D} = \text{Curl } \mathbf{A}. \quad (11)$$

The referential vectors  $\mathbf{E}$  and  $\mathbf{D}$  can be expressed as the pull-backs of the electric field and displacement in the current (deformed) configuration,  $\mathbf{e}$  and  $\mathbf{d}$ , as [22]

$$\mathbf{E} = \mathbf{F}^\top \mathbf{e} \quad \text{and} \quad \mathbf{D} = J \mathbf{F}^{-1} \mathbf{d}. \quad (12)$$

Within the electroelastic solid, the constitutive relation

$$\mathbf{E} = \Omega_{\mathbf{D}} \quad (13)$$

relates  $\mathbf{E}$  and  $\mathbf{D}$  via the total energy density  $\Omega$  of the material. In free space,  $\mathbf{e}$  and  $\mathbf{d}$  are related through the electric permittivity of vacuum  $\varepsilon_0$  as

$$\mathbf{e} = \varepsilon_0^{-1} \mathbf{d}. \quad (14)$$

174 *3.2. Potential energy functional*

The toroidal membrane occupies the region  $\mathcal{B}_0$  in the reference configuration and its total internal energy density per unit volume  $\Omega$  is parameterised by the deformation gradient  $\mathbf{F}$  and the referential electric displacement  $\mathbf{D}$ . Under an applied pressure  $\tilde{P}$ , the total potential energy of the system can be written as

$$\mathfrak{E}(\boldsymbol{\chi}, \mathbf{A}) = \int_{\mathcal{B}_0} \Omega(\mathbf{F}, \mathbf{D}) dv_0 - \int_{V_0}^{V_0+\Delta V} \tilde{P} dV. \quad (15)$$

175 We note here that the first integral is over the region occupied by the solid membrane while the second  
 176 integral of pressure work is over the volume of fluid enclosed by the inflated membrane (that is the  
 177 region lying in the interior of the torus). Hence the differentials are distinguished as  $dv_0$  and  $dV$ . Since  
 178 the electric potential is specified on the inner and outer surfaces of the torus, we assume that the electric  
 179 field does not leak out and therefore there is no contribution to the energy in the region outside the  
 180 membrane given by  $\mathbb{R}^3 \setminus \mathcal{B}_0$ .

As the membrane is considered to be thin ( $H/R_s \ll 1$ ) with negligible bending stiffness, the deformation field  $\boldsymbol{\chi}$  is determined by the functions  $\tilde{\varrho}$  and  $\tilde{\eta}$  which describe the geometry of the mid-surface of the membrane (see Figure 1b). The potential energy functional  $\mathfrak{E}$  (15) can therefore be reparametrised as

$$E(\tilde{\varrho}, \tilde{\eta}, \mathbf{A}) = H \int_0^{2\pi} \int_0^{2\pi} \Omega(\mathbf{F}, \mathbf{D}) \sqrt{G} d\theta d\phi - \frac{1}{2} \int_0^{2\pi} \int_0^{2\pi} \tilde{P} \tilde{\varrho}^2 \tilde{\eta}_\theta d\theta d\phi. \quad (16)$$

181 The modification of the second term for the pressure work is based on the calculations provided in  
 182 Appendix A (supporting file).

183 *3.3. First variation and equations of equilibrium*

At equilibrium, the total potential energy of the inflated toroidal membrane will be stationary, that is

$$\delta E \equiv \delta E((\tilde{\varrho}, \tilde{\eta}, \mathbf{A}); (\delta \tilde{\varrho}, \delta \tilde{\eta}, \delta \mathbf{A})) = 0, \quad (17)$$

$$\begin{aligned} \text{with } \delta E = H \int_0^{2\pi} \int_0^{2\pi} & \left[ \Omega_{\tilde{\varrho}} \delta \tilde{\varrho} + \Omega_{\tilde{\varrho}_\theta} \delta \tilde{\varrho}_\theta + \Omega_{\tilde{\eta}_\theta} \delta \tilde{\eta}_\theta + \Omega_{\tilde{\varrho}_\phi} \delta \tilde{\varrho}_\phi + \Omega_{\tilde{\eta}_\phi} \delta \tilde{\eta}_\phi + \Omega_{\mathbf{D}} \cdot \delta \mathbf{D} \right] \sqrt{G} \\ & - \frac{1}{2H} \tilde{P} \left[ 2 \tilde{\varrho} \tilde{\eta}_\theta \delta \tilde{\varrho} + \tilde{\varrho}^2 \delta \tilde{\eta}_\theta \right] d\theta d\phi = 0. \end{aligned} \quad (18)$$

As shown in Figure 1a, the geometry of the toroidal membrane is axisymmetric with respect to  $\mathbf{E}_3$ . Thus, the principle solutions  $\tilde{\varrho}$  and  $\tilde{\eta}$  should be constant along the  $\phi$  direction, which implies

$\tilde{\varrho}_\phi = \tilde{\eta}_\phi = 0$ . Thus Equation (18) can be simplified as

$$\begin{aligned} \delta E = 2\pi H \int_0^{2\pi} & \left[ \Omega_{\tilde{\varrho}} \delta \tilde{\varrho} + \Omega_{\tilde{\varrho}_\theta} \delta \tilde{\varrho}_\theta + \Omega_{\tilde{\eta}_\theta} \delta \tilde{\eta}_\theta + \Omega_{\mathbf{D}} \cdot \delta \mathbf{D} \right] \sqrt{G} \\ & - \frac{1}{2H} \tilde{P} [2 \tilde{\varrho} \tilde{\eta}_\theta \delta \tilde{\varrho} + \tilde{\varrho}^2 \delta \tilde{\eta}_\theta] \, d\theta = 0. \end{aligned} \quad (19)$$

184

The rotational symmetry of the torus leads to the periodic boundary conditions

$$\delta \tilde{\varrho} |_{\theta=0} = \delta \tilde{\varrho} |_{\theta=2\pi}, \quad \delta \tilde{\eta} |_{\theta=0} = \delta \tilde{\eta} |_{\theta=2\pi}, \quad (20)$$

while a perturbation of equation (11) gives  $\delta \mathbf{D} = \text{Curl } \delta \mathbf{A}$ . Thus we can express the variations of all the quantities in equation (19) in terms of the variations  $\delta \tilde{\varrho}$ ,  $\delta \tilde{\eta}$  and  $\delta \mathbf{A}$ , as desired. Using integration by parts on the terms containing  $\delta \tilde{\varrho}_\theta$  and  $\delta \tilde{\eta}_\theta$ , the vector identity

$$[\nabla \times \mathbf{u}] \cdot \mathbf{v} = \nabla \cdot [\mathbf{u} \times \mathbf{v}] + [\nabla \times \mathbf{v}] \cdot \mathbf{u}, \quad \mathbf{u}, \mathbf{v} \in \mathbb{R}^3 \quad (21)$$

for the terms containing  $\text{Curl } \delta \mathbf{A}$ , and the arbitrariness of the variations results in the following Euler-Lagrange equations for this system

$$\sqrt{G} \Omega_{\tilde{\varrho}} - \frac{d}{d\theta} \left( \sqrt{G} \Omega_{\tilde{\varrho}_\theta} \right) - \frac{\tilde{P} \tilde{\varrho} \tilde{\eta}_\theta}{H} = 0, \quad (22a)$$

$$\frac{d}{d\theta} \left( \sqrt{G} \Omega_{\tilde{\eta}_\theta} - \frac{\tilde{P} \tilde{\varrho}^2}{2H} \right) = 0, \quad (22b)$$

$$\text{Curl } \mathbb{E} = \mathbf{0}, \quad (22c)$$

185 for  $\theta \in (0, 2\pi]$  along with the boundary conditions (20) and a specified potential difference  $\Phi_0$  across  
186 the torus thickness.

For the thin-walled membrane considered, the electric field can be reasonably approximated as [80]

$$\mathbf{e} = \frac{\Phi_0}{h} \mathbf{n}. \quad (23)$$

Thus, from (13) the electric field in reference configuration is given by

$$\mathbb{E} = \frac{\Phi_0}{\lambda_3 H} \mathbf{F}^\top \mathbf{n}, \quad (24)$$

187 which also satisfies the governing equation (22c).

188 *3.4. Energy density function*

The total energy density  $\Omega$  can be further decomposed into an elastic energy density  $\widehat{W}$  and an electric contribution as follows, see [19]

$$\Omega(\mathbf{F}, \mathbf{D}) = \widehat{W}(\mathbf{F}) + \beta[\mathbf{C} \mathbf{D}] \cdot \mathbf{D}, \quad (25)$$

where  $\beta$  is a positive material constant representing electroelastic coupling and the term  $[\mathbf{C} \mathbf{D}] \cdot \mathbf{D}$  is a scalar invariant. This allows the electric field in the reference configuration to be expressed as

$$\mathbb{E} = \Omega_{\mathbf{D}} = 2\beta \mathbf{C} \mathbf{D}. \quad (26)$$

On comparing equations (23) and (26), the electric displacement in the reference configuration can be expressed as

$$\mathbf{D} = \frac{\Phi_0}{2\beta\lambda_3 H} \mathbf{F}^{-1} \mathbf{n} = \frac{\Phi_0}{2\beta H} \mathbf{C}^{-1} \mathbf{N}, \quad (27)$$

189 where  $\mathbf{n}$  and  $\mathbf{N}$  are unit vectors along the outward normal in current (deformed) and reference con-  
 190 figurations, respectively. Here Nanson's relation is employed to relate the normal vectors as  $\mathbf{n} da =$   
 191  $J \mathbf{F}^{-\top} \mathbf{N} dA$  with  $da = \lambda_1 \lambda_2 dA$ .

We consider an incompressible Mooney–Rivlin constitutive model for the elastic energy density  $\widehat{W}$  given in terms of two material constants  $C_1$  and  $C_2$  where

$$\widehat{W}(I_1, I_2) = C_1[I_1 - 3] + C_2[I_2 - 3], \quad (28a)$$

$$\text{with } I_1 = \lambda_1^2 + \lambda_2^2 + \lambda_3^2 \quad \text{and} \quad I_2 = \lambda_1^{-2} + \lambda_2^{-2} + \lambda_3^{-2}. \quad (28b)$$

The energy density  $\Omega$  in Equation (25) can therefore be expressed as

$$\Omega = C_1[I_1 - 3] + C_2[I_2 - 3] + \beta[\mathbf{C} \mathbf{D}] \cdot \mathbf{D}. \quad (29)$$

192 The derivatives of  $\Omega$  required for the subsequent derivations and computations are tabulated in Ap-  
 193 pendix B (supporting file).

194 *3.5. Governing equations*

We introduce the following dimensionless versions of pressure  $P$  and electric loading  $\mathcal{E}$  to simplify our calculations

$$P = \frac{\widetilde{P} R_b}{C_1 H}, \quad \mathcal{E} = \frac{\Phi_0^2}{C_1 \beta H^2}. \quad (30)$$

Further introducing a dimensionless parameter  $\alpha = C_2/C_1$ , the ordinary differential equations (22a) and (22b) can be written in dimensionless form for  $\theta \in [0, \pi]$  as

$$\begin{aligned} \frac{d}{d\theta} \left( [1 + \gamma \cos \theta] \left[ \frac{2\varrho_\theta}{\gamma^2} [1 + \alpha\lambda_2^2] \left[ 1 - \frac{1}{\lambda_1^4\lambda_2^2} \right] - \frac{\rho_\theta \mathcal{E} \lambda_2^2}{2\gamma^2} \right] \right) \\ - 2\lambda_2 [1 + \alpha\lambda_1^2] \left[ 1 - \frac{1}{\lambda_1^2\lambda_2^4} \right] + \frac{\mathcal{E} \lambda_2 \lambda_1^2}{2} + \frac{P \varrho \eta_\theta}{\gamma} = 0, \end{aligned} \quad (31a)$$

$$\frac{d}{d\theta} \left( [1 + \gamma \cos \theta] \left[ \frac{2\eta_\theta}{\gamma^2} [1 + \alpha\lambda_2^2] \left[ 1 - \frac{1}{\lambda_1^4\lambda_2^2} \right] - \frac{\eta_\theta \mathcal{E} \lambda_2^2}{2\gamma^2} \right] - \frac{P \varrho^2}{2\gamma} \right) = 0, \quad (31b)$$

along with the boundary conditions, accounting for the additional assumption of a reflection symmetry of the system with respect to the  $Y^1 - Y^2$  plane, given by

$$\varrho_\theta = 0, \quad \eta = 0 \quad \text{at} \quad \theta = 0 \quad (32a)$$

$$\text{and } \varrho_\theta = 0, \quad \eta = 0 \quad \text{at} \quad \theta = \pi. \quad (32b)$$

195

### 196 3.6. Numerical solution procedure

The governing equations (31a) and (31b) are coupled nonlinear second-order ordinary differential equations. These can be converted to a system of first-order ODEs by defining

$$y_1 = \varrho, \quad y_2 = \varrho_\theta, \quad y_3 = \eta, \quad y_4 = \eta_\theta, \quad (33)$$

and rewriting the system as

$$\underbrace{\begin{bmatrix} 1 & 0 & 0 & 0 \\ 0 & A_1 & 0 & A_2 \\ 0 & 0 & 1 & 0 \\ 0 & B_1 & 0 & B_2 \end{bmatrix}}_{\mathbf{A}} \underbrace{\begin{bmatrix} y_1' \\ y_2' \\ y_3' \\ y_4' \end{bmatrix}}_{\mathbf{y}} = \underbrace{\begin{bmatrix} y_2 \\ -A_3 \\ y_4 \\ -B_3 \end{bmatrix}}_{\mathbf{b}}, \quad (34)$$

where  $(\bullet)'$  denotes the derivative with respect to  $\theta$ , together with boundary conditions

$$y_2 = 0, \quad y_3 = 0 \quad \text{at} \quad \theta = 0 \quad \text{and} \quad \theta = \pi. \quad (35)$$

197 The components of matrices  $\mathbf{A}$  and  $\mathbf{b}$  are derived in Appendix D (supporting file).

198 We discretise the reference configuration of the membrane into  $n_\theta$  segments as shown in Figure 2. The  
199  $n_\theta + 1$  discretised points in the deformed configuration are denoted by  $\mathbf{x}^i(\theta)$ , where  $i = 0, 1, 2, \dots, n_\theta$ .  
200 For each  $\theta^i$ , the matrix  $\mathbf{A}$  and the right hand vector  $\mathbf{b}$  can be computed given the mechanical and  
201 electrical loads  $P$  and  $\mathcal{E}$  that are independent of  $\theta$ .  $P$  is only present in the vector  $\mathbf{b}$  as the mechanical

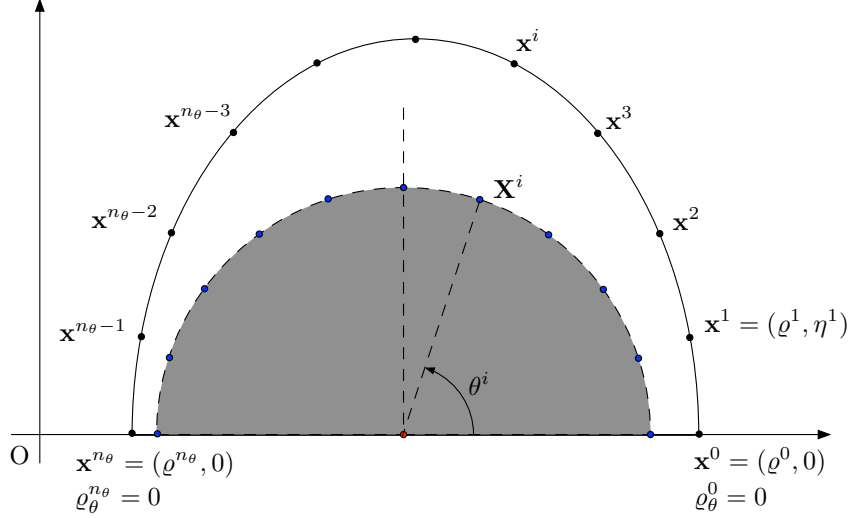


Figure 2: Half of the cross-section is discretised into  $n_\theta$  segments with respect to  $\theta$  and the boundary conditions (32) are applied at  $\theta = 0$  and  $\pi$ .

load does not affect the material “stiffness”. However,  $\mathcal{E}$  appears in both the matrix  $\mathbf{A}$  and the vector  $\mathbf{b}$  since the electrical load affects not only the boundary conditions but also changes the material behaviour.

The system (34) and (35) is solved using a variation of the shooting method [51] employing arc-control [59]. We use the `ode45` solver in `Matlab` [43] for the numerical approximation of the ODEs.  $y_2^0$  and  $y_3^0$  are zero as per the boundary conditions (35) and a value of  $y_1^0$  is chosen. To solve the system of equation, a reasonable initial guess for the variables  $y_4^0$  and  $P$  is required. Then the function `ode45` can be used to solve for the unknowns  $y_1^i, y_2^i, y_3^i, y_4^i$  for any  $i = 0, 1, 2, 3, \dots, n_\theta$ . A cost function  $f_c = \sqrt{[y_2^{n_\theta}]^2 + [y_3^{n_\theta}]^2}$  is introduced to ensure satisfaction of the boundary conditions; this is required to be minimised as part of the shooting method. Then the function `fminsearchbnd` [16] is used to search for a pair of  $y_4^0$  and  $P$  such that the cost function  $f_c$  is less than a tolerance  $\epsilon = 10^{-6}$ . Once  $f_c < \epsilon$ , the values of  $y_4^0$  and  $P$  are assumed sufficiently converged and the values of  $y_1^i, y_2^i, y_3^i, y_4^i$  for all  $i = 0, 1, 2, 3, \dots, n_\theta$  are computed. The arc-length control (by specifying  $y_1^0$  and computing  $P$ ) helps in the evaluation of solutions between the snap-through path, see Figure 3.

Since the solutions are computed using a minimisation procedure, convergence is dependent upon the initial guess of  $P$  and  $y_4^0$ . In general, the values of  $y_4^0$  and  $P$  from the previous load step can be used as initial guesses for the updated deformed profile, thereby allowing the inflation of the toroidal membrane to be simulated. However, in the initial stages of the inflation of the membrane, a relatively large pressure increase results in a very small deformation. This is due to the high initial stiffness as shown in Figure 3. In this initial region, the gradient of  $P$  with respect to volume change is very high

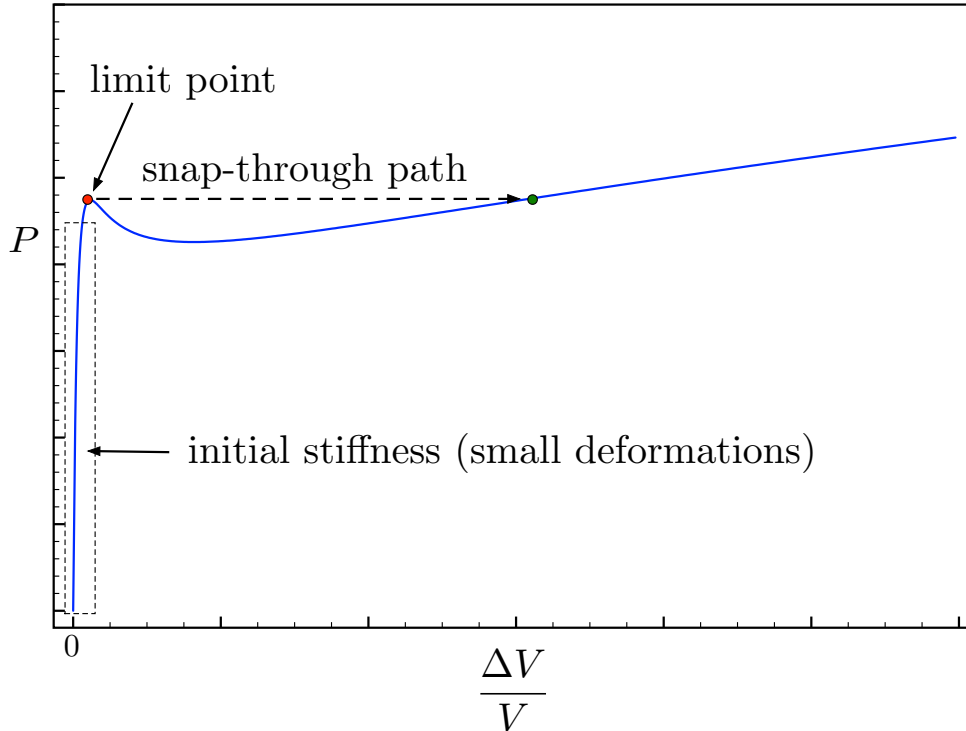


Figure 3: A sketch of the initial stiffness and snap-through path for an ideal electroelastic toroidal membrane under large inflation. For a membrane with imperfections, snap-through may occur prior to reaching the limit point.

222 and convergence of the method using `fminsearchbnd` is problematic. To simulate the inflation in this  
 223 region, one should seek solutions close to the limit point and then solve for a less deformed membrane  
 224 profile by decreasing  $dy_1^0$  with a small decrement. Convergence is also improved by introducing a scaling  
 225 coefficient  $\kappa = |dP/dy_1^0|$ , where the change of pressure  $dP$  is estimated based on the previous solutions.  
 226 Then, instead of searching for  $y_4^0$  and  $P$  to achieve  $f_c = 0$ , one searches for  $P$  and  $\kappa y_4^0$ . Following this  
 227 approach, the convergence of the `fminsearchbnd` is greatly improved and the method is robust. A  
 228 computer code employing the above-described scheme is available at [40].

#### 229 4. Wrinkling instability analysis

230 A membrane structure can only sustain tensile loading and has no resistance to compressive stress.  
 231 When an in-plane compressive stress is about to occur in a membrane structure, the membrane tends  
 232 to develop localised out-of-plane deformation to lower the energy. This phenomenon is known as wrin-  
 233 kling. For the problem considered here, when the toroidal membrane inflates and gradually undergoes  
 234 increasing deformation, the tensile stresses in inner regions ( $\theta \approx \pi$ ) are gradually reduced. Eventually,  
 235 this will lead to wrinkling in the inner regions of the toroidal membrane. Post wrinkle formation, the  
 236 principle governing equations (31a) and (31b) are no longer descriptors of the state of the system. An



237 energy relaxation method is then adopted to modify the governing equations and compute new solutions  
 238 valid for the post-wrinkling regime.

#### 239 4.1. In-plane stress components

The total Piola stress tensor  $\mathbf{P}$  for the incompressible case is given by [19]

$$\mathbf{P} = \Omega_{\mathbf{F}} - p \mathbf{F}^{-\top}, \quad (36)$$

where  $p$  is a Lagrange multiplier associated with the constraint of incompressibility. The total Cauchy stress is (as  $J = 1$ )

$$\boldsymbol{\sigma} = \mathbf{P} \mathbf{F}^{\top} = \Omega_{\mathbf{F}} \mathbf{F}^{\top} - p \mathbf{i}, \quad (37)$$

where  $\mathbf{i}$  is the second-order unit tensor in the current configuration. Let the local orthonormal coordinate system in the membrane mid-surface be given by  $\{\mathbf{n}, \mathbf{t}_1, \mathbf{t}_2\}$ , where the unit normal  $\mathbf{n}$  is defined in Appendix A (supporting file) and  $\mathbf{t}_1$  and  $\mathbf{t}_2$  are unit vectors in the tangent plane of the membrane. Following the discussion in Section 2, the tensor  $\mathbf{F}$  and subsequently the Cauchy stress  $\boldsymbol{\sigma}$  are represented by diagonal matrices in this local basis. We can compute the in-plane stress components as

$$s_{11} = [\boldsymbol{\sigma} \mathbf{t}_1] \cdot \mathbf{t}_1, \quad s_{22} = [\boldsymbol{\sigma} \mathbf{t}_2] \cdot \mathbf{t}_2, \quad s_{12} = s_{21} = [\boldsymbol{\sigma} \mathbf{t}_2] \cdot \mathbf{t}_1 = 0, \quad (38)$$

Using the balance of traction at the inner boundary,

$$\boldsymbol{\sigma} \mathbf{n} + \tilde{P} \mathbf{n} = \mathbf{0}, \quad (39)$$

One determines the Lagrange multiplier  $p$  as

$$p = \tilde{P} + [\Omega_{\mathbf{F}} \mathbf{F}^{\top} \mathbf{n}] \cdot \mathbf{n}, \quad (40)$$

using which one can write the two in-plane stress components as

$$\begin{aligned} s_{11} &= [\Omega_{\mathbf{F}} \mathbf{F}^{\top} \mathbf{t}_1] \cdot \mathbf{t}_1 - \tilde{P} - [\Omega_{\mathbf{F}} \mathbf{F}^{\top} \mathbf{n}] \cdot \mathbf{n}, \\ s_{22} &= [\Omega_{\mathbf{F}} \mathbf{F}^{\top} \mathbf{t}_2] \cdot \mathbf{t}_2 - \tilde{P} - [\Omega_{\mathbf{F}} \mathbf{F}^{\top} \mathbf{n}] \cdot \mathbf{n}. \end{aligned} \quad (41)$$

Substituting in the specific form of  $\Omega$  from equations (25) and (28a), and making use of (27), yields

$$\Omega_{\mathbf{F}} \mathbf{F}^{\top} = 2C_1 \mathbf{b} + 2C_2 [I_1 \mathbf{b} - \mathbf{b}^2] + \frac{\Phi_0^2}{2\beta\lambda_3^2 H^2} \mathbf{n} \otimes \mathbf{n}, \quad (42)$$

allowing one to rewrite the in-plane principal stress components as

$$s_{11} = C_1 \left[ -\frac{PH}{R_b} + 2\lambda_1^2 + 2\alpha\lambda_1^2 \left[ \lambda_2^2 + \frac{1}{\lambda_1^2\lambda_2^2} \right] - \frac{2}{\lambda_1^2\lambda_2^2} - 2\alpha \left[ \frac{1}{\lambda_1^2} + \frac{1}{\lambda_2^2} \right] - \frac{\mathcal{E}\lambda_1^2\lambda_2^2}{2} \right], \quad (43a)$$

$$s_{22} = C_1 \left[ -\frac{PH}{R_b} + 2\lambda_2^2 + 2\alpha\lambda_2^2 \left[ \lambda_1^2 + \frac{1}{\lambda_1^2\lambda_2^2} \right] - \frac{2}{\lambda_1^2\lambda_2^2} - 2\alpha \left[ \frac{1}{\lambda_1^2} + \frac{1}{\lambda_2^2} \right] - \frac{\mathcal{E}\lambda_1^2\lambda_2^2}{2} \right]. \quad (43b)$$

240 Note that the thinness assumption of the membrane,  $H/R_s \ll 1$ , nullifies the influence of the pressure  
 241 term on the in-plane membrane stresses [12]. A constant value  $H/R_s = \gamma^{-1}10^{-4}$  is thus adopted in all  
 242 numerical examples.

#### 243 4.2. Energy Relaxation

244 Adopting the tension field theory developed by [57, 67] for hyperelastic membranes and later ex-  
 245 tended to electroelastic membranes by [15, 26], we introduce the concept of a *generalised natural state*.  
 246 In the current problem, the key kinematic variables in the total energy density function  $\Omega(\mathbf{F}, \mathbf{D})$  are  
 247  $\{\lambda_1, \lambda_2, \mathcal{E}\}$  and hence  $\Omega = \widehat{\Omega}(\lambda_1, \lambda_2, \mathcal{E})$ .

If the membrane is mechanically stretched along one direction with stretch  $\lambda_1 > 1$  (resp.  $\lambda_2 > 1$ )  
 and an electric load  $\mathcal{E}$  is applied, then the value of  $\lambda_2$  (resp.  $\lambda_1$ ) that sets the principal stress component  
 $s_{22}$  (resp.  $s_{11}$ ) to zero is denoted as the *natural width*  $w_1$ . This natural width is given by

$$w_1(\lambda_1, \mathcal{E}) := \lambda_2^* \quad \text{such that} \quad s_{22}(\lambda_1, \lambda_2^*, \mathcal{E}) = 0, \quad (44)$$

where  $\lambda_2^{*2}$  can be expressed as a function of  $\lambda_1$  and  $\mathcal{E}$  as

$$\lambda_2^{*2}(\lambda_1, \mathcal{E}) = \frac{\frac{PH}{R_b} \lambda_1 + \sqrt{\frac{P^2 H^2}{R_b^2} \lambda_1^2 - 4\alpha \mathcal{E} \lambda_1^4 + 16\alpha^2 \lambda_1^4 + 32\alpha \lambda_1^2 - 4\mathcal{E} \lambda_1^2 + 16}}{4\lambda_1 + 4\alpha \lambda_1^3 - \mathcal{E} \lambda_1^3}. \quad (45)$$

The relaxed energy is then given by

$$\Omega^*(\lambda_1, \lambda_2^*) = C_1[I_1^* - 3] + C_2[I_2^* - 3] + \beta[\mathbf{C} \mathbf{D}] \cdot \mathbf{D}, \quad (46)$$

where

$$I_1^*(\lambda_1, \lambda_2^*) = \lambda_1^2 + \lambda_2^{*2} + \frac{1}{\lambda_1^2 \lambda_2^{*2}}, \quad I_2^*(\lambda_1, \lambda_2^*) = \frac{1}{\lambda_1^2} + \frac{1}{\lambda_2^{*2}} + \lambda_1^2 \lambda_2^{*2}, \quad (47)$$

and

$$\beta[\mathbf{C} \mathbf{D}] \cdot \mathbf{D} = \frac{C_1 \mathcal{E}}{4} \lambda_1^2 \lambda_2^{*2}. \quad (48)$$

Since  $\lambda_2^*$  is a function of  $\lambda_1$  and  $\mathcal{E}$  as shown in (45),  $I_1^*$  and  $I_2^*$  are only functions of  $\lambda_1$  and  $\mathcal{E}$ .  
 Similarly,  $\beta[\mathbf{C} \mathbf{D}] \cdot \mathbf{D}$  is a function of  $\lambda_1$  and  $\mathcal{E}$ . Hence

$$\Omega^*(\lambda_1, \mathcal{E}) = C_1[I_1^* - 3] + C_2[I_2^* - 3] + \beta[\mathbf{C} \mathbf{D}] \cdot \mathbf{D}. \quad (49)$$

The governing equations (31) thus become

$$\begin{aligned} [1 + \gamma \cos \theta] \frac{d}{d\theta} \left( \frac{\partial \Omega^*}{\partial \varrho_\theta} \right) - \gamma \sin \theta \frac{\partial \Omega^*}{\partial \varrho_\theta} - \frac{\partial \Omega^*}{\partial \varrho} [1 + \gamma \cos \theta] + \frac{\tilde{P} R_b \varrho \eta_\theta}{\gamma H} &= 0, \\ [1 + \gamma \cos \theta] \frac{d}{d\theta} \left( \frac{\partial \Omega^*}{\partial \eta_\theta} \right) - \gamma \sin \theta \frac{\partial \Omega^*}{\partial \eta_\theta} - \frac{d}{d\theta} \left( \frac{\tilde{P} R_b \varrho^2}{2\gamma H} \right) &= 0. \end{aligned} \quad (50)$$

248 These can be rearranged into a matrix form as in (34). The reformulation is given in Appendix E  
 249 (supporting file). The same shooting method described in Section 3.6 is used to solve these modified  
 250 equations.

## 251 5. Loss of symmetry in the $\phi$ direction

252 This section considers the loss of symmetry of the principal solution obtained in Section 3 due to  
 253 a perturbation along the outer equator which is an instability of the toroidal membrane. If the second  
 254 variation of the potential energy functional vanishes, the solution bifurcates to a lower energy branch  
 255 that is no longer symmetric.

### 256 5.1. Second variation of the potential energy functional

For the analysis of the critical point  $(\mathbf{X}, \mathbf{A})$  of instability, one seeks  $\Delta \mathbf{X} := (\Delta \tilde{\varrho}, \Delta \tilde{\eta})$  and  $\Delta \mathbf{A}$  such that the following bilinear functional vanishes

$$\delta^2 E[\mathbf{X}, \mathbf{A}; (\delta \mathbf{X}, \delta \mathbf{A}), (\Delta \mathbf{X}, \Delta \mathbf{A})] = 0. \quad (51)$$

The principal solution has no dependence on the  $\phi$  coordinate, but one might be interested in perturbations along the  $\phi$  direction. Hence, we derive a more general Taylor expansion of the functional  $E$  in (16) considering  $\tilde{\varrho}$  and  $\tilde{\eta}$  to have dependence on both  $\theta$  and  $\phi$ , i.e.  $\tilde{\varrho}(\theta, \phi)$  and  $\tilde{\eta}(\theta, \phi)$ . This yields

$$\begin{aligned} E[\tilde{\varrho} + \delta \tilde{\varrho}, \tilde{\eta} + \delta \tilde{\eta}, \mathbf{A} + \delta \mathbf{A}] &= H \int_0^{2\pi} \int_0^{2\pi} \left[ \Omega + \Omega_{\tilde{\varrho}} \delta \tilde{\varrho} + \Omega_{\tilde{\varrho}_\theta} \delta \tilde{\varrho}_\theta + \Omega_{\tilde{\varrho}_\phi} \delta \tilde{\varrho}_\phi + \Omega_{\tilde{\eta}_\theta} \delta \tilde{\eta}_\theta \right. \\ &+ \Omega_{\tilde{\eta}_\phi} \delta \tilde{\eta}_\phi + \Omega_{\mathbb{D}} \cdot \delta \mathbb{D} + \frac{1}{2} \left[ \Omega_{\tilde{\varrho}\tilde{\varrho}} \delta \tilde{\varrho} \delta \tilde{\varrho} + \Omega_{\tilde{\varrho}_\theta \tilde{\varrho}_\theta} \delta \tilde{\varrho}_\theta \delta \tilde{\varrho}_\theta + \Omega_{\tilde{\varrho}_\phi \tilde{\varrho}_\phi} \delta \tilde{\varrho}_\phi \delta \tilde{\varrho}_\phi \right. \\ &+ \Omega_{\tilde{\eta}_\theta \tilde{\eta}_\theta} \delta \tilde{\eta}_\theta \delta \tilde{\eta}_\theta + \Omega_{\tilde{\eta}_\phi \tilde{\eta}_\phi} \delta \tilde{\eta}_\phi \delta \tilde{\eta}_\phi + \delta \mathbb{D} \cdot [\Omega_{\mathbb{D}\mathbb{D}} \delta \mathbb{D}] + 2\Omega_{\tilde{\varrho}\tilde{\varrho}_\theta} \delta \tilde{\varrho} \delta \tilde{\varrho}_\theta + 2\Omega_{\tilde{\varrho}\tilde{\varrho}_\phi} \delta \tilde{\varrho} \delta \tilde{\varrho}_\phi \\ &+ 2\Omega_{\tilde{\varrho}\tilde{\eta}_\theta} \delta \tilde{\varrho} \delta \tilde{\eta}_\theta + 2\Omega_{\tilde{\varrho}\tilde{\eta}_\phi} \delta \tilde{\varrho} \delta \tilde{\eta}_\phi + 2\delta \mathbb{D} \cdot \Omega_{\tilde{\varrho}\mathbb{D}} \delta \tilde{\varrho} + 2\Omega_{\tilde{\varrho}_\theta \tilde{\varrho}_\theta} \delta \tilde{\varrho}_\theta \delta \tilde{\varrho}_\theta + 2\Omega_{\tilde{\varrho}_\theta \tilde{\eta}_\theta} \delta \tilde{\varrho}_\theta \delta \tilde{\eta}_\theta \\ &+ 2\Omega_{\tilde{\varrho}_\theta \tilde{\eta}_\phi} \delta \tilde{\varrho}_\theta \delta \tilde{\eta}_\phi + 2\delta \mathbb{D} \cdot \Omega_{\tilde{\varrho}_\theta \mathbb{D}} \delta \tilde{\varrho}_\theta + 2\Omega_{\tilde{\varrho}_\phi \tilde{\eta}_\theta} \delta \tilde{\varrho}_\phi \delta \tilde{\eta}_\theta + 2\Omega_{\tilde{\varrho}_\phi \tilde{\eta}_\phi} \delta \tilde{\varrho}_\phi \delta \tilde{\eta}_\phi \\ &\left. + 2\delta \mathbb{D} \cdot \Omega_{\tilde{\varrho}_\phi \mathbb{D}} \delta \tilde{\varrho}_\phi + 2\Omega_{\tilde{\eta}_\theta \tilde{\eta}_\theta} \delta \tilde{\eta}_\theta \delta \tilde{\eta}_\theta + 2\delta \mathbb{D} \cdot \Omega_{\tilde{\eta}_\theta \mathbb{D}} \delta \tilde{\eta}_\theta + 2\delta \mathbb{D} \cdot \Omega_{\tilde{\eta}_\phi \mathbb{D}} \delta \tilde{\eta}_\phi \right] \sqrt{G} d\theta d\phi \\ &- \frac{1}{2} \int_0^{2\pi} \int_0^{2\pi} \tilde{P} [[\tilde{\varrho} + \delta \tilde{\varrho}]^2 [\tilde{\eta}_\theta + \delta \tilde{\eta}_\theta]] d\theta d\phi. \end{aligned} \quad (52)$$

Application of integration by parts and making use of the vector identity (21), the second variation is

expressed as

$$\begin{aligned}
\delta^2 E[\boldsymbol{\chi}, \mathbf{A}; (\delta \boldsymbol{\chi}, \delta \mathbf{A}), (\Delta \boldsymbol{\chi}, \Delta \mathbf{A})] = & -H \int_0^{2\pi} \int_0^{2\pi} \left[ \right. \\
& \left[ \sqrt{G} \left[ -\Omega_{\tilde{\varrho}} \tilde{\varrho} \Delta \tilde{\varrho} - \Omega_{\tilde{\varrho} \tilde{\varrho}_\theta} \Delta \tilde{\varrho}_\theta - \Omega_{\tilde{\varrho} \tilde{\varrho}_\phi} \Delta \tilde{\varrho}_\phi - \Omega_{\tilde{\varrho} \tilde{\eta}_\theta} \Delta \tilde{\eta}_\theta - \Omega_{\tilde{\varrho} \tilde{\eta}_\phi} \Delta \tilde{\eta}_\phi - \Omega_{\tilde{\varrho} \mathbf{D}} \cdot \Delta \mathbf{D} \right] \right. \\
& + \frac{d}{d\theta} \left( \left[ \Omega_{\tilde{\varrho}_\theta \tilde{\varrho}_\theta} \Delta \tilde{\varrho}_\theta + \Omega_{\tilde{\varrho} \tilde{\varrho}_\theta} \Delta \tilde{\varrho} + \Omega_{\tilde{\varrho}_\theta \tilde{\varrho}_\phi} \Delta \tilde{\varrho}_\phi + \Omega_{\tilde{\varrho}_\theta \tilde{\eta}_\theta} \Delta \tilde{\eta}_\theta + \Omega_{\tilde{\varrho}_\theta \tilde{\eta}_\phi} \Delta \tilde{\eta}_\phi + \Omega_{\tilde{\varrho}_\theta \mathbf{D}} \cdot \Delta \mathbf{D} \right] \sqrt{G} \right) \\
& + \frac{d}{d\phi} \left( \left[ \Omega_{\tilde{\varrho}_\phi \tilde{\varrho}_\phi} \Delta \tilde{\varrho}_\phi + \Omega_{\tilde{\varrho} \tilde{\varrho}_\phi} \Delta \tilde{\varrho} + \Omega_{\tilde{\varrho}_\theta \tilde{\varrho}_\phi} \Delta \tilde{\varrho}_\theta + \Omega_{\tilde{\varrho}_\phi \tilde{\eta}_\theta} \Delta \tilde{\eta}_\theta + \Omega_{\tilde{\varrho}_\phi \tilde{\eta}_\phi} \Delta \tilde{\eta}_\phi + \Omega_{\tilde{\varrho}_\phi \mathbf{D}} \cdot \Delta \mathbf{D} \right] \sqrt{G} \right) \delta \tilde{\varrho} \\
& + \left[ \frac{d}{d\theta} \left( \left[ \Omega_{\tilde{\eta}_\theta \tilde{\eta}_\theta} \Delta \tilde{\eta}_\theta + \Omega_{\tilde{\varrho} \tilde{\eta}_\theta} \Delta \tilde{\varrho} + \Omega_{\tilde{\varrho}_\theta \tilde{\eta}_\theta} \Delta \tilde{\varrho}_\theta + \Omega_{\tilde{\varrho}_\phi \tilde{\eta}_\theta} \Delta \tilde{\varrho}_\phi + \Omega_{\tilde{\eta}_\theta \tilde{\eta}_\phi} \Delta \tilde{\eta}_\phi + \Omega_{\tilde{\eta}_\theta \mathbf{D}} \cdot \Delta \mathbf{D} \right] \sqrt{G} \right) \right. \\
& + \left. \frac{d}{d\phi} \left( \left[ \Omega_{\tilde{\eta}_\phi \tilde{\eta}_\phi} \Delta \tilde{\eta}_\phi + \Omega_{\tilde{\varrho} \tilde{\eta}_\phi} \Delta \tilde{\varrho} + \Omega_{\tilde{\varrho}_\theta \tilde{\eta}_\phi} \Delta \tilde{\varrho}_\theta + \Omega_{\tilde{\varrho}_\phi \tilde{\eta}_\phi} \Delta \tilde{\varrho}_\phi + \Omega_{\tilde{\eta}_\theta \tilde{\eta}_\phi} \Delta \tilde{\eta}_\theta + \Omega_{\tilde{\eta}_\phi \mathbf{D}} \cdot \Delta \mathbf{D} \right] \sqrt{G} \right) \right] \delta \tilde{\eta} \\
& - \text{Curl} \left[ \Omega_{\mathbf{D} \mathbf{D}} \Delta \mathbf{D} + \Omega_{\tilde{\varrho} \mathbf{D}} \Delta \tilde{\varrho} + \Omega_{\tilde{\varrho}_\theta \mathbf{D}} \Delta \tilde{\varrho}_\theta + \Omega_{\tilde{\varrho}_\phi \mathbf{D}} \Delta \tilde{\varrho}_\phi + \Omega_{\tilde{\eta}_\theta \mathbf{D}} \Delta \tilde{\eta}_\theta + \Omega_{\tilde{\eta}_\phi \mathbf{D}} \Delta \tilde{\eta}_\phi \right] \cdot \delta \mathbf{A} \sqrt{G} \Big] d\theta d\phi \\
& - \int_0^{2\pi} \int_0^{2\pi} \tilde{P} \left[ [\tilde{\varrho} \Delta \tilde{\eta}_\theta + \tilde{\eta}_\theta \Delta \tilde{\varrho}] \delta \tilde{\varrho} - [\tilde{\varrho}_\theta \Delta \tilde{\varrho} + \tilde{\varrho} \Delta \tilde{\varrho}_\theta] \delta \tilde{\eta} \right] d\theta d\phi. \tag{53}
\end{aligned}$$

257 The Euler-Lagrange equations corresponding to (51) are derived in dimensionless form as

$$\begin{aligned}
& \left[ -\Omega_{\varrho} \varrho \Delta \varrho - \Omega_{\varrho \varrho_\theta} \Delta \varrho_\theta - \Omega_{\varrho \varrho_\phi} \Delta \varrho_\phi - \Omega_{\varrho \eta_\theta} \Delta \eta_\theta - \Omega_{\varrho \eta_\phi} \Delta \eta_\phi - \Omega_{\varrho \mathbf{D}} \cdot \Delta \mathbf{D} \right] [1 + \gamma \cos \theta] \\
& + \frac{d}{d\theta} \left( \left[ \Omega_{\varrho_\theta \varrho_\theta} \Delta \varrho_\theta + \Omega_{\varrho \varrho_\theta} \Delta \varrho + \Omega_{\varrho_\theta \varrho_\phi} \Delta \varrho_\phi + \Omega_{\varrho_\theta \eta_\theta} \Delta \eta_\theta + \Omega_{\varrho_\theta \eta_\phi} \Delta \eta_\phi + \Omega_{\varrho_\theta \mathbf{D}} \cdot \Delta \mathbf{D} \right] [1 + \gamma \cos \theta] \right) \\
& + \frac{d}{d\phi} \left( \left[ \Omega_{\varrho_\phi \varrho_\phi} \Delta \varrho_\phi + \Omega_{\varrho \varrho_\phi} \Delta \varrho + \Omega_{\varrho_\theta \varrho_\phi} \Delta \varrho_\theta + \Omega_{\varrho_\phi \eta_\theta} \Delta \eta_\theta + \Omega_{\varrho_\phi \eta_\phi} \Delta \eta_\phi + \Omega_{\varrho_\phi \mathbf{D}} \cdot \Delta \mathbf{D} \right] [1 + \gamma \cos \theta] \right) \\
& + \frac{C_1 P}{\gamma} \left[ \varrho \Delta \eta_\theta + \eta_\theta \Delta \varrho \right] = 0, \tag{54}
\end{aligned}$$

$$\begin{aligned}
& \frac{d}{d\theta} \left( \left[ \Omega_{\eta_\theta \eta_\theta} \Delta \eta_\theta + \Omega_{\varrho \eta_\theta} \Delta \varrho + \Omega_{\varrho_\theta \eta_\theta} \Delta \varrho_\theta + \Omega_{\varrho_\phi \eta_\theta} \Delta \varrho_\phi + \Omega_{\eta_\theta \eta_\phi} \Delta \eta_\phi + \Omega_{\eta_\theta \mathbf{D}} \cdot \Delta \mathbf{D} \right] [1 + \gamma \cos \theta] \right) \\
& + \frac{d}{d\phi} \left( \left[ \Omega_{\eta_\phi \eta_\phi} \Delta \eta_\phi + \Omega_{\varrho \eta_\phi} \Delta \varrho + \Omega_{\varrho_\theta \eta_\phi} \Delta \varrho_\theta + \Omega_{\varrho_\phi \eta_\phi} \Delta \varrho_\phi + \Omega_{\eta_\theta \eta_\phi} \Delta \eta_\theta + \Omega_{\eta_\phi \mathbf{D}} \cdot \Delta \mathbf{D} \right] [1 + \gamma \cos \theta] \right) \\
& - \frac{C_1 P}{\gamma} \left[ \varrho \Delta \varrho_\theta + \varrho_\theta \Delta \varrho \right] = 0, \tag{55}
\end{aligned}$$

$$\text{Curl} \left[ \Omega_{\mathbf{D} \mathbf{D}} \Delta \mathbf{D} + \Omega_{\varrho \mathbf{D}} \Delta \varrho + \Omega_{\varrho_\theta \mathbf{D}} \Delta \varrho_\theta + \Omega_{\varrho_\phi \mathbf{D}} \Delta \varrho_\phi + \Omega_{\eta_\theta \mathbf{D}} \Delta \eta_\theta + \Omega_{\eta_\phi \mathbf{D}} \Delta \eta_\phi \right] = \mathbf{0}, \tag{56}$$

with periodic boundary conditions along  $\theta$  and  $\phi$  given by

$$\{\Delta \varrho, \Delta \eta, \Delta \mathbf{D}, \Delta \varrho_\theta, \Delta \varrho_\phi, \Delta \eta_\theta, \Delta \eta_\phi\}|_{\phi=0} = \{\Delta \varrho, \Delta \eta, \Delta \mathbf{D}, \Delta \varrho_\theta, \Delta \varrho_\phi, \Delta \eta_\theta, \Delta \eta_\phi\}|_{\phi=2\pi}, \quad (57)$$

$$\{\Delta \varrho, \Delta \eta, \Delta \mathbf{D}, \Delta \varrho_\theta, \Delta \varrho_\phi, \Delta \eta_\theta, \Delta \eta_\phi\}|_{\theta=0} = \{\Delta \varrho, \Delta \eta, \Delta \mathbf{D}, \Delta \varrho_\theta, \Delta \varrho_\phi, \Delta \eta_\theta, \Delta \eta_\phi\}|_{\theta=2\pi}. \quad (58)$$

Since  $\varrho_\phi$  and  $\eta_\phi$  vanish at the bifurcation point,  $\Omega_{\varrho\varrho\varrho}$ ,  $\Omega_{\varrho\eta\phi}$ ,  $\Omega_{\varrho\theta\varrho\phi}$ ,  $\Omega_{\varrho\theta\eta\phi}$ ,  $\Omega_{\varrho\phi\mathbf{D}}$  and  $\Omega_{\eta\phi\mathbf{D}}$  are also zero as shown in Appendix C (supporting file). Rearranging equations (54) and (55) gives

$$\begin{aligned} & \left[1 + \gamma \cos \theta\right] \left[-\Omega_{\varrho\varrho} + \frac{d\Omega_{\varrho\varrho\theta}}{d\theta}\right] - \gamma \sin \theta \Omega_{\varrho\varrho\theta} + \frac{C_1 P}{\gamma} \eta_\theta \Delta \varrho \\ & + \left[1 + \gamma \cos \theta\right] \left[-\Omega_{\varrho\varrho\theta} + \frac{d\Omega_{\varrho\varrho\theta\theta}}{d\theta}\right] - \gamma \sin \theta \Omega_{\varrho\varrho\theta\theta} \Delta \varrho_\theta \\ & + \left[1 + \gamma \cos \theta\right] \Omega_{\varrho\theta\varrho\theta} \Delta \varrho_{\theta\theta} + \left[1 + \gamma \cos \theta\right] \left[\frac{d\Omega_{\varrho\phi\varrho\phi}}{d\phi}\right] \Delta \varrho_\phi \\ & + \left[1 + \gamma \cos \theta\right] \Omega_{\varrho\phi\varrho\phi} \Delta \varrho_{\phi\phi} + \left[1 + \gamma \cos \theta\right] \left[-\Omega_{\varrho\eta\theta} + \frac{d\Omega_{\varrho\theta\eta\theta}}{d\theta}\right] - \gamma \sin \theta \Omega_{\varrho\theta\eta\theta} + \frac{C_1 P}{\gamma} \varrho \Delta \eta_\theta \\ & + \left[1 + \gamma \cos \theta\right] \Omega_{\varrho\theta\eta\theta} \Delta \eta_{\theta\theta} + \left[1 + \gamma \cos \theta\right] \left[\frac{d\Omega_{\varrho\phi\eta\phi}}{d\phi}\right] \Delta \eta_\phi + \left[1 + \gamma \cos \theta\right] \Omega_{\varrho\phi\eta\phi} \Delta \eta_{\phi\phi} \\ & + \left[1 + \gamma \cos \theta\right] \left[-\Omega_{\varrho\mathbf{D}} + \frac{d\Omega_{\varrho\theta\mathbf{D}}}{d\theta}\right] - \gamma \sin \theta \Omega_{\varrho\theta\mathbf{D}} \cdot \Delta \mathbf{D} + \left[1 + \gamma \cos \theta\right] \Omega_{\varrho\theta\mathbf{D}} \cdot \frac{d\Delta \mathbf{D}}{d\theta} = 0 \end{aligned} \quad (59)$$

$$\begin{aligned} & \left[1 + \gamma \cos \theta\right] \frac{d\Omega_{\varrho\eta\theta}}{d\theta} - \gamma \sin \theta \Omega_{\varrho\eta\theta} - \frac{C_1 P}{\gamma} \varrho_\theta \Delta \varrho \\ & + \left[1 + \gamma \cos \theta\right] \left[\Omega_{\varrho\eta\theta} + \frac{d\Omega_{\varrho\theta\eta\theta}}{d\theta}\right] - \gamma \sin \theta \Omega_{\varrho\theta\eta\theta} - \frac{C_1 P}{\gamma} \varrho \Delta \varrho_\theta \\ & + \left[1 + \gamma \cos \theta\right] \Omega_{\varrho\theta\eta\theta} \Delta \varrho_{\theta\theta} + \left[1 + \gamma \cos \theta\right] \frac{d\Omega_{\varrho\phi\eta\phi}}{d\phi} \Delta \varrho_\phi \\ & + \left[1 + \gamma \cos \theta\right] \Omega_{\varrho\phi\eta\phi} \Delta \varrho_{\phi\phi} + \left[1 + \gamma \cos \theta\right] \frac{d\Omega_{\eta\theta\eta\theta}}{d\theta} - \gamma \sin \theta \Omega_{\eta\theta\eta\theta} \Delta \eta_\theta \\ & + \left[1 + \gamma \cos \theta\right] \Omega_{\eta\theta\eta\theta} \Delta \eta_{\theta\theta} + \left[1 + \gamma \cos \theta\right] \frac{d\Omega_{\eta\phi\eta\phi}}{d\phi} \Delta \eta_\phi \\ & + \left[1 + \gamma \cos \theta\right] \Omega_{\eta\phi\eta\phi} \Delta \eta_{\phi\phi} + \left[1 + \gamma \cos \theta\right] \frac{d\Omega_{\eta\theta\mathbf{D}}}{d\theta} - \gamma \sin \theta \Omega_{\eta\theta\mathbf{D}} \cdot \Delta \mathbf{D} \\ & + \left[1 + \gamma \cos \theta\right] \Omega_{\eta\theta\mathbf{D}} \cdot \frac{d\Delta \mathbf{D}}{d\theta} = 0 \end{aligned} \quad (60)$$

The third governing equation (56) physically means that the curl of the perturbed electrical field is zero, i.e.  $\text{Curl}(\Delta \mathbf{E}) = \mathbf{0}$ . As the electrical field does not change in the normal directions, i.e.  $\frac{d}{d\mathbf{N}}(\Delta \mathbf{E}) = \mathbf{0}$ , (56) reduces to

$$[\Omega_{\mathbf{D}\mathbf{D}} \Delta \mathbf{D} + \Omega_{\varrho\mathbf{D}} \Delta \varrho + \Omega_{\varrho\theta\mathbf{D}} \Delta \varrho_\theta + \Omega_{\varrho\phi\mathbf{D}} \Delta \varrho_\phi + \Omega_{\eta\theta\mathbf{D}} \Delta \eta_\theta + \Omega_{\eta\phi\mathbf{D}} \Delta \eta_\phi] \cdot \mathbf{N} = 0. \quad (61)$$

To study prismatic-type bifurcation of the solution along the  $\phi$  coordinate, we consider the following perturbations of the fields superimposed upon the principal solution

$$\Delta \varrho = \mathcal{F} \exp(im\phi), \quad \Delta \eta = \mathcal{G} \exp(im\phi), \quad \Delta \mathbb{D} = \frac{\Phi_0}{\beta H} \mathcal{H} \exp(im\phi) \mathbf{N}, \quad m \in \mathbb{Z}^+. \quad (62)$$

Here we have assumed  $\mathcal{F}, \mathcal{G}$  and  $\mathcal{H}$  are constants and, invoking the thin-membrane assumption, we restrict the solution  $\Delta \mathbb{D}$  to along the thickness direction  $\mathbf{N}$ . Upon substitution of (62), the equations (59), (60) and (61) can be expressed in terms of three unknown variables  $\mathcal{F}, \mathcal{G}$  and  $\mathcal{H}$  as

$$\underbrace{\left[ [1 + \gamma \cos \theta] \left[ -\Omega_{\varrho\varrho} + \frac{d\Omega_{\varrho\varrho}}{d\theta} \right] - \gamma \sin \theta \Omega_{\varrho\varrho\theta} + \frac{C_1 P}{\gamma} \eta_\theta - m^2 [1 + \gamma \cos \theta] \Omega_{\varrho\phi\varrho\phi} \right]}_{M_{11}} \mathcal{F} \quad (63)$$

$$\underbrace{-m^2 [1 + \gamma \cos \theta] \Omega_{\varrho\phi\eta\phi}}_{M_{12}} \mathcal{G} + \underbrace{\frac{\Phi_0}{\beta H} \left[ [1 + \gamma \cos \theta] \left[ -\Omega_{\varrho\mathbb{D}} + \frac{d\Omega_{\varrho\mathbb{D}}}{d\theta} \right] - \gamma \sin \theta \Omega_{\varrho\theta\mathbb{D}} \right] \cdot \mathbf{N}}_{M_{13}} \mathcal{H} = 0, \quad (64)$$

$$\underbrace{\left[ [1 + \gamma \cos \theta] \frac{d\Omega_{\varrho\eta\theta}}{d\theta} - \gamma \sin \theta \Omega_{\varrho\eta\theta} - \frac{C_1 P}{\gamma} \varrho_\theta - m^2 [1 + \gamma \cos \theta] \Omega_{\varrho\phi\eta\phi} \right]}_{M_{21}} \mathcal{F}$$

$$\underbrace{-m^2 [1 + \gamma \cos \theta] \Omega_{\eta\phi\eta\phi}}_{M_{22}} \mathcal{G} + \underbrace{\frac{\Phi_0}{\beta H} \left[ [1 + \gamma \cos \theta] \frac{d\Omega_{\eta\theta\mathbb{D}}}{d\theta} - \gamma \sin \theta \Omega_{\eta\theta\mathbb{D}} \right] \cdot \mathbf{N}}_{M_{23}} \mathcal{H} = 0, \quad (65)$$

$$\underbrace{\Omega_{\varrho\mathbb{D}} \cdot \mathbf{N}}_{M_{31}} \mathcal{F} + \underbrace{\left[ \frac{\Phi_0}{\beta H} \Omega_{\mathbb{D}\mathbb{D}} \right]}_{M_{33}} \mathcal{H} = 0. \quad (66)$$

Finally the governing system of equations (64), (65) and (66) can be expressed in a matrix form as

$$\underbrace{\begin{bmatrix} M_{11} & M_{12} & M_{13} \\ M_{21} & M_{22} & M_{23} \\ M_{31} & 0 & M_{33} \end{bmatrix}}_{\mathbf{M}} \begin{bmatrix} \mathcal{F} \\ \mathcal{G} \\ \mathcal{H} \end{bmatrix} = \begin{bmatrix} 0 \\ 0 \\ 0 \end{bmatrix}. \quad (67)$$

259 If  $\det(\mathbf{M}) = 0$ , the system of equations has a solution, which means the toroidal membrane could lose  
 260 stability due to a bifurcation in the  $\phi$  direction.

## 261 6. Numerical examples

262 Section 6.1 presents numerical results obtained by solving the governing equations (31a) and (31b)  
 263 with associated boundary conditions (32). These results are only valid before the torus loses stability.

264 Recall that as the membrane inflates, there are three kinds of possible instabilities considered here. They  
 265 are snap-through, wrinkling, and bifurcation in the  $\phi$  direction. If wrinkling happens first, the energy  
 266 relaxation method is adopted and the governing equation are modified as described in Section 4.2. The  
 267 new solutions obtained with the energy relaxation method are computed in Section 6.2 and compared  
 268 with the principle solutions. If the bifurcation happens first, the toroidal membrane loses its symmetry  
 269 along the  $\phi$  direction at the critical point as demonstrated in Section 6.3. The principle solution becomes  
 270 unstable after the bifurcation point.

### 271 6.1. Principal solution and limit point instability

272 We first consider the behaviour of an inflating electro-elastic toroidal membrane under different  
 273 electrical loads. Figure 4 shows the plots of pressure against volume change for a toroidal membrane  
 274 with aspect ratio  $\gamma = 0.6$ , material coefficient  $\alpha = 0.2$  and an electrical load  $\mathcal{E}$  increasing from 0 to  
 275 0.3. The profiles of these plots are similar. The solution without electrical load is verified using the  
 276 results in [59]. At small deformation, the membrane has a large stiffness against inflation. Thus the  
 277 ratio of pressure to volume change is large at the beginning. The ratio stays the same under different  
 278 electrical loads. As the electrical load increases the limit point also occurs at a similar volume change,  
 279 but the limit point pressure is significantly decreased. After the limit point for different electrical loads,  
 280 the pressures all decrease with increasing volume. After a finite volume change, the membrane regains  
 281 stiffness and the pressures start to increase as the volume increases. The same trend can be seen in  
 282 Figures 8 and 9 for a toroidal membrane with  $\gamma = 0.4$  and  $\alpha = 0.1, 0.2$  and 0.3.

283 Figure 5 compares and visualises the inflation of purely elastic membranes and electroelastic mem-  
 284 branes with  $\mathcal{E} = 0.3$ . The principle solutions are solved for increasing  $\rho$  at  $\theta = 0$  and the deformed  
 285 profiles for both cases are coloured by the pressure  $P$ . The electroelastic membrane can achieve the  
 286 same volume change as the elastic membrane under considerably less pressure. We also note the  
 287 significant difference in inflation profiles of stout ( $\gamma = 0.4$ ) and slender ( $\gamma = 0.1$ ) tori. For large  $\gamma$   
 288 values shown in Figure 5a, the inflation (prescribed by position of outer end  $\rho$  at  $\theta = 0$ ) causes the  
 289 inner end ( $\theta = \pi$ ) to move slightly inwards. However, for small  $\gamma$  values the inner end ( $\theta = \pi$ ) first  
 290 moves outward and then inwards as shown in Figure 5b. The level of inward movement is significantly  
 291 accentuated in the presence of the electric field. This dependence of  $\rho(\pi)$  and  $\rho(0)$  on the aspect ratio  
 292 and material properties is of significance while designing actuator mechanisms from EAPs as detailed  
 293 in [77].

294 In an experimental setting, inflation of the membrane can be accomplished using either a pressure  
 295 controlled or a volume controlled process. During the inflation of the membrane, one can control

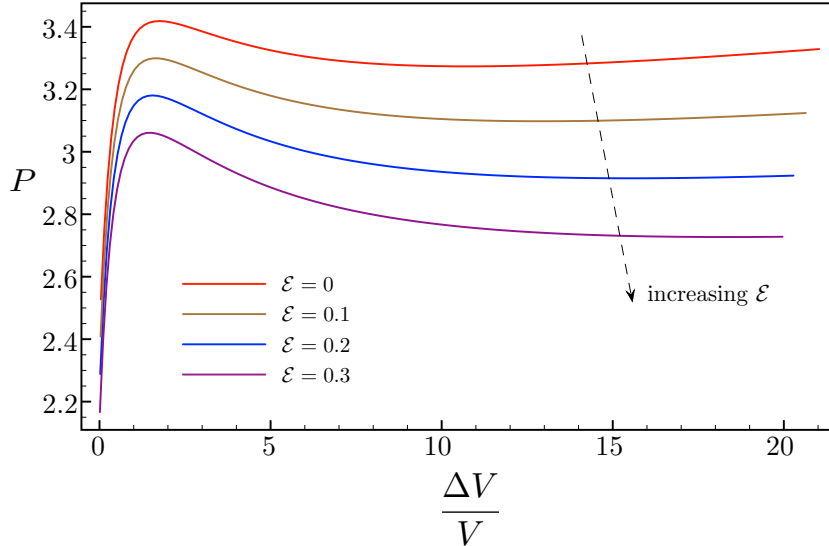


Figure 4: Plot of pressure against volume change for a toroidal membrane with geometry parameter  $\gamma = 0.6$  and material parameter  $\alpha = 0.2$  for different electrical loads  $\mathcal{E}$ .

the pressure inside the membrane. When the pressure reach the limit point in a pressure controlled experiment, there will be a sudden volume change of the membrane. This is known as a snap-through buckling of the hyperelastic membrane as described in Figures 3 and 5a. We also note that it would be possible for snap-through to occur prior to reaching the limit point if there are imperfections. The post bifurcation state can be analysed using a range of techniques including the Maxwell criterion [72, 71].

Figure 5b shows the inflation process for a toroidal membrane with a smaller aspect ratio,  $\gamma = 0.1$  and  $\alpha = 0.2$ . The pressure to reach the limit point is much higher than a toroidal membrane with  $\gamma = 0.4$ . For such tori, the snap-through path is significantly longer and cannot be shown in Figure 5b.

The snap-through phenomenon can be eliminated if the torus is inflated in a volume-controlled experiment. Our calculations show that the snap-through phenomenon can also be eliminated in a mass-controlled experiment (assuming ideal gas law under constant temperature, mass is proportional to  $PV$ ) since mass and volume increase monotonically for an electroelastic torus.

## 6.2. Computation of wrinkling instability

Wrinkling occurs during inflation when the in-plane stress in any direction becomes zero. The two in-plane principal stress components are calculated using the principal solutions obtained from (41). For the toroidal membrane, wrinkling first occurs at the inner region where  $\theta \approx \pi$ . Figures 6a and 6b are two examples of membranes with negative stresses calculated from the principal solutions. Figure 6a shows a half cross section of the membrane with aspect ratio  $\gamma = 0.4$ , material parameter  $\alpha = 0.3$ , and the electrical load  $\mathcal{E} = 0.1$ . Wrinkles start to form when  $\varrho \approx 5.16$  at  $\theta = 0$ . When  $\varrho \approx 5.68$  at  $\theta = 0$ ,



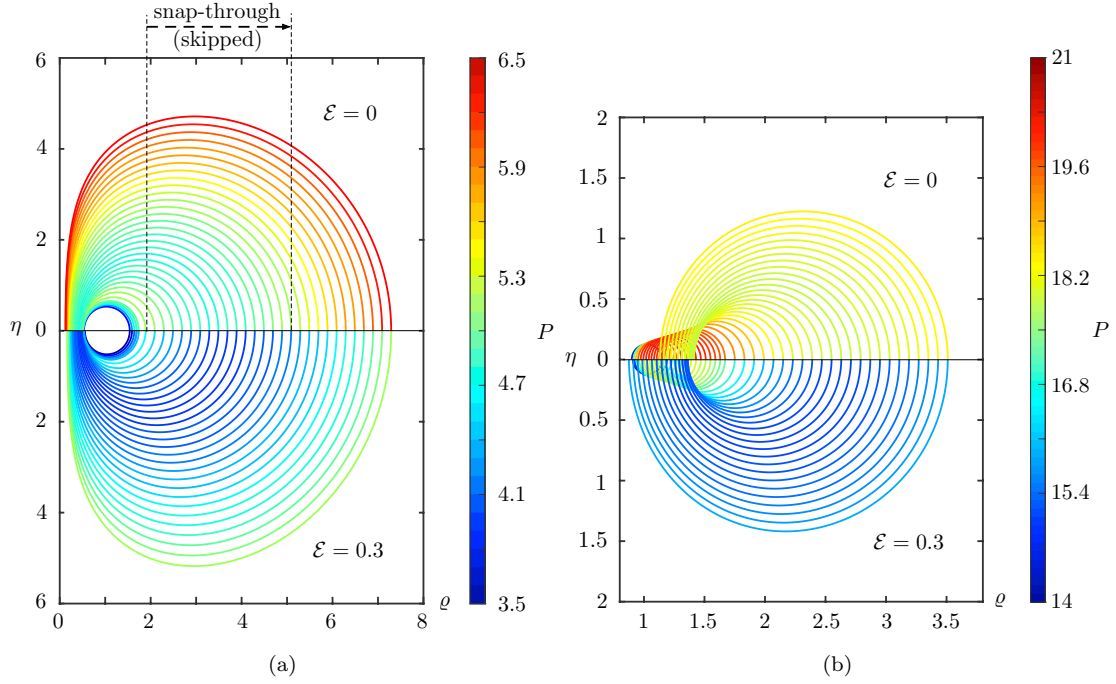


Figure 5: Cross-section profiles during inflation for toroidal membrane with (a)  $\gamma = 0.4$  and (b)  $\gamma = 0.1$ . The material parameter  $\alpha = 0.2$  for both cases. The upper halves represent the deformation under pure elastic loads. The lower halves represent the deformation with an electrical load  $\mathcal{E} = 0.3$ .

315 the wrinkling region is between  $\theta = (29/30)\pi$  to  $\pi$ . Keeping the material parameter and electrical load  
 316 the same, a torus with large aspect ratio  $\gamma = 0.6$  starts to wrinkles when  $\rho \approx 2.78$  at  $\theta = 0$ . When  
 317  $\rho \approx 3.38$ , the wrinkling region is between  $\theta = (29/30)\pi$  to  $\pi$ .

318 The relaxed form of the energy density (46) is adopted when negative stresses are detected. The  
 319 modified ODE system (50) is used for computing the profile of the wrinkled membrane. Figures 7a  
 320 and 7b compare the membrane profiles of the principal solution with the solution obtained using the re-  
 321 laxed energy density function for tori with two different aspect ratios ( $\gamma = 0.4$  and  $\gamma = 0.6$ ). Figures 8a  
 322 and 8b compare the plots of the pressure against the volume change with different electrical loads. Two  
 323 toroidal membranes with same aspect ratio  $\gamma = 0.4$  but different material parameters,  $\alpha = 0.2$  and  
 324  $0.3$ , are investigated. The red dots indicate the first appearance of wrinkling during inflation. The  
 325 loading curve post the occurrence of wrinkling is dashed to demonstrate the unstable region. As the  
 326 electrical loads increase, the wrinkles occur even at low values of pressure and inflation. However, we  
 327 note that the volume change for the first appearance of wrinkling does not decrease monotonically with  
 328 increasing  $\mathcal{E}$ . Significant variable changes in the onset points of wrinkling are observed in both cases  
 329 when  $\mathcal{E} < 0.1$ .

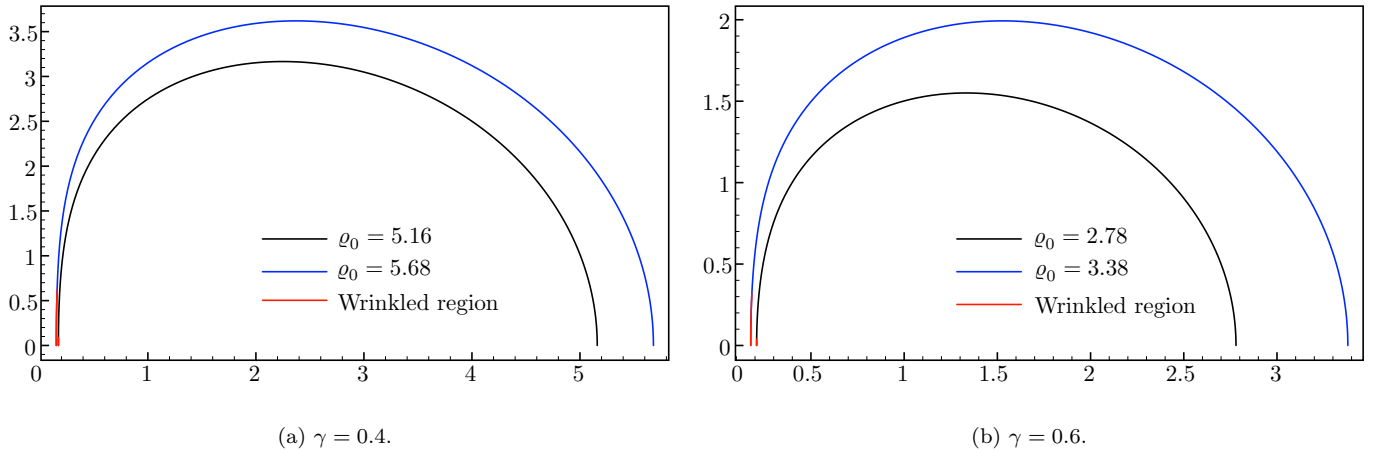
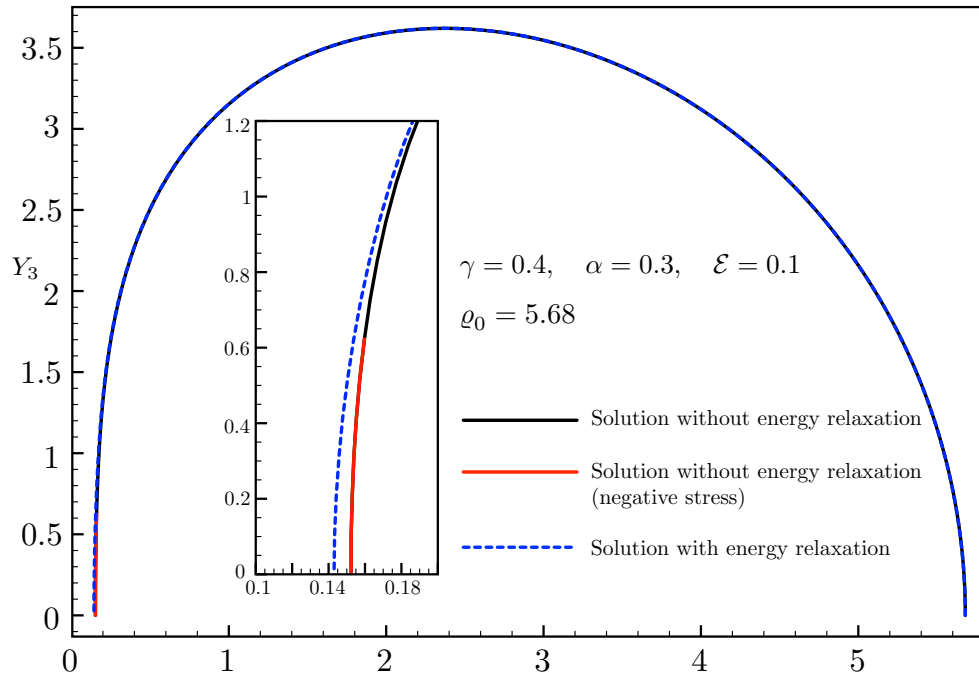


Figure 6: Membrane profiles showing wrinkling regions. The black profile shows the wrinkling starting to form and the blue profile indicate the wrinkling region is  $\theta = (29/30)\pi$  to  $\pi$ . Both cases have the same material property  $\alpha = 0.3$ , Electrical load is  $\mathcal{E} = 0.1$ . A toroidal membrane with larger aspect ratio wrinkles with less inflation.

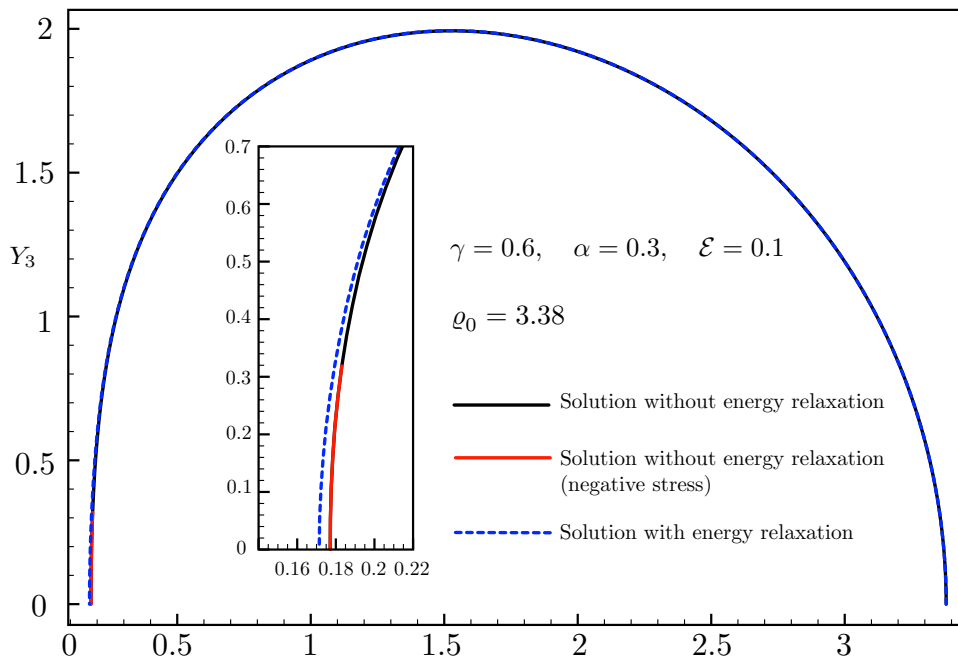
### 330 6.3. Loss of symmetry

331 The loss of symmetry along the  $\phi$  direction during inflation is examined. This bifurcation occurs  
 332 when the second variation of the energy density function is zero as computed by checking the determi-  
 333 nant of matrix  $\mathbf{M}$  in Equation (67). Three toroidal membranes with the same aspect ratio  $\gamma = 0.4$  but  
 334 different material parameter  $\alpha = 0.1, 0.2$  and  $0.3$  are compared. Figure 9a shows the plot of pressure  
 335 against volume change for increasing electrical load  $\mathcal{E} = 0, 0.1, 0.2$  and  $0.3$  and the material parameter  
 336  $\alpha = 0.1$ . The bifurcation occurs close to the limit points which is similar to the neo-Hookean material  
 337 investigated in [77]. Figures 9b and 9c show the same plots for membranes with  $\alpha = 0.2$  and  $0.3$ .  
 338 In this case bifurcation occurs at the strain hardening stage. All the bifurcation points are found at  
 339 buckling mode  $m = 1$ . However, the electrical load significantly influences the onset of bifurcation.  
 340 When the electrical load remain small, it delays the appearance of bifurcation. After the electrical load  
 341 exceeds a certain value, bifurcation happens with a smaller volume change. For very large electrical  
 342 loads, bifurcation occurs close to the limit point as shown for  $\mathcal{E} = 0.4$  in Figure 9b.

343 Finally, we investigate the combined effect of both wrinkling and loss of symmetry. We compare the  
 344 response of membranes with same geometry ( $\gamma = 0.4$ ) and different material parameter ( $\alpha = 0.2, 0.3$ ) in  
 345 Figures 10a and 10b, and membranes with same material parameter ( $\alpha = 0.3$ ) and different geometry  
 346 ( $\gamma = 0.4, 0.5$ ) in Figures 10b and 10c. Wrinkling is the dominant instability mode for membranes with a  
 347 large aspect ratio  $\gamma = 0.5$  irrespective as to the electrical load. For membranes with a lower aspect ratio  
 348  $\gamma = 0.4$ , the combined effect of the material parameter  $\alpha$  and the electrical load  $\mathcal{E}$  dictates the instability  
 349 mode. Typically loss of symmetry occurs before wrinkling for very small and very large electrical loads,



(a)



(b)

Figure 7: Comparison of the membrane profiles computed using the principal solution and the relaxed energy solution.

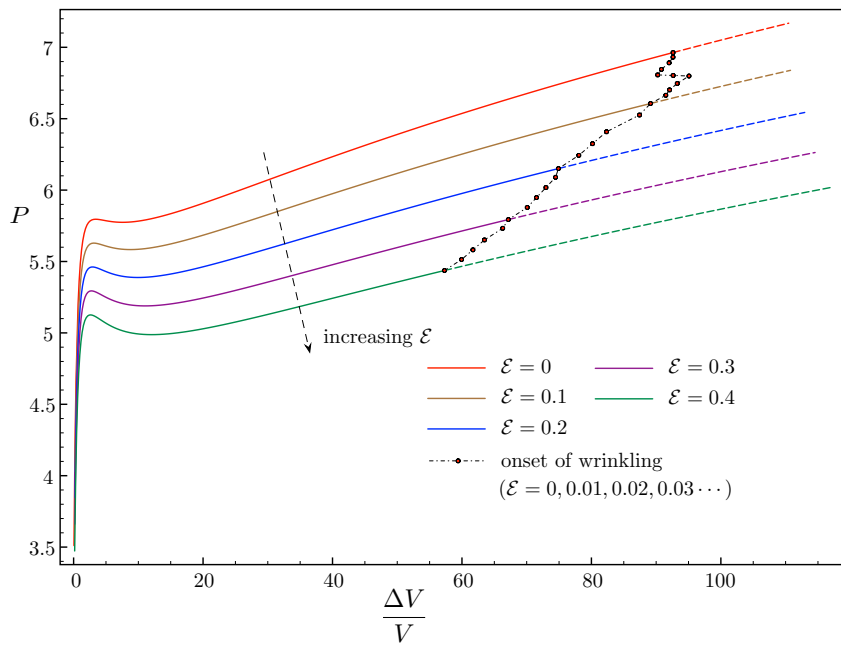
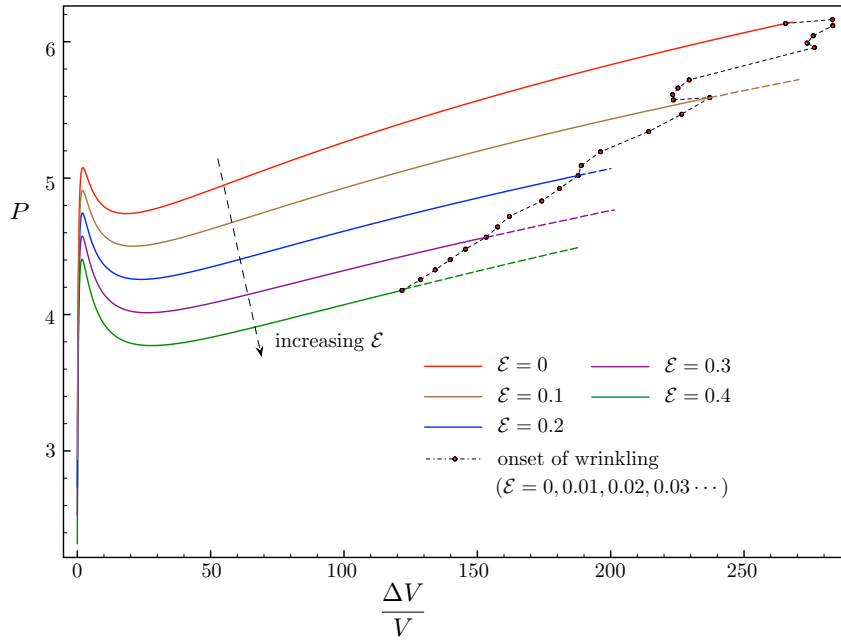
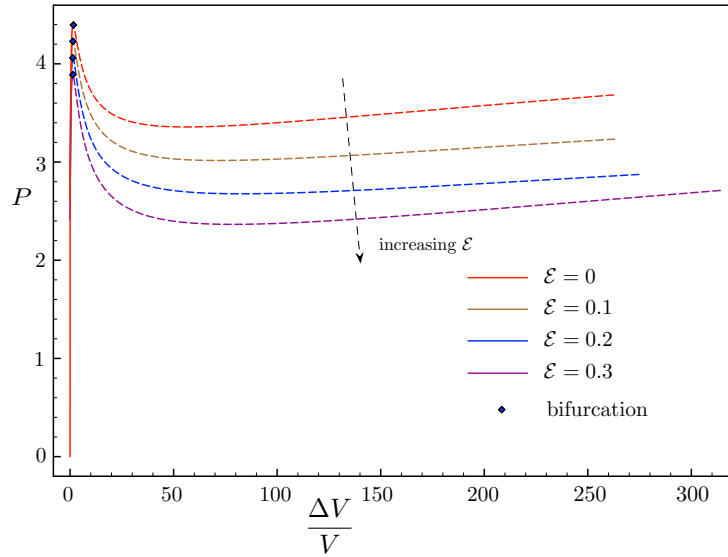
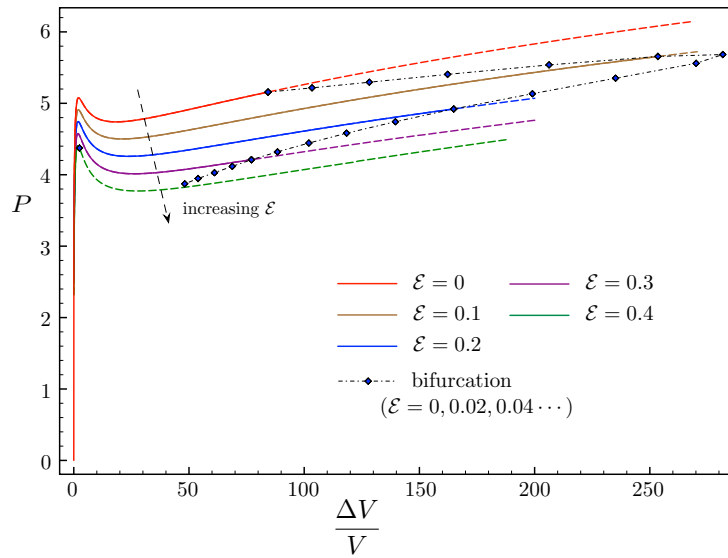


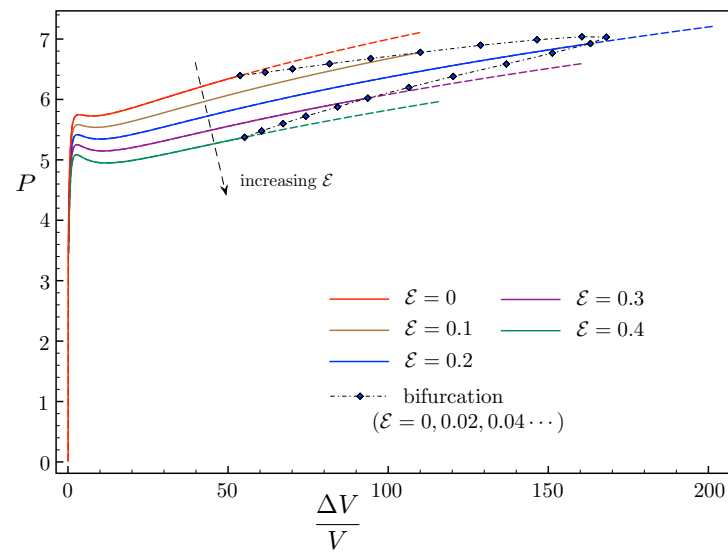
Figure 8: Plots of the pressure against the volume change with different electrical loads. Red dots indicate where the first wrinkles occur. The dashed portions of the loading curves denote the unstable region post-wrinkling.



(a)  $\gamma = 0.4, \alpha = 0.1$



(b)  $\gamma = 0.4, \alpha = 0.2$



(c)  $\gamma = 0.4, \alpha = 0.3$

Figure 9: Plots of the pressure against the volume change with different electrical loads. Blue diamonds indicate the onset of bifurcation that causes loss of symmetry. The dashed portions of the loading curves denote the unstable region after loss of symmetry

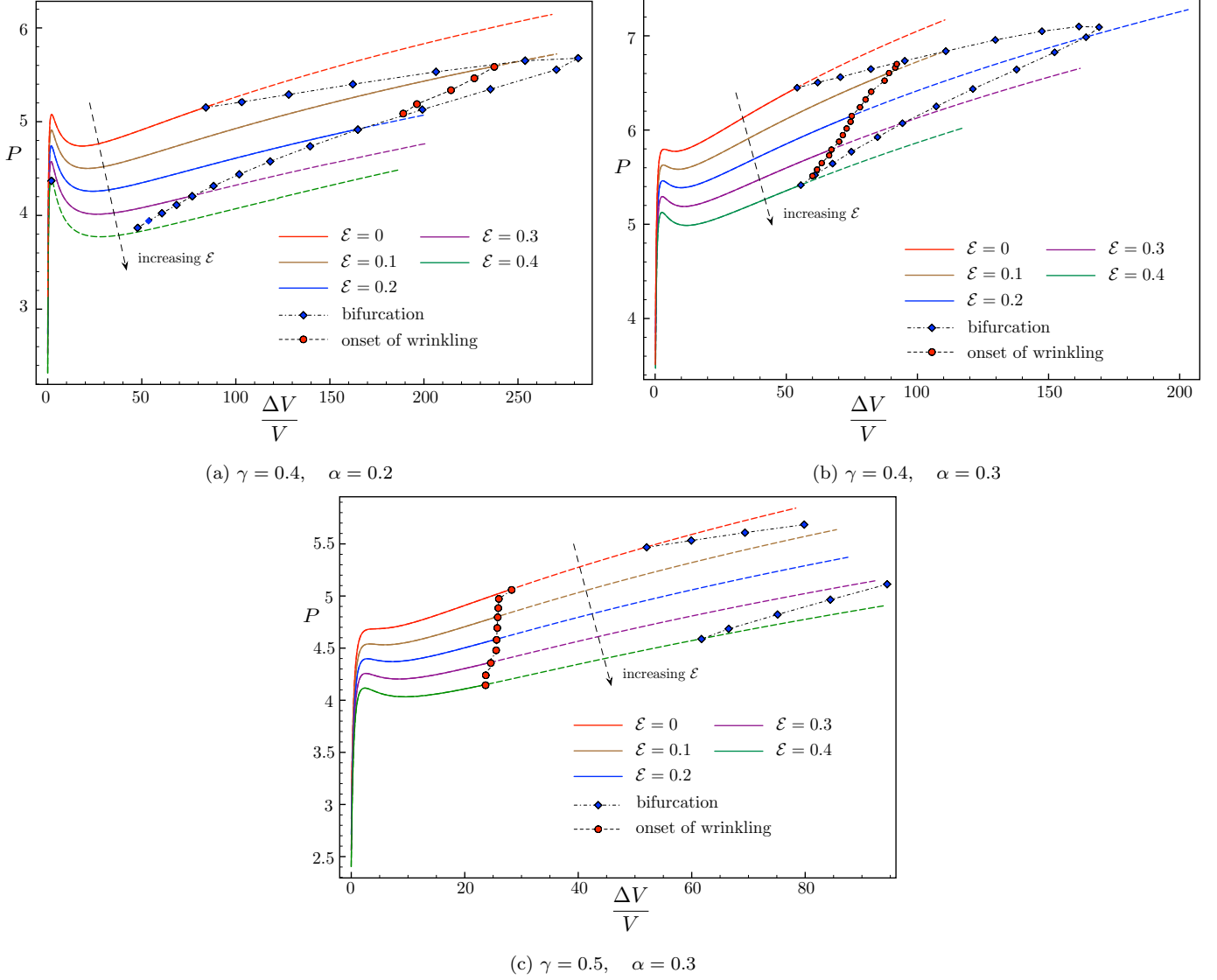


Figure 10: Plots of the pressure against the volume change with different electrical loads. Red dots indicate where the first wrinkle occurs. Blue diamonds indicate where the bifurcation points. As the electric load increases, the bifurcation occurs at a larger volume change. However, after a certain value of  $\mathcal{E}$ , the bifurcation occurs earlier.

350 and wrinkling is preferred for moderate  $\mathcal{E}$  values. A larger value of the material parameter  $\alpha$  can  
 351 increase the zone in which wrinkling is preferred.

352 This interesting interaction between the various modes of instabilities can be used as an actuation  
 353 mechanism. For example, consider the idealised phase-space diagram depicted in Figure 11 based on  
 354 the response in Figure 10. An initial loading can be performed in the presence of electric field along  
 355 the path  $A \rightarrow B \rightarrow C$ . Moving from B to C induces wrinkles in the torus. Upon reducing the intensity of  
 356 the electric load while keeping the volume constant, one can remove wrinkles by moving to the state D.  
 357 Upon further reducing the electric load while keeping the volume constant, one can move to the state  
 358 E where the torus is no longer symmetric.

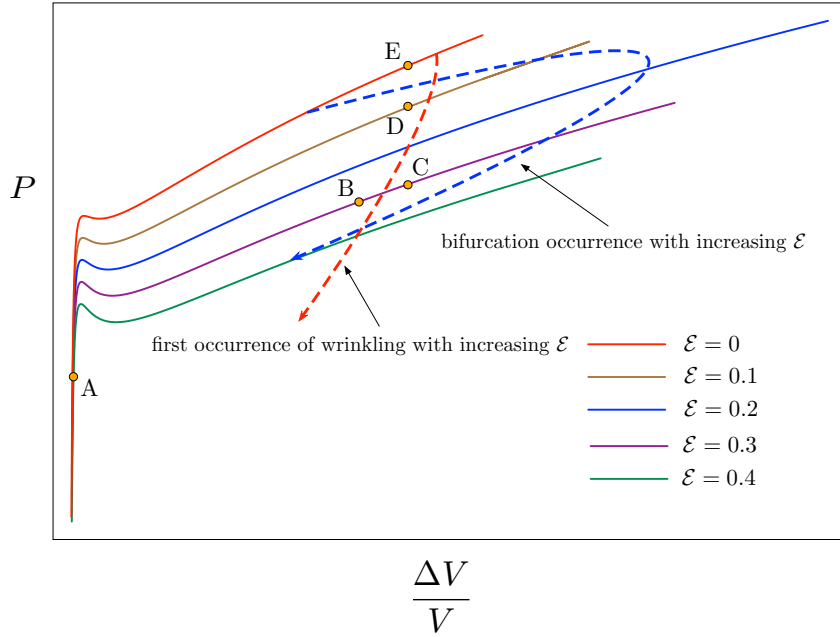


Figure 11: Instability interaction diagram. One can induce (or eliminate) wrinkles and loss of symmetry in a reversible manner by controlling the applied electric load  $\mathcal{E}$  and the volume of fluid in the membrane; for example by traversing the path  $A \rightarrow B \rightarrow C \rightarrow D \rightarrow E$ .

## 359 7. Conclusions

360 A study of the mechanics of inflation of a toroidal membrane under large coupled electromechanical  
 361 loading has been presented. A numerical scheme has been developed to solve the highly nonlinear  
 362 coupled ODEs to capture the rapidly changing solution for small inflation values together with the aid  
 363 of an arc-length method. The classical limit point instability for inflated membranes is recovered and  
 364 the limit point pressure can be significantly reduced upon the application of a potential difference across  
 365 the thickness of the torus. Wrinkling instability has been modelled using an extension of the tension  
 366 field theory to electroelasticity by employing a relaxed energy approach. The torus loses its rotational  
 367 symmetry at large values of inflation and this instability has been computed using a second variation  
 368 based analysis. This critical bifurcation point varies nonlinearly with the electrical load - it is delayed  
 369 for moderate electric loads and is then favoured for large electric loads.

370 This interaction between the various instability modes can be exploited for the development of  
 371 actuation mechanisms. One such example has been demonstrated in Figure 11. The phase space of this  
 372 problem can be traversed by controlling the electric load and either one of the pressure or the volume  
 373 thereby providing a great deal of flexibility in engineering design. Such features will be exploited in  
 374 future works.

375 **Acknowledgements**

376 This work was supported by the UK Engineering and Physical Sciences Research Council grant  
377 EP/R008531/1 for the Glasgow Computational Engineering Centre.

378 Basant Lal Sharma acknowledges the partial support of MATRICS grant number MTR/2017/000013  
379 from the Science and Engineering Research Board.

380 Paul Steinmann also gratefully acknowledges financial support for this work by the Deutsche Forschungs-  
381 gemeinschaft under GRK2495/B.



## 382 References

- 383 [1] Adams, W., Sridar, S., Thalman, C.M., Copenhaver, B., Elsaad, H., Polygerinos, P., 2018. Water  
384 pipe robot utilizing soft inflatable actuators, in: 2018 IEEE International Conference on Soft  
385 Robotics (RoboSoft), IEEE. pp. 321–6.
- 386 [2] Ahmad, D., Patra, K., Hossain, M., 2020. Experimental study and phenomenological modelling  
387 of flaw sensitivity of two polymers used as dielectric elastomers. *Continuum Mechanics and Ther-*  
388 *modynamics* 32, 489–500.
- 389 [3] Araromi, O.A., Gavrilovich, I., Shintake, J., Rosset, S., Richard, M., Gass, V., Shea, H.R., 2014.  
390 Rollable multisegment dielectric elastomer minimum energy structures for a deployable microsattel-  
391 lite gripper. *IEEE/ASME Transactions on mechatronics* 20, 438–46.
- 392 [4] Ask, A., Menzel, A., Ristinmaa, M., 2012. Electrostriction in electro-viscoelastic polymers. *Me-*  
393 *chanics of Materials* 50, 9–21.
- 394 [5] Bar-Cohen, Y., et al., 2001. Electroactive polymer actuators as artificial muscles. SPIE, Washing-  
395 ton .
- 396 [6] Barsotti, R., 2015. Approximated Solutions for Axisymmetric Wrinkled Inflated Membranes. *Jour-*  
397 *nal of Applied Mechanics* 82.
- 398 [7] Benedict, R., Wineman, A., Yang, W.H., 1979. The determination of limiting pressure in simul-  
399 taneous elongation and inflation of nonlinear elastic tubes. *International Journal of Solids and*  
400 *Structures* 15, 241–9.
- 401 [8] Budiansky, B., 1974. Theory of buckling and post-buckling behavior of elastic structures, in:  
402 *Advances in applied mechanics*. Elsevier. volume 14, pp. 1–65.
- 403 [9] Bustamante, R., Dorfmann, A., Ogden, R.W., 2009. Nonlinear electroelastostatics: a variational  
404 framework. *Zeitschrift für angewandte Mathematik und Physik* 60, 154–77.
- 405 [10] Carroll, M., 1987. Pressure maximum behavior in inflation of incompressible elastic hollow spheres  
406 and cylinders. *Quarterly of applied mathematics* 45, 141–54.
- 407 [11] Chaudhuri, A., Dasgupta, A., 2014. On the static and dynamic analysis of inflated hyperelastic  
408 circular membranes. *Journal of the Mechanics and Physics of Solids* 64, 302–15.

- 409 [12] Crandall, S.H., Dahl, N.C., Lardner, T.J., 1972. An Introduction to the Mechanics of Solids.  
410 McGraw-Hill.
- 411 [13] De Melo, F.J., Pereira, A.B., Morais, A.B., 2018. The simulation of an automotive air spring  
412 suspension using a pseudo-dynamic procedure. *Applied Sciences* 8, 1049.
- 413 [14] De Tommasi, D., Puglisi, G., Saccomandi, G., Zurlo, G., 2010. Pull-in and wrinkling instabilities  
414 of electroactive dielectric actuators. *Journal of Physics D: Applied Physics* 43, 325501.
- 415 [15] De Tommasi, D., Puglisi, G., Zurlo, G., 2011. Compression-induced failure of electroactive poly-  
416 meric thin films. *Applied Physics Letters* 98.
- 417 [16] D’Errico, J., 2020. `fminsearchbnd`, `fminsearchcon`. URL: [https://www.mathworks.com/  
418 matlabcentral/fileexchange/8277-fminsearchbnd-fminsearchcon](https://www.mathworks.com/matlabcentral/fileexchange/8277-fminsearchbnd-fminsearchcon).
- 419 [17] Di Biasio, A., Ambrosone, L., Cametti, C., 2014. Dielectric response of shelled toroidal parti-  
420 cles carrying localized surface charge distributions. the effect of concentric and confocal shells.  
421 *Bioelectrochemistry* 98, 76–86.
- 422 [18] Dorfmann, A., Ogden, R., 2005. Nonlinear electroelasticity. *Acta Mechanica* 174, 167–83.
- 423 [19] Dorfmann, A., Ogden, R., 2006. Nonlinear electroelastic deformations. *Journal of Elasticity* 82,  
424 99–127.
- 425 [20] Dorfmann, L., Ogden, R.W., 2014a. Instabilities of an electroelastic plate. *International Journal*  
426 *of Engineering Science* 77, 79–101.
- 427 [21] Dorfmann, L., Ogden, R.W., 2014b. Nonlinear response of an electroelastic spherical shell. *Inter-*  
428 *national Journal of Engineering Science* 85, 163–74.
- 429 [22] Dorfmann, L., Ogden, R.W., 2014c. Nonlinear theory of electroelastic and magnetoelastic interac-  
430 tions. Springer.
- 431 [23] Dorfmann, L., Ogden, R.W., 2017. Nonlinear electroelasticity: material properties, continuum the-  
432 ory and applications. *Proceedings of the Royal Society A: Mathematical, Physical and Engineering*  
433 *Sciences* 473, 20170311.
- 434 [24] Dorfmann, L., Ogden, R.W., 2019. Instabilities of soft dielectrics. *Philosophical Transactions of*  
435 *the Royal Society A* 377, 20180077.

- 436 [25] Eringen, A.C., 1963. On the foundations of electroelastostatics. *International Journal of Engineer-*  
437 *ing Science* 1, 127–53.
- 438 [26] Greaney, P., Meere, M., Zurlo, G., 2019. The out-of-plane behaviour of dielectric membranes:  
439 Description of wrinkling and pull-in instabilities. *Journal of the Mechanics and Physics of Solids*  
440 122, 84–97.
- 441 [27] Hingorani, M.M., O’Donnell, M., 1998. Toroidal proteins: running rings around dna. *Current*  
442 *Biology* 8, R83–6.
- 443 [28] Hossain, M., Vu, D.K., Steinmann, P., 2014. A comprehensive characterization of the electro-  
444 mechanically coupled properties of VHB 4910 polymer. *Archive of Applied Mechanics* 85, 523–37.
- 445 [29] Khayat, R.E., Derdorri, A., García-Rejón, A., 1992. Inflation of an elastic cylindrical membrane:  
446 non-linear deformation and instability. *International journal of solids and structures* 29, 69–87.
- 447 [30] Kofod, G., Paajanen, M., Bauer, S., 2006. Self-organized minimum-energy structures for dielectric  
448 elastomer actuators. *Applied Physics A* 85, 141–3.
- 449 [31] Kofod, G., Wirges, W., Paajanen, M., Bauer, S., 2007. Energy minimization for self-organized  
450 structure formation and actuation. *Applied Physics Letters* 90, 081916.
- 451 [32] Koiter, W.T., 1970. The stability of elastic equilibrium. Technical Report. Stanford Univ Ca Dept  
452 of Aeronautics and Astronautics.
- 453 [33] Kollosche, M., Zhu, J., Suo, Z., Kofod, G., 2012. Complex interplay of nonlinear processes in  
454 dielectric elastomers. *Physical Review E* 85, 051801.
- 455 [34] Lau, G.K., Heng, K.R., Ahmed, A.S., Shrestha, M., 2017. Dielectric elastomer fingers for versatile  
456 grasping and nimble pinching. *Applied Physics Letters* 110, 182906.
- 457 [35] Leo-Macias, A., Katz, G., Wei, H., Alimova, A., Katz, A., Rice, W.J., Diaz-Avalos, R., Hu, G.B.,  
458 Stokes, D.L., Gottlieb, P., 2011. Toroidal surface complexes of bacteriophage  $\phi$ 12 are responsible  
459 for host-cell attachment. *Virology* 414, 103–9.
- 460 [36] Li, T., Keplinger, C., Baumgartner, R., Bauer, S., Yang, W., Suo, Z., 2013. Giant voltage-induced  
461 deformation in dielectric elastomers near the verge of snap-through instability. *Journal of the*  
462 *Mechanics and Physics of Solids* 61, 611–28.

- 463 [37] Li, X., Steigmann, D.J., 1995a. Finite deformation of a pressurized toroidal membrane. Interna-  
464 tional Journal of Non-Linear Mechanics 30, 583–95.
- 465 [38] Li, X., Steigmann, D.J., 1995b. Point loads on a hemispherical elastic membrane. International  
466 Journal of Non-Linear Mechanics 30, 569–81.
- 467 [39] Liu, L., 2013. On energy formulations of electrostatics for continuum media. Journal of the  
468 Mechanics and Physics of Solids 61, 968–90.
- 469 [40] Liu, Z., 2020. Electroelastic torodial membrane. URL: [https://doi.org/10.5281/zenodo.](https://doi.org/10.5281/zenodo.3768563)  
470 [3768563](https://doi.org/10.5281/zenodo.3768563).
- 471 [41] Lu, T., Ma, C., Wang, T., 2020. Mechanics of dielectric elastomer structures: A review. Extreme  
472 Mechanics Letters , 100752.
- 473 [42] Mao, G., Wu, L., Fu, Y., Liu, J., Qu, S., 2018. Voltage-controlled radial wrinkles of a trumpet-like  
474 dielectric elastomer structure. AIP Advances 8.
- 475 [43] MATLAB, 2018. version 9.5.0 (R2018b). The MathWorks Inc., Natick, Massachusetts.
- 476 [44] McMeeking, R.M., Landis, C.M., 2005. Electrostatic forces and stored energy for deformable  
477 dielectric materials. Journal of Applied Mechanics 72, 581–90.
- 478 [45] Mehnert, M., Hossain, M., Steinmann, P., 2019. Experimental and numerical investigations of the  
479 electro-viscoelastic behavior of vhb 4905tm. European Journal of Mechanics - A/Solids 77, 103797.
- 480 [46] Melnikov, A., Ogden, R.W., 2018. Bifurcation of finitely deformed thick-walled electroelastic  
481 cylindrical tubes subject to a radial electric field. Zeitschrift fur Angewandte Mathematik und  
482 Physik 69, 1–27.
- 483 [47] Michel, S., Bormann, A., Jordi, C., Fink, E., 2008. Feasibility studies for a bionic propulsion  
484 system of a blimp based on dielectric elastomers. Proceedings of SPIE - EAPAD 4332, 1–15.
- 485 [48] Miehe, C., Vallicotti, D., Zäh, D., 2015. Computational structural and material stability analysis in  
486 finite electro-elasto-statics of electro-active materials. International Journal for Numerical Methods  
487 in Engineering 102, 1605–37.
- 488 [49] Mooney, M., 1940. A theory of large elastic deformation. Journal of applied physics 11, 582–92.

- 489 [50] Moretti, G., Papini, G.P.R., Daniele, L., Forehand, D., Ingram, D., Vertechy, R., Fontana, M.,  
490 2019. Modelling and field testing of a wave energy converter based on dielectric elastomer gener-  
491 ators. *Proceedings of the Royal Society A: Mathematical, Physical and Engineering Sciences* 475,  
492 20180566.
- 493 [51] Morrison, D.D., Riley, J.D., Zancanaro, J.F., 1962. Multiple shooting method for two-point bound-  
494 ary value problems. *Communications of the ACM* 5, 613–4.
- 495 [52] Müller, I., Struchtrup, H., 2002. Inflating a rubber balloon. *Mathematics and Mechanics of Solids*  
496 7, 569–77.
- 497 [53] Nayyar, V., Ravi-Chandar, K., Huang, R., 2011. Stretch-induced stress patterns and wrinkles in  
498 hyperelastic thin sheets. *International journal of solids and structures* 48, 3471–83.
- 499 [54] O’Halloran, A., O’Malley, F., McHugh, P., 2008. A review on dielectric elastomer actuators,  
500 technology, applications, and challenges. *Journal of Applied Physics* 104, 71101–10.
- 501 [55] Ozsecen, M.Y., Sivak, M., Mavroidis, C., 2010. Haptic interfaces using dielectric electroactive  
502 polymers, in: Tomizuka, M., Yun, C.B., Giurgiutiu, V., Lynch, J.P. (Eds.), *Proceedings of SPIE -*  
503 *Sensors and Smart Structures Technologies for Civil, Mechanical, and Aerospace Systems*, p. 7647.
- 504 [56] Pelrine, R., Kornbluh, R., Pei, Q., Joseph, J., 2000. High-speed electrically actuated elastomers  
505 with strain greater than 100%. *Science* 287, 836–9.
- 506 [57] Pipkin, A.C., 1986. The Relaxed Energy Density for Isotropic Elastic Membranes. *IMA Journal*  
507 *of Applied Mathematics* 36, 85–99.
- 508 [58] Purnell, M.C., Butawan, M.B., Ramsey, R.D., 2018. Bio-field array: a dielectrophoretic elec-  
509 tromagnetic toroidal excitation to restore and maintain the golden ratio in human erythrocytes.  
510 *Physiological reports* 6, e13722.
- 511 [59] Reddy, N.H., Saxena, P., 2017. Limit points in the free inflation of a magnetoelastic toroidal  
512 membrane. *International Journal of Non-Linear Mechanics* 95, 248–63.
- 513 [60] Reddy, N.H., Saxena, P., 2018. Instabilities in the axisymmetric magnetoelastic deformation of a  
514 cylindrical membrane. *International Journal of Solids and Structures* 136, 203–19.

- 515 [61] Rivlin, R., 1948. Large elastic deformations of isotropic materials. i. fundamental concepts. Philo-  
516 sopherical Transactions of the Royal Society of London. Series A, Mathematical and Physical Sciences  
517 240, 459–90.
- 518 [62] Rudykh, S., Bhattacharya, K., deBotton, G., 2012. Snap-through actuation of thick-wall electroac-  
519 tive balloons. *International Journal of Non-Linear Mechanics* 47, 206–9.
- 520 [63] Saxena, P., Reddy, N.H., Pradhan, S.P., 2019. Magnetoelastic deformation of a circular membrane:  
521 wrinkling and limit point instabilities. *International Journal of Non-Linear Mechanics* 116, 250–61.
- 522 [64] Saxena, P., Sharma, B.L., 2020. On equilibrium equations and their perturbations using three  
523 different variational formulations of nonlinear electroelastostatics. *Mathematics and Mechanics of*  
524 *Solids* .
- 525 [65] Saxena, P., Vu, D.K., Steinmann, P., 2014. On rate-dependent dissipation effects in electro-  
526 elasticity. *International Journal of Non-Linear Mechanics* 62, 1–11.
- 527 [66] Shintake, J., Cacucciolo, V., Floreano, D., Shea, H., 2018. Soft robotic grippers. *Advanced*  
528 *Materials* 30, 1707035.
- 529 [67] Steigmann, D.J., 1990. Tension-Field Theory. *Proceedings of the Royal Society A: Mathematical,*  
530 *Physical and Engineering Sciences* 429, 141–73.
- 531 [68] Suo, Z., 2010. Theory of dielectric elastomers. *Acta Mechanica Solida Sinica* 23, 549–78.
- 532 [69] Swain, D., Gupta, A., 2015. Interfacial growth during closure of a cutaneous wound: Stress  
533 generation and wrinkle formation. *Soft Matter* 11, 6499–508.
- 534 [70] Tamadapu, G., Dhavale, N.N., DasGupta, A., 2013. Geometrical feature of the scaling behavior  
535 of the limit-point pressure of inflated hyperelastic membranes. *Physical Review E* 88, 053201.
- 536 [71] Thompson, J.M.T., 2015. Advances in shell buckling: theory and experiments. *International*  
537 *Journal of Bifurcation and Chaos* 25, 1530001.
- 538 [72] Thompson, J.M.T., Van der Heijden, G., 2014. Quantified” shock-sensitivity” above the Maxwell  
539 load. *International Journal of Bifurcation and Chaos* 24, 1430009.
- 540 [73] Tiersten, H.F., 1978. Perturbation theory for linear electroelastic equations for small fields super-  
541 posed on a bias. *The Journal of the Acoustical Society of America* 64, 832–7.

- 542 [74] Tiersten, H.F., 1981. Electroelastic interactions and the piezoelectric equations. The Journal of  
543 the Acoustical Society of America 70, 1567–76.
- 544 [75] Toupin, R.A., 1956. The elastic dielectric. Journal of Rational Mechanics and Analysis 5, 849–915.
- 545 [76] Toupin, R.A., 1963. A dynamical theory of elastic dielectrics. International Journal of Engineering  
546 Science 1, 101–26.
- 547 [77] Venkata, S.P., Saxena, P., 2020. Instabilities in the free inflation of a nonlinear hyperelastic toroidal  
548 membrane. Journal of Mechanics of Materials and Structures 14, 473–96.
- 549 [78] Vu, D., Steinmann, P., Possart, G., 2007. Numerical modelling of non-linear electroelasticity.  
550 International Journal for Numerical Methods in Engineering 70, 685–704.
- 551 [79] Wong, W., Pellegrino, S., 2006. Wrinkled membranes II: analytical models. Journal of Mechanics  
552 of Materials and Structures 1, 27–61.
- 553 [80] Xie, Y.X., Liu, J.C., Fu, Y.B., 2016. Bifurcation of a dielectric elastomer balloon under pressurized  
554 inflation and electric actuation. International Journal of Solids and Structures 78-79, 182–8.
- 555 [81] Zang, H., Liao, B., Lang, X., Zhao, Z.L., Yuan, W., Feng, X.Q., 2020. Bionic torus as a self-  
556 adaptive soft grasper in robots. Applied Physics Letters 116, 023701.
- 557 [82] Zhang, C., Sun, W., Chen, H., Liu, L., Li, B., Li, D., 2016. Electromechanical deformation of  
558 conical dielectric elastomer actuator with hydrogel electrodes. Journal of Applied Physics 119.
- 559 [83] Zhao, X., Suo, Z., 2007. Method to analyze electromechanical stability of dielectric elastomers.  
560 Applied Physics Letters 91, 061921.

## 561 **Appendix A. Pressure term in the variational formulation**

The pressure term in the total potential energy functional

$$\int_{V_0}^{V_0+\Delta V} \tilde{P} dV \quad (\text{A.1})$$

should be such that upon taking its first variation, the virtual work ( $\delta V$ ) obtained is of the form [63]

$$\delta V = \int_{\Gamma} [\tilde{P} \mathbf{n} ds_0] \cdot \delta \mathbf{x} \quad (\text{A.2})$$

where  $\Gamma$  is the domain comprising the deformed mid-surface of the membrane and  $\delta \mathbf{x}$  is a virtual displacement of a point on the mid-surface. The normal vector is given by

$$\mathbf{n} = \frac{1}{\sqrt{g}} [\tilde{\varrho} \tilde{\eta}_\theta \cos \phi \mathbf{E}_1 + \tilde{\varrho} \tilde{\eta}_\theta \sin \phi \mathbf{E}_2 - \tilde{\varrho} \tilde{\varrho}_\theta \mathbf{E}_3] \quad \text{where} \quad \sqrt{g} = \tilde{\varrho} [\tilde{\varrho}_\theta^2 + \tilde{\eta}_\theta^2]^{1/2}. \quad (\text{A.3})$$

From equations (3) and (A.3), one obtains

$$\delta V = \int_0^{2\pi} \int_0^{2\pi} \tilde{P} [\tilde{\varrho} \tilde{\eta}_\theta \delta \tilde{\varrho} - \tilde{\varrho} \tilde{\varrho}_\theta \delta \tilde{\eta}] d\theta d\phi. \quad (\text{A.4})$$

It can be shown that this is the first variation of the functional following

$$\frac{1}{2} \int_0^{2\pi} \int_0^{2\pi} \tilde{P} \tilde{\varrho}^2 \tilde{\eta}_\theta d\theta d\phi, \quad (\text{A.5})$$

562 after using the condition  $\delta \eta|_{\theta=0} = \delta \eta|_{\theta=2\pi}$ .

Further note that total volume of the deformed torus is given by

$$V(\tilde{\varrho}, \tilde{\eta}) = 2 \int_{\tilde{\varrho}(\pi)}^{\tilde{\varrho}(0)} 2\pi \tilde{\varrho} \tilde{\eta} d\tilde{\varrho} = -4\pi \int_0^\pi \tilde{\varrho} \tilde{\varrho}_\theta \tilde{\eta} d\theta. \quad (\text{A.6})$$

In the domain  $\theta \in [0, 2\pi]$ , it can be shown that the function  $\tilde{\varrho}$  is even while  $\tilde{\varrho}_\theta$  and  $\tilde{\eta}$  are odd with respect to the point  $\theta = \pi$ . Thus the product  $\tilde{\varrho} \tilde{\varrho}_\theta \tilde{\eta}$  is an even function and the above integrals can be written as

$$V(\tilde{\varrho}, \tilde{\eta}) = -2\pi \int_0^{2\pi} \tilde{\varrho} \tilde{\varrho}_\theta \tilde{\eta} d\theta = - \int_0^{2\pi} \int_0^{2\pi} \tilde{\varrho} \tilde{\varrho}_\theta \tilde{\eta} d\theta d\phi. \quad (\text{A.7})$$

Upon using the identity

$$\int_0^{2\pi} [\tilde{\varrho}^2 \tilde{\eta}]_\theta d\theta = 0 \quad \Rightarrow \quad \int_0^{2\pi} \tilde{\varrho}^2 \tilde{\eta}_\theta d\theta = -2 \int_0^{2\pi} \tilde{\varrho} \tilde{\varrho}_\theta \tilde{\eta} d\theta, \quad (\text{A.8})$$

we can write the above volume integral as

$$V(\tilde{\varrho}, \tilde{\eta}) = \frac{1}{2} \int_0^{2\pi} \int_0^{2\pi} \tilde{\varrho}^2 \tilde{\eta}_\theta d\theta d\phi. \quad (\text{A.9})$$

If the torus deforms from the reference configuration with volume  $V_0$  to the current configuration with volume  $V$  at constant pressure  $\tilde{P}$  then the total work done can be written as

$$\frac{1}{2} \int_0^{2\pi} \int_0^{2\pi} \tilde{P} \tilde{\varrho}^2 \tilde{\eta}_\theta d\theta d\phi - \tilde{P} V_0, \quad (\text{A.10})$$

563 which is the same expression as (A.5) barring the constant term.



## Appendix B. Derivatives of the energy density function

The first derivatives of the right Cauchy–Green deformation tensor  $\mathbf{C}$  as expressed in Equation (8) with respect to  $\varrho$ ,  $\varrho_\theta$ ,  $\eta$  and  $\eta_\theta$  are given by

$$\begin{aligned}\mathbf{C}_\varrho &= \text{diag} \left( 0, \frac{2\lambda_2}{1 + \gamma \cos \theta}, \frac{-2}{\lambda_1^2 \lambda_2^3 [1 + \gamma \cos \theta]} \right), \\ \mathbf{C}_{\varrho_\theta} &= \text{diag} \left( \frac{2\varrho_\theta}{\gamma^2}, 0, \frac{-2\varrho_\theta}{\lambda_1^4 \lambda_2^2 \gamma^2} \right), \\ \mathbf{C}_\eta &= \mathbf{0}, \\ \mathbf{C}_{\eta_\theta} &= \text{diag} \left( \frac{2\eta_\theta}{\gamma^2}, 0, \frac{-2\eta_\theta}{\lambda_1^4 \lambda_2^2 \gamma^2} \right).\end{aligned}\tag{B.1}$$

Then non-zero second derivatives of  $\mathbf{C}$  are

$$\begin{aligned}\mathbf{C}_{\varrho\varrho} &= \text{diag} \left( 0, \frac{2}{[1 + \gamma \cos \theta]^2}, \frac{6}{\lambda_1^2 \lambda_2^4 [1 + \gamma \cos \theta]^2} \right), \\ \mathbf{C}_{\varrho\varrho_\theta} &= \text{diag} \left( 0, 0, \frac{4\varrho_\theta}{\gamma^2 \lambda_1^4 \lambda_2^3 [1 + \gamma \cos \theta]} \right), \\ \mathbf{C}_{\varrho\eta_\theta} &= \text{diag} \left( 0, 0, \frac{4\eta_\theta}{\gamma^2 \lambda_1^4 \lambda_2^3 [1 + \gamma \cos \theta]} \right), \\ \mathbf{C}_{\varrho_\theta\varrho_\theta} &= \text{diag} \left( \frac{2}{\gamma^2}, 0, \frac{8\varrho_\theta^2}{\gamma^4 \lambda_1^6 \lambda_2^2} - \frac{2}{\gamma^2 \lambda_1^4 \lambda_2^2} \right), \\ \mathbf{C}_{\eta_\theta\eta_\theta} &= \text{diag} \left( \frac{2}{\gamma^2}, 0, \frac{8\eta_\theta^2}{\gamma^4 \lambda_1^6 \lambda_2^2} - \frac{2}{\gamma^2 \lambda_1^4 \lambda_2^2} \right), \\ \mathbf{C}_{\varrho_\theta\eta_\theta} &= \text{diag} \left( 0, 0, \frac{8\varrho_\theta\eta_\theta}{\gamma^4 \lambda_1^6 \lambda_2^2} \right).\end{aligned}\tag{B.2}$$

The full derivatives of some of the second derivatives with respect to  $\theta$  are computed as

$$\begin{aligned}\frac{d\mathbf{C}_{\varrho\varrho}}{d\theta} &= \text{diag} \left( 0, 0, \frac{4}{\gamma^2} \left[ \frac{\varrho_{\theta\theta}}{\lambda_1^4 \lambda_2^3 [1 + \gamma \cos \theta]} + \frac{\varrho_\theta \gamma \sin \theta}{\lambda_1^4 \lambda_2^3 [1 + \gamma \cos \theta]^2} - \frac{3\varrho_\theta \lambda_{2\theta}}{\lambda_1^4 \lambda_2^4 [1 + \gamma \cos \theta]} - \frac{4\varrho_\theta \lambda_{1\theta}}{\lambda_1^5 \lambda_2^3 [1 + \gamma \cos \theta]} \right] \right), \\ \frac{d\mathbf{C}_{\varrho\eta_\theta}}{d\theta} &= \text{diag} \left( 0, 0, \frac{4}{\gamma^2} \left[ \frac{\eta_{\theta\theta}}{\lambda_1^4 \lambda_2^3 [1 + \gamma \cos \theta]} + \frac{\eta_\theta \gamma \sin \theta}{\lambda_1^4 \lambda_2^3 [1 + \gamma \cos \theta]^2} - \frac{3\eta_\theta \lambda_{2\theta}}{\lambda_1^4 \lambda_2^4 [1 + \gamma \cos \theta]} - \frac{4\eta_\theta \lambda_{1\theta}}{\lambda_1^5 \lambda_2^3 [1 + \gamma \cos \theta]} \right] \right), \\ \frac{d\mathbf{C}_{\varrho_\theta\varrho_\theta}}{d\theta} &= \text{diag} \left( 0, 0, \frac{8\varrho_{\theta\theta}\eta_\theta}{\gamma^4 \lambda_1^6 \lambda_2^2} + \frac{8\varrho_\theta\eta_{\theta\theta}}{\gamma^4 \lambda_1^6 \lambda_2^2} - \frac{16\varrho_\theta\eta_\theta\lambda_{2\theta}}{\gamma^4 \lambda_1^6 \lambda_2^3} - \frac{48\varrho_\theta\eta_\theta\lambda_{1\theta}}{\gamma^4 \lambda_1^7 \lambda_2^2} \right), \\ \frac{d\mathbf{C}_{\eta_\theta\eta_\theta}}{d\theta} &= \text{diag} \left( 0, 0, \frac{8}{\gamma^4} \left[ \frac{2\eta_{\theta\theta}\eta_{\theta\theta}}{\lambda_1^6 \lambda_2^2} - \frac{6\eta_\theta^2}{\lambda_1^7 \lambda_2^2} \lambda_{1\theta} - \frac{2\eta_\theta^2}{\lambda_1^6 \lambda_2^3} \lambda_{2\theta} \right] + \frac{2}{\gamma^2} \left[ \frac{4}{\lambda_1^5 \lambda_2^2} \lambda_{1\theta} + \frac{2}{\lambda_1^4 \lambda_2^3} \lambda_{2\theta} \right] \right).\end{aligned}\tag{B.3}$$

Given the energy density function in equation (29), the first derivatives of the energy density with respect to  $\varrho$  is computed as

$$\begin{aligned}\Omega_\varrho &= C_1 \frac{\partial I_1}{\partial \varrho} + C_2 \frac{\partial I_2}{\partial \varrho} + \beta [\mathbf{C}_\varrho \mathbf{D}] \cdot \mathbf{D} \\ &= C_1 \frac{2\lambda_2}{[1 + \gamma \cos \theta]} \left[ [1 + \alpha \lambda_1^2] \left[ 1 - \frac{1}{\lambda_1^2 \lambda_2^4} \right] \right] - \frac{\Phi_0^2 \lambda_2 \lambda_1^2}{2\beta H^2 [1 + \gamma \cos \theta]}.\end{aligned}\tag{B.4}$$

Similarly, other first derivatives of energy density function  $\Omega$  are given by

$$\begin{aligned}
\Omega_{\mathbf{D}} &= 2\beta \mathbf{C} \mathbf{D}, \\
\Omega_{\varrho\theta} &= C_1 \frac{2\varrho\theta}{\gamma^2} \left[ [1 + \alpha\lambda_2^2] \left[ 1 - \frac{1}{\lambda_1^4\lambda_2^2} \right] \right] - \frac{\varrho\theta \Phi_0^2 \lambda_2^2}{2\beta H^2 \gamma^2}, \\
\Omega_{\eta\theta} &= C_1 \frac{2\eta\theta}{\gamma^2} \left[ [1 + \alpha\lambda_2^2] \left[ 1 - \frac{1}{\lambda_1^4\lambda_2^2} \right] \right] - \frac{\eta\theta \Phi_0^2 \lambda_2^2}{2\beta H^2 \gamma^2}, \\
\Omega_{\eta} &= 0.
\end{aligned} \tag{B.5a}$$

The non-zero second derivatives of the energy density are given by

$$\begin{aligned}
\Omega_{\varrho\varrho} &= 2C_1 \frac{[1 + \alpha\lambda_1^2]}{[1 + \gamma \cos \theta]^2} \left[ 1 + \frac{3}{\lambda_1^2\lambda_2^4} \right] + \frac{3\Phi_0^2\lambda_1^2}{2\beta H^2 [1 + \gamma \cos \theta]^2}, \\
\Omega_{\varrho\varrho\theta} &= C_1 \frac{4\lambda_2}{[1 + \gamma \cos \theta]} \frac{\varrho\theta}{\gamma^2} \left[ \alpha + \frac{1}{\lambda_1^4\lambda_2^4} \right] + \frac{\varrho\theta}{\gamma^2} \frac{\Phi_0^2\lambda_2}{\beta H^2 [1 + \gamma \cos \theta]}, \\
\Omega_{\varrho\eta\theta} &= C_1 \frac{4\lambda_2}{[1 + \gamma \cos \theta]} \frac{\eta\theta}{\gamma^2} \left[ \alpha + \frac{1}{\lambda_1^4\lambda_2^4} \right] + \frac{\eta\theta}{\gamma^2} \frac{\Phi_0^2\lambda_2}{\beta H^2 [1 + \gamma \cos \theta]}, \\
\Omega_{\varrho\theta\varrho\theta} &= \frac{2C_1}{\gamma^2} [1 + \alpha\lambda_2^2] \left[ \left[ 1 - \frac{1}{\lambda_1^4\lambda_2^2} \right] + \frac{4\varrho\theta^2}{\gamma^2\lambda_1^6\lambda_2^2} \right] + \frac{2\Phi_0^2\varrho\theta^2\lambda_2^2}{\beta H^2 \gamma^4 \lambda_1^2} - \frac{\Phi_0^2\lambda_2^2}{2\beta H^2 \gamma^2}, \\
\Omega_{\varrho\theta\eta\theta} &= 8C_1 \frac{\varrho\theta\eta\theta}{\gamma^4} [1 + \alpha\lambda_2^2] \frac{1}{\lambda_1^6\lambda_2^2} + \frac{\varrho\theta\eta\theta}{\gamma^4} \frac{2\Phi_0^2\lambda_2^2}{\beta H^2 \lambda_1^2}, \\
\Omega_{\eta\theta\eta\theta} &= \frac{2C_1}{\gamma^2} [1 + \alpha\lambda_2^2] \left[ \left[ 1 - \frac{1}{\lambda_1^4\lambda_2^2} \right] + \frac{4\eta\theta^2}{\gamma^2\lambda_1^6\lambda_2^2} \right] + \frac{2\Phi_0^2\eta\theta^2\lambda_2^2}{\beta H^2 \gamma^4 \lambda_1^2} - \frac{\Phi_0^2\lambda_2^2}{2\beta H^2 \gamma^2}.
\end{aligned} \tag{B.6}$$

Full derivatives of some second derivatives of the energy density function with respect to  $\theta$  are computed

as

$$\begin{aligned}
\frac{d\Omega_{\eta\theta\eta\theta}}{d\theta} &= \frac{2C_1}{\gamma^2} \left[ 2\alpha\lambda_2\lambda_{2\theta} \left[ \left[ 1 - \frac{1}{\lambda_1^4\lambda_2^2} \right] + \frac{4\eta_\theta^2}{\gamma^2\lambda_1^6\lambda_2^2} \right] \right. \\
&\quad \left. + [1 + \alpha\lambda_2^2] \left[ \frac{4\lambda_{1\theta}}{\lambda_1^5\lambda_2^2} + \frac{2\lambda_{2\theta}}{\lambda_1^4\lambda_2^3} + \frac{4}{\gamma^2} \left[ \frac{2\eta_\theta\eta_{\theta\theta}}{\lambda_1^6\lambda_2^2} - \frac{6\eta_\theta^2\lambda_{1\theta}}{\lambda_1^7\lambda_2^2} - \frac{2\eta_\theta^2\lambda_{2\theta}}{\lambda_1^6\lambda_2^3} \right] \right] \right] \\
&\quad + \frac{\Phi_0^2}{\beta H^2} \left[ \frac{2}{\gamma^4} \left[ \frac{2\eta_\theta\eta_{\theta\theta}\lambda_2^2}{\lambda_1^2} - \frac{6\eta_\theta^2\lambda_2^2}{\lambda_1^3}\lambda_{1\theta} - \frac{2\eta_\theta^2\lambda_2}{\lambda_1^2}\lambda_{2\theta} \right] + \frac{1}{2\gamma^2} \left[ \frac{4\lambda_2^2}{\lambda_1}\lambda_{1\theta} + 2\lambda_2\lambda_{2\theta} \right] \right] \\
\frac{d\Omega_{\varrho\varrho\theta}}{d\theta} &= \frac{4C_1}{\gamma^2} \left[ \left[ \frac{\varrho_\theta\gamma\sin\theta}{[1+\gamma\cos\theta]^2} + \frac{\varrho_{\theta\theta}}{[1+\gamma\cos\theta]} \right] \left[ \alpha\lambda_2 + \frac{1}{\lambda_1^4\lambda_2^3} \right] \right. \\
&\quad \left. + \frac{\varrho_\theta}{[1+\gamma\cos\theta]} \left[ \alpha\lambda_{2\theta} - \frac{4}{\lambda_1^5\lambda_2^3}\lambda_{1\theta} - \frac{3}{\lambda_1^4\lambda_2^4}\lambda_{2\theta} \right] \right] \\
&\quad - \frac{\Phi_0^2}{\beta H^2\gamma^2} \left[ \frac{\varrho_{\theta\theta}\lambda_2}{[1+\gamma\cos\theta]} + \frac{\varrho_\theta\gamma\sin\theta\lambda_2}{[1+\gamma\cos\theta]^2} - \frac{3\varrho_\theta\lambda_{2\theta}}{[1+\gamma\cos\theta]} - \frac{4\varrho_\theta\lambda_2\lambda_{1\theta}}{\lambda_1[1+\gamma\cos\theta]} \right] \\
\frac{d\Omega_{\varrho\eta\theta}}{d\theta} &= \frac{4C_1}{\gamma^2} \left[ \left[ \frac{\eta_\theta\gamma\sin\theta}{[1+\gamma\cos\theta]^2} + \frac{\eta_{\theta\theta}}{[1+\gamma\cos\theta]} \right] \left[ \alpha\lambda_2 + \frac{1}{\lambda_1^4\lambda_2^3} \right] \right. \\
&\quad \left. + \frac{\eta_\theta}{[1+\gamma\cos\theta]} \left[ \alpha\lambda_{2\theta} - \frac{4}{\lambda_1^5\lambda_2^3}\lambda_{1\theta} - \frac{3}{\lambda_1^4\lambda_2^4}\lambda_{2\theta} \right] \right] \\
&\quad - \frac{\Phi_0^2}{\beta H^2\gamma^2} \left[ \frac{\eta_{\theta\theta}\lambda_2}{[1+\gamma\cos\theta]} + \frac{\eta_\theta\gamma\sin\theta\lambda_2}{[1+\gamma\cos\theta]^2} - \frac{3\eta_\theta\lambda_{2\theta}}{[1+\gamma\cos\theta]} - \frac{4\eta_\theta\lambda_2\lambda_{1\theta}}{\lambda_1[1+\gamma\cos\theta]} \right] \\
\frac{d\Omega_{\varrho\theta\eta\theta}}{d\theta} &= \frac{8C_1}{\gamma^4} \left[ [\varrho_{\theta\theta}\eta_\theta + \varrho_\theta\eta_{\theta\theta}] [1 + \alpha\lambda_2^2] \frac{1}{\lambda_1^6\lambda_2^2} + \varrho_\theta\eta_\theta [2\alpha\lambda_2\lambda_{2\theta}] \frac{1}{\lambda_1^6\lambda_2^2} \right. \\
&\quad \left. - \varrho_\theta\eta_\theta\gamma^4 [1 + \alpha\lambda_2^2] \left[ \frac{6\lambda_{1\theta}}{\lambda_1^7\lambda_2^2} + \frac{2\lambda_{2\theta}}{\lambda_1^6\lambda_2^3} \right] \right] \\
&\quad + \frac{\Phi_0^2}{\beta H^2} \left[ \frac{2\varrho_{\theta\theta}\eta_\theta\lambda_2^2}{\gamma^4\lambda_1^2} + \frac{2\varrho_\theta\eta_{\theta\theta}\lambda_2^2}{\gamma^4\lambda_1^2} - \frac{4\varrho_\theta\eta_\theta\lambda_{2\theta}\lambda_2}{\gamma^4\lambda_1^2} - \frac{12\varrho_\theta\eta_\theta\lambda_{1\theta}\lambda_2^2}{\gamma^4\lambda_1^3} \right] \tag{B.7}
\end{aligned}$$

where

$$\lambda_{1\theta} = \frac{\varrho_\theta\varrho_{\theta\theta} + \eta_\theta\eta_{\theta\theta}}{\gamma[\varrho_\theta^2 + \eta_\theta^2]^{1/2}} = \frac{\varrho_\theta\varrho_{\theta\theta} + \eta_\theta\eta_{\theta\theta}}{\gamma^2\lambda_1}, \quad \lambda_{2\theta} = \frac{\varrho_\theta}{1 + \gamma\cos\theta} + \frac{\varrho_\theta\gamma\sin\theta}{[1 + \gamma\cos\theta]^2}. \tag{B.8}$$

The second various derivatives of  $\Omega$  with respect to  $\mathbb{D}$  are computed as

$$\begin{aligned}
\Omega_{\mathbb{D}\mathbb{D}} &= 2\beta \mathbf{C}, \\
\Omega_{\mathbb{D}\varrho} &= 2\beta \mathbf{C}_{\varrho} \mathbb{D} = \frac{\Phi_0}{H} \mathbf{C}_{\varrho} \mathbf{C}^{-1} \mathbf{N}, \\
\Omega_{\mathbb{D}\varrho\theta} &= 2\beta \mathbf{C}_{\varrho\theta} \mathbb{D} = \frac{\Phi_0}{H} \mathbf{C}_{\varrho\theta} \mathbf{C}^{-1} \mathbf{N}, \\
\Omega_{\mathbb{D}\eta\theta} &= 2\beta \mathbf{C}_{\eta\theta} \mathbb{D} = \frac{\Phi_0}{H} \mathbf{C}_{\eta\theta} \mathbf{C}^{-1} \mathbf{N}, \\
\frac{d\Omega_{\mathbb{D}\varrho\theta}}{d\theta} &= 2\beta \mathbf{C}_{\varrho\theta\theta} \mathbb{D} = \frac{\Phi_0}{H} \frac{d\mathbf{C}_{\varrho\theta}}{d\theta} \mathbf{C}^{-1} \mathbf{N}, \\
\frac{d\Omega_{\mathbb{D}\eta\theta}}{d\theta} &= 2\beta \mathbf{C}_{\eta\theta\theta} \mathbb{D} = \frac{\Phi_0}{H} \frac{d\mathbf{C}_{\eta\theta}}{d\theta} \mathbf{C}^{-1} \mathbf{N},
\end{aligned} \tag{B.9a}$$

where

$$\frac{d\mathbf{C}_{\varrho\theta}}{d\theta} = \text{diag} \left( -\frac{2\varrho_{\theta\theta}}{\gamma^2}, 0, -\frac{2}{\gamma^2} \left( \frac{\varrho_{\theta\theta}}{\lambda_1^4 \lambda_2^2} - \frac{4\varrho_{\theta}}{\lambda_1^5 \lambda_2^2} \lambda_{1\theta} - \frac{2\varrho_{\theta}}{\lambda_1^4 \lambda_2^3} \lambda_{2\theta} \right) \right), \tag{B.10a}$$

$$\frac{d\mathbf{C}_{\eta\theta}}{d\theta} = \text{diag} \left( -\frac{2\eta_{\theta\theta}}{\gamma^2}, 0, -\frac{2}{\gamma^2} \left( \frac{\eta_{\theta\theta}}{\lambda_1^4 \lambda_2^2} - \frac{4\eta_{\theta}}{\lambda_1^5 \lambda_2^2} \lambda_{1\theta} - \frac{2\eta_{\theta}}{\lambda_1^4 \lambda_2^3} \lambda_{2\theta} \right) \right). \tag{B.10b}$$

Upon rewriting, we get

$$\Omega_{\mathbb{D}\mathbb{D}} = 2\beta \text{diag} (\lambda_1^2, \lambda_2^2, \lambda_3^2), \tag{B.11a}$$

$$\Omega_{\mathbb{D}\varrho} = \frac{\Phi_0}{H} \text{diag} \left( 0, \frac{2}{\lambda_2(1 + \gamma \cos(\theta))}, -\frac{2}{\lambda_2(1 + \gamma \cos(\theta))} \right) \mathbf{N}, \tag{B.11b}$$

$$\Omega_{\mathbb{D}\varrho\theta} = \frac{\Phi_0}{H} \text{diag} \left( \frac{2\varrho_{\theta}}{\lambda_1^2 \gamma^2}, 0, \frac{-2\varrho_{\theta}}{\lambda_1^2 \gamma^2} \right) \mathbf{N}, \tag{B.11c}$$

$$\Omega_{\mathbb{D}\eta\theta} = \frac{\Phi_0}{H} \text{diag} \left( \frac{2\eta_{\theta}}{\lambda_1^2 \gamma^2}, 0, \frac{-2\eta_{\theta}}{\lambda_1^2 \gamma^2} \right) \mathbf{N}, \tag{B.11d}$$

$$\frac{d\Omega_{\mathbb{D}\varrho\theta}}{d\theta} = \frac{\Phi_0}{H} \text{diag} \left( -\frac{2\varrho_{\theta\theta}}{\gamma^2 \lambda_1^2}, 0, -\frac{2}{\gamma^2} \left( \frac{\varrho_{\theta\theta}}{\lambda_1^2} - \frac{4\varrho_{\theta}}{\lambda_1^3} \lambda_{1\theta} - \frac{2\varrho_{\theta}}{\lambda_1^2 \lambda_2} \lambda_{2\theta} \right) \right) \mathbf{N}, \tag{B.11e}$$

$$\frac{d\Omega_{\mathbb{D}\eta\theta}}{d\theta} = \frac{\Phi_0}{H} \text{diag} \left( -\frac{2\eta_{\theta\theta}}{\gamma^2 \lambda_1^2}, 0, -\frac{2}{\gamma^2} \left( \frac{\eta_{\theta\theta}}{\lambda_1^2} - \frac{4\eta_{\theta}}{\lambda_1^3} \lambda_{1\theta} - \frac{2\eta_{\theta}}{\lambda_1^2 \lambda_2} \lambda_{2\theta} \right) \right) \mathbf{N}. \tag{B.11f}$$

## 565 Appendix C. Second derivatives for computing the second variation of the potential en- 566 ergy

In Section 5, the loss of symmetry in the  $\phi$  direction was considered. Bifurcation occurs when the second variation of the potential energy function becomes zero. However, the symmetric assumption in solutions is no longer valid and  $\lambda_1$ ,  $\lambda_2$  and  $\lambda_3$  in the right Cauchy–Green deformation tensor are computed using the full expressions (6) and (7). The second derivatives of the energy density function with respect to  $\varrho$  is expressed as

$$\Omega_{\varrho\varrho} = C_1 [I_{1\varrho\varrho} + \alpha I_{2\varrho\varrho}] + \beta [\mathbf{C}_{\varrho\varrho} \mathbb{D}] \cdot \mathbb{D}, \tag{C.1}$$

where

$$\begin{aligned} I_{1_{\varrho\varrho}} &= \lambda_{1_{\varrho\varrho}}^2 + \lambda_{2_{\varrho\varrho}}^2 + \lambda_{3_{\varrho\varrho}}^2, \\ I_{2_{\varrho\varrho}} &= \lambda_{1_{\varrho\varrho}}^{-2} + \lambda_{2_{\varrho\varrho}}^{-2} + \lambda_{3_{\varrho\varrho}}^{-2}. \end{aligned} \quad (\text{C.2})$$

On substituting the expressions (6) and (7) into the previous equations, one obtains

$$\begin{aligned} I_{1_{\varrho\varrho}} &= \frac{2}{[1 + \gamma \cos \theta]^2} - \frac{2\gamma^2[1 + \gamma \cos \theta]^2[\varrho_\theta^2 + \eta_\theta^2]}{[[\varrho_\theta \eta_\phi - \varrho_\phi \eta_\theta]^2 + \varrho^2[\varrho_\theta^2 + \eta_\theta^2]]^2} + \frac{8\gamma^2[1 + \gamma \cos \theta]^2 \varrho^2[\varrho_\theta^2 + \eta_\theta^2]^2}{[[\varrho_\theta \eta_\phi - \varrho_\phi \eta_\theta]^2 + \varrho^2[\varrho_\theta^2 + \eta_\theta^2]]^3} \\ I_{2_{\varrho\varrho}} &= \frac{2\gamma^2}{[\varrho_\theta \eta_\phi - \varrho_\phi \eta_\theta]^2 + \varrho^2[\varrho_\theta^2 + \eta_\theta^2]} - \frac{4\gamma^2 \varrho^2[\varrho_\theta^2 + \eta_\theta^2]}{[[\varrho_\theta \eta_\phi - \varrho_\phi \eta_\theta]^2 + \varrho^2[\varrho_\theta^2 + \eta_\theta^2]]^2} \\ &\quad - \frac{2[\varrho_\theta^2 + \eta_\theta^2] [\gamma^2[\varrho_\phi^2 + \eta_\phi^2 + \varrho^2] + [\varrho_\theta^2 + \eta_\theta^2][1 + \gamma \cos \theta]^2]}{[[\varrho_\theta \eta_\phi - \varrho_\phi \eta_\theta]^2 + \varrho^2[\varrho_\theta^2 + \eta_\theta^2]]^2} \\ &\quad + \frac{8 \varrho^2[\varrho_\theta^2 + \eta_\theta^2]^2 [\gamma^2[\varrho_\phi^2 + \eta_\phi^2 + \varrho^2] + [\varrho_\theta^2 + \eta_\theta^2][1 + \gamma \cos \theta]^2]}{[[\varrho_\theta \eta_\phi - \varrho_\phi \eta_\theta]^2 + \varrho^2[\varrho_\theta^2 + \eta_\theta^2]]^3} + \frac{2[\varrho_\theta^2 + \eta_\theta^2]}{\gamma^2[1 + \gamma \cos \theta]^2}, \end{aligned} \quad (\text{C.3})$$

and

$$\beta[\mathbf{C}_{\varrho\varrho} \mathbf{D}] \cdot \mathbf{D} = \frac{2\Phi_0^2 \varrho^2[\varrho_\theta^2 + \eta_\theta^2]^2}{\beta H^2 \gamma^2 [1 + \gamma \cos \theta]^2 [[\varrho_\theta \eta_\phi - \varrho_\phi \eta_\theta]^2 + \varrho^2[\varrho_\theta^2 + \eta_\theta^2]]} - \frac{\Phi_0^2[\varrho_\theta^2 + \eta_\theta^2]}{2\beta H^2 \gamma^2 [1 + \gamma \cos \theta]^2}. \quad (\text{C.4})$$

Similarly, the second derivative of  $\Omega$  with respect to  $\varrho$  and  $\varrho_\theta$  can be computed as

$$\Omega_{\varrho\varrho_\theta} = C_1[I_{1_{\varrho\varrho_\theta}} + \alpha I_{2_{\varrho\varrho_\theta}}] + \beta[\mathbf{C}_{\varrho\varrho_\theta} \mathbf{D}] \cdot \mathbf{D}, \quad (\text{C.5})$$

where

$$I_{1_{\varrho\varrho_\theta}} = \frac{4\gamma^2 \varrho[\varrho_\theta^2 + \eta_\theta^2] [2 \varrho^2 \varrho_\theta + 2\eta_\phi[\eta_\phi \varrho_\theta - \varrho_\phi \eta_\theta]] [1 + \gamma \cos \theta]^2}{[[\varrho_\theta \eta_\phi - \varrho_\phi \eta_\theta]^2 + \varrho^2[\varrho_\theta^2 + \eta_\theta^2]]^3} - \frac{4\gamma^2 \varrho \varrho_\theta [1 + \gamma \cos \theta]^2}{[[\varrho_\theta \eta_\phi - \varrho_\phi \eta_\theta]^2 + \varrho^2[\varrho_\theta^2 + \eta_\theta^2]]^2}, \quad (\text{C.6})$$

$$\begin{aligned} I_{2_{\varrho\varrho_\theta}} &= -\frac{4\gamma^2 \varrho [2 \varrho^2 \varrho_\theta + 2\eta_\phi[\eta_\phi \varrho_\theta - \varrho_\phi \eta_\theta]]}{[[\varrho_\theta \eta_\phi - \varrho_\phi \eta_\theta]^2 + \varrho^2[\varrho_\theta^2 + \eta_\theta^2]]^2} - \frac{4 \varrho \varrho_\theta [\varrho_\theta^2 + \eta_\theta^2][1 + \gamma \cos \theta]^2}{[[\varrho_\theta \eta_\phi - \varrho_\phi \eta_\theta]^2 + \varrho^2[\varrho_\theta^2 + \eta_\theta^2]]^2} \\ &\quad - \frac{4 \varrho \varrho_\theta [[\varrho_\theta^2 + \eta_\theta^2][1 + \gamma \cos \theta]^2 + [\varrho_\phi^2 + \eta_\phi^2 + \varrho^2]\gamma^2]}{[[\varrho_\theta \eta_\phi - \varrho_\phi \eta_\theta]^2 + \varrho^2[\varrho_\theta^2 + \eta_\theta^2]]^2} \\ &\quad + \frac{4 \varrho[\varrho_\theta^2 + \eta_\theta^2] [2 \varrho^2 \varrho_\theta + 2\eta_\phi[\eta_\phi \varrho_\theta - \varrho_\phi \eta_\theta]] [[\varrho_\theta^2 + \eta_\theta^2][1 + \gamma \cos \theta]^2 + [\varrho_\phi^2 + \eta_\phi^2 + \varrho^2]\gamma^2]}{[[\varrho_\theta \eta_\phi - \varrho_\phi \eta_\theta]^2 + \varrho^2[\varrho_\theta^2 + \eta_\theta^2]]^3} + \frac{4 \varrho \varrho_\theta}{\gamma^2[1 + \gamma \cos \theta]^2}, \end{aligned} \quad (\text{C.7})$$

$$\beta[\mathbf{C}_{\varrho\varrho_\theta} \mathbf{D}] \cdot \mathbf{D} = \frac{\Phi_0^2 \varrho[\varrho_\theta^2 + \eta_\theta^2][2 \varrho^2 \varrho_\theta + 2\eta_\phi[\eta_\phi \varrho_\theta - \varrho_\phi \eta_\theta]]}{\beta H^2 [[\varrho_\theta \eta_\phi - \varrho_\phi \eta_\theta]^2 + \varrho^2[\varrho_\theta^2 + \eta_\theta^2]] \gamma^2[1 + \gamma \cos \theta]^2} - \frac{\Phi_0^2 \varrho \varrho_\theta}{\beta H^2 \gamma^2 [1 + \gamma \cos \theta]^2}. \quad (\text{C.8})$$

The second derivative of  $\Omega$  with respect to  $\varrho$  and  $\eta_\theta$  can be computed as

$$\Omega_{\varrho\eta_\theta} = C_1[I_{1_{\varrho\eta_\theta}} + \alpha I_{2_{\varrho\eta_\theta}}] + \beta[\mathbf{C}_{\varrho\eta_\theta} \mathbf{D}] \cdot \mathbf{D}, \quad (\text{C.9})$$

where

$$I_{1_{\varrho\eta\theta}} = \frac{4\gamma^2 \varrho[\varrho_\theta^2 + \eta_\theta^2] [2\varrho^2\eta_\theta - 2\varrho_\phi[\eta_\phi\varrho_\theta - \varrho_\phi\eta_\theta]] [1 + \gamma \cos \theta]^2}{[[\varrho_\theta\eta_\phi - \varrho_\phi\eta_\theta]^2 + \varrho^2[\varrho_\theta^2 + \eta_\theta^2]]^3} - \frac{4\gamma^2 \varrho\eta_\theta[1 + \gamma \cos \theta]^2}{[[\varrho_\theta\eta_\phi - \varrho_\phi\eta_\theta]^2 + \varrho^2[\varrho_\theta^2 + \eta_\theta^2]]^2}, \quad (\text{C.10})$$

$$\begin{aligned} I_{2_{\varrho\eta\theta}} = & -\frac{4\gamma^2 \varrho [2\varrho^2\eta_\theta - 2\varrho_\phi[\eta_\phi\varrho_\theta - \varrho_\phi\eta_\theta]]}{[[\varrho_\theta\eta_\phi - \varrho_\phi\eta_\theta]^2 + \varrho^2[\varrho_\theta^2 + \eta_\theta^2]]^2} - \frac{4\varrho\eta_\theta[\varrho_\theta^2 + \eta_\theta^2][1 + \gamma \cos \theta]^2}{[[\varrho_\theta\eta_\phi - \varrho_\phi\eta_\theta]^2 + \varrho^2[\varrho_\theta^2 + \eta_\theta^2]]^2} \\ & - \frac{4\varrho\eta_\theta [[\varrho_\theta^2 + \eta_\theta^2][1 + \gamma \cos \theta]^2 + [\varrho_\phi^2 + \eta_\phi^2 + \varrho^2]\gamma^2]}{[[\varrho_\theta\eta_\phi - \varrho_\phi\eta_\theta]^2 + \varrho^2[\varrho_\theta^2 + \eta_\theta^2]]^2} \\ & + \frac{4\varrho[\varrho_\theta^2 + \eta_\theta^2] [2\varrho^2\eta_\theta - 2\varrho_\phi[\eta_\phi\varrho_\theta - \varrho_\phi\eta_\theta]] [[\varrho_\theta^2 + \eta_\theta^2][1 + \gamma \cos \theta]^2 + [\varrho_\phi^2 + \eta_\phi^2 + \varrho^2]\gamma^2]}{[[\varrho_\theta\eta_\phi - \varrho_\phi\eta_\theta]^2 + \varrho^2[\varrho_\theta^2 + \eta_\theta^2]]^3} \\ & + \frac{4\varrho\eta_\theta}{\gamma^2[1 + \gamma \cos \theta]^2}, \end{aligned} \quad (\text{C.11})$$

$$\beta[\mathbf{C}_{\varrho\eta\theta} \mathbf{D}] \cdot \mathbf{D} = \frac{\Phi_0^2 \varrho[\varrho_\theta^2 + \eta_\theta^2][2\varrho^2\eta_\theta - 2\varrho_\phi[\eta_\phi\varrho_\theta - \varrho_\phi\eta_\theta]]}{\beta H^2 [[\varrho_\theta\eta_\phi - \varrho_\phi\eta_\theta]^2 + \varrho^2[\varrho_\theta^2 + \eta_\theta^2]] \gamma^2[1 + \gamma \cos \theta]^2} - \frac{\Phi_0^2 \varrho\eta_\theta}{\beta H^2 \gamma^2[1 + \gamma \cos \theta]^2} \quad (\text{C.12})$$

The second derivative of  $\Omega$  with respect to  $\varrho$  and  $\varrho_\phi$  can be computed as

$$\Omega_{\varrho\varrho_\phi} = C_1[I_{1_{\varrho\varrho_\phi}} + \alpha I_{2_{\varrho\varrho_\phi}}] + \beta[\mathbf{C}_{\varrho\varrho_\phi} \mathbf{D}] \cdot \mathbf{D}, \quad (\text{C.13})$$

where

$$I_{1_{\varrho\varrho_\phi}} = -\frac{8\varrho\eta_\theta[\eta_\phi\varrho_\theta - \varrho_\phi\eta_\theta][\varrho_\theta^2 + \eta_\theta^2]\gamma^2[1 + \gamma \cos \theta]^2}{[[\varrho_\theta\eta_\phi - \varrho_\phi\eta_\theta]^2 + \varrho^2[\varrho_\theta^2 + \eta_\theta^2]]^3}, \quad (\text{C.14})$$

$$\begin{aligned} I_{2_{\varrho\varrho_\phi}} = & \frac{4\varrho\gamma^2\eta_\theta[\varrho_\theta\eta_\phi - \varrho_\phi\eta_\theta]}{[[\varrho_\theta\eta_\phi - \varrho_\phi\eta_\theta]^2 + \varrho^2[\varrho_\theta^2 + \eta_\theta^2]]^2} - \frac{4\varrho_\phi\varrho[\varrho_\theta^2 + \eta_\theta^2]\gamma^2}{[[\varrho_\theta\eta_\phi - \varrho_\phi\eta_\theta]^2 + \varrho^2[\varrho_\theta^2 + \eta_\theta^2]]^2} \\ & - \frac{8\varrho\eta_\theta[\varrho_\theta\eta_\phi - \varrho_\phi\eta_\theta][\varrho_\theta^2 + \eta_\theta^2] [[\varrho_\theta^2 + \eta_\theta^2][1 + \gamma \cos \theta]^2 + [\varrho_\phi^2 + \eta_\phi^2 + \varrho^2]\gamma^2]}{[[\varrho_\theta\eta_\phi - \varrho_\phi\eta_\theta]^2 + \varrho^2[\varrho_\theta^2 + \eta_\theta^2]]^3}, \end{aligned} \quad (\text{C.15})$$

$$\beta[\mathbf{C}_{\varrho\varrho_\phi} \mathbf{D}] \cdot \mathbf{D} = -\frac{2\Phi_0^2 \varrho\eta_\theta[\eta_\phi\varrho_\theta - \varrho_\phi\eta_\theta][\varrho_\theta^2 + \eta_\theta^2]}{\beta H^2 [[\varrho_\theta\eta_\phi - \varrho_\phi\eta_\theta]^2 + \varrho^2[\varrho_\theta^2 + \eta_\theta^2]] \gamma^2[1 + \gamma \cos \theta]^2}. \quad (\text{C.16})$$

The second derivative of  $\Omega$  with respect to  $\varrho$  and  $\eta_\phi$  is given by

$$\Omega_{\varrho\eta_\phi} = C_1[I_{1_{\varrho\eta_\phi}} + \alpha I_{2_{\varrho\eta_\phi}}] + \beta[\mathbf{C}_{\varrho\eta_\phi} \mathbf{D}] \cdot \mathbf{D}, \quad (\text{C.17})$$

where

$$I_{1\varrho\eta_\phi} = \frac{8\varrho\varrho_\theta[\eta_\phi\varrho_\theta - \varrho_\phi\eta_\theta][\varrho_\theta^2 + \eta_\theta^2]\gamma^2[1 + \gamma\cos\theta]^2}{[[\varrho_\theta\eta_\phi - \varrho_\phi\eta_\theta]^2 + \varrho^2[\varrho_\theta^2 + \eta_\theta^2]]^3}, \quad (\text{C.18})$$

$$I_{2\varrho\eta_\phi} = -\frac{4\varrho\gamma^2\varrho_\theta[\varrho_\theta\eta_\phi - \varrho_\phi\eta_\theta]}{[[\varrho_\theta\eta_\phi - \varrho_\phi\eta_\theta]^2 + \varrho^2[\varrho_\theta^2 + \eta_\theta^2]]^2} - \frac{4\eta_\phi\varrho[\varrho_\theta^2 + \eta_\theta^2]\gamma^2}{[[\varrho_\theta\eta_\phi - \varrho_\phi\eta_\theta]^2 + \varrho^2[\varrho_\theta^2 + \eta_\theta^2]]^2} + \frac{8\varrho\varrho_\theta[\varrho_\theta\eta_\phi - \varrho_\phi\eta_\theta][\varrho_\theta^2 + \eta_\theta^2][[\varrho_\theta^2 + \eta_\theta^2][1 + \gamma\cos\theta] + [\varrho_\phi^2 + \eta_\phi^2 + \varrho^2]\gamma^2]}{[[\varrho_\theta\eta_\phi - \varrho_\phi\eta_\theta]^2 + \varrho^2[\varrho_\theta^2 + \eta_\theta^2]]^3}, \quad (\text{C.19})$$

$$\beta[\mathbf{C}_{\varrho\varrho_\phi} \mathbf{D}] \cdot \mathbf{D} = \frac{2\Phi_0^2\varrho\varrho_\theta[\eta_\phi\varrho_\theta - \varrho_\phi\eta_\theta][\varrho_\theta^2 + \eta_\theta^2]}{\beta H^2 [[\varrho_\theta\eta_\phi - \varrho_\phi\eta_\theta]^2 + \varrho^2[\varrho_\theta^2 + \eta_\theta^2]] \gamma^2[1 + \gamma\cos\theta]^2} \quad (\text{C.20})$$

The second derivative of  $\Omega$  with respect to  $\varrho_\theta$  is given by

$$\Omega_{\varrho_\theta\varrho_\theta} = C_1[I_{1\varrho_\theta\varrho_\theta} + \alpha I_{2\varrho_\theta\varrho_\theta}] + \beta[\mathbf{C}_{\varrho_\theta\varrho_\theta} \mathbf{D}] \cdot \mathbf{D}, \quad (\text{C.21})$$

where

$$I_{1\varrho_\theta\varrho_\theta} = \frac{2}{\gamma^2} + \frac{2\gamma^2[1 + \gamma\cos\theta]^2[2\eta_\phi^2\varrho_\theta - 2\eta_\phi\varrho_\phi\eta_\theta + 2\varrho^2\varrho_\theta]^2}{[[\varrho_\theta\eta_\phi - \varrho_\phi\eta_\theta]^2 + \varrho^2[\varrho_\theta^2 + \eta_\theta^2]]^3} - \frac{\gamma^2[1 + \gamma\cos\theta]^2[2\eta_\phi^2 + 2\varrho^2]}{[[\varrho_\theta\eta_\phi - \varrho_\phi\eta_\theta]^2 + \varrho^2[\varrho_\theta^2 + \eta_\theta^2]]^2}, \quad (\text{C.22})$$

$$I_{2\varrho_\theta\varrho_\theta} = \frac{2\varrho^2 + 2\eta_\phi^2}{\gamma^2[1 + \gamma\cos\theta]^2} - \frac{4\varrho_\theta[1 + \gamma\cos\theta]^2[2\varrho^2\varrho_\theta + 2\eta_\phi^2\varrho_\theta - 2\eta_\theta\varrho_\phi\eta_\phi]}{[[\varrho_\theta\eta_\phi - \varrho_\phi\eta_\theta]^2 + \varrho^2[\varrho_\theta^2 + \eta_\theta^2]]^2} + \frac{2[1 + \gamma\cos\theta]^2}{[\varrho_\theta\eta_\phi - \varrho_\phi\eta_\theta]^2 + \varrho^2[\varrho_\theta^2 + \eta_\theta^2]} + \frac{2[[\varrho_\theta^2 + \eta_\theta^2][1 + \gamma\cos\theta]^2 + [\varrho_\phi^2 + \eta_\phi^2 + \varrho^2]\gamma^2][2\eta_\phi^2\varrho_\theta - 2\eta_\phi\varrho_\phi\eta_\theta + 2\varrho^2\varrho_\theta]^2}{[[\varrho_\theta\eta_\phi - \varrho_\phi\eta_\theta]^2 + \varrho^2[\varrho_\theta^2 + \eta_\theta^2]]^3} - \frac{[[\varrho_\theta^2 + \eta_\theta^2][1 + \gamma\cos\theta]^2 + [\varrho_\phi^2 + \eta_\phi^2 + \varrho^2]\gamma^2][2\eta_\phi^2 + 2\varrho^2]}{[[\varrho_\theta\eta_\phi - \varrho_\phi\eta_\theta]^2 + \varrho^2[\varrho_\theta^2 + \eta_\theta^2]]^2}, \quad (\text{C.23})$$

$$\beta[\mathbf{C}_{\varrho_\theta\varrho_\theta} \mathbf{D}] \cdot \mathbf{D} = \frac{2\Phi_0^2[\eta_\phi^2\varrho_\theta - \eta_\phi\varrho_\phi\eta_\theta + \varrho^2\varrho_\theta]^2}{\beta H^2 [[\varrho_\theta\eta_\phi - \varrho_\phi\eta_\theta]^2 + \varrho^2[\varrho_\theta^2 + \eta_\theta^2]] \gamma^2[1 + \gamma\cos\theta]^2} - \frac{\Phi_0^2[\eta_\phi^2 + \varrho^2]}{2\beta H^2 \gamma^2[1 + \gamma\cos\theta]^2}. \quad (\text{C.24})$$

The second derivative of  $\Omega$  with respect to  $\varrho_\theta$  and  $\eta_\theta$  is given by

$$\Omega_{\varrho_\theta\eta_\theta} = C_1[I_{1\varrho_\theta\eta_\theta} + \alpha I_{2\varrho_\theta\eta_\theta}] + \beta[\mathbf{C}_{\varrho_\theta\eta_\theta} \mathbf{D}] \cdot \mathbf{D}, \quad (\text{C.25})$$

where

$$I_{1_{\varrho_\theta \eta_\theta}} = \frac{2\gamma^2[1 + \gamma \cos \theta]^2[2\varrho_\phi^2 \eta_\theta - 2\eta_\phi \varrho_\phi \varrho_\theta + 2\varrho^2 \eta_\theta][2\varrho^2 \varrho_\theta + 2\varrho_\theta \eta_\phi^2 - 2\varrho_\phi \eta_\phi \eta_\theta]}{[[\varrho_\theta \eta_\phi - \varrho_\phi \eta_\theta]^2 + \varrho^2[\varrho_\theta^2 + \eta_\theta^2]]^3}, \quad (\text{C.26})$$

$$\begin{aligned} & - \frac{2\varrho_\phi \eta_\phi \gamma^2 [1 + \gamma \cos \theta]^2}{[[\varrho_\theta \eta_\phi - \varrho_\phi \eta_\theta]^2 + \varrho^2[\varrho_\theta^2 + \eta_\theta^2]]^2} \\ I_{2_{\varrho_\theta \eta_\theta}} &= -\frac{2\varrho_\phi \eta_\phi}{\gamma^2 [1 + \gamma \cos \theta]^2} - \frac{2\varrho_\theta [1 + \gamma \cos \theta]^2 [2\varrho^2 \eta_\theta - 2\varrho_\phi \eta_\phi \varrho_\theta + 2\varrho_\phi^2 \eta_\theta]}{[[\varrho_\theta \eta_\phi - \varrho_\phi \eta_\theta]^2 + \varrho^2[\varrho_\theta^2 + \eta_\theta^2]]^2} \\ & - \frac{2\eta_\theta [1 + \gamma \cos \theta]^2 [2\varrho^2 \varrho_\theta + 2\eta_\phi^2 \varrho_\theta - 2\eta_\phi \varrho_\phi \eta_\theta]}{[[\varrho_\theta \eta_\phi - \varrho_\phi \eta_\theta]^2 + \varrho^2[\varrho_\theta^2 + \eta_\theta^2]]^2} + \frac{2\varrho_\phi \eta_\phi [[\varrho_\theta^2 + \eta_\theta^2][1 + \gamma \cos \theta]^2 + [\varrho_\phi^2 + \eta_\phi^2 + \varrho^2]\gamma^2]}{[[\varrho_\theta \eta_\phi - \varrho_\phi \eta_\theta]^2 + \varrho^2[\varrho_\theta^2 + \eta_\theta^2]]^2} \\ & + \frac{2[2\varrho^2 \eta_\theta - 2\varrho_\phi \eta_\phi \varrho_\theta + 2\varrho_\phi^2 \eta_\theta][2\varrho^2 \varrho_\theta + 2\eta_\phi^2 \varrho_\theta - 2\eta_\phi \varrho_\phi \eta_\theta] [[\varrho_\theta^2 + \eta_\theta^2][1 + \gamma \cos \theta]^2 + [\varrho_\phi^2 + \eta_\phi^2 + \varrho^2]\gamma^2]}{[[\varrho_\theta \eta_\phi - \varrho_\phi \eta_\theta]^2 + \varrho^2[\varrho_\theta^2 + \eta_\theta^2]]^3}, \end{aligned} \quad (\text{C.27})$$

$$\beta[\mathbf{C}_{\varrho_\theta \eta_\theta} \mathbf{D}] \cdot \mathbf{D} = \frac{2\Phi_0^2[\varrho_\phi^2 \eta_\theta - \eta_\phi \varrho_\phi \varrho_\theta + \varrho^2 \eta_\theta][\varrho^2 \varrho_\theta + \varrho_\theta \eta_\phi^2 - \varrho_\phi \eta_\phi \eta_\theta]}{\beta H^2 [[\varrho_\theta \eta_\phi - \varrho_\phi \eta_\theta]^2 + \varrho^2[\varrho_\theta^2 + \eta_\theta^2]] \gamma^2 [1 + \gamma \cos \theta]^2} - \frac{\Phi_0^2 \varrho_\phi \eta_\phi}{2\beta H^2 \gamma^2 [1 + \gamma \cos \theta]^2}. \quad (\text{C.28})$$

The second derivative of  $\Omega$  with respect to  $\eta_\theta$  and  $\varrho_\phi$  is computed as

$$\Omega_{\eta_\theta \varrho_\phi} = C_1[I_{1_{\eta_\theta \varrho_\phi}} + \alpha I_{2_{\eta_\theta \varrho_\phi}}] + \beta[\mathbf{C}_{\eta_\theta \varrho_\phi} \mathbf{D}] \cdot \mathbf{D}, \quad (\text{C.29})$$

where

$$\begin{aligned} I_{1_{\eta_\theta \varrho_\phi}} &= -\frac{4\gamma^2[1 + \gamma \cos \theta]^2[\varrho_\theta \eta_\theta \eta_\phi - \eta_\theta^2 \varrho_\phi][2\varrho_\phi^2 \eta_\theta - 2\eta_\phi \varrho_\phi \varrho_\theta + 2\varrho^2 \eta_\theta]}{[[\varrho_\theta \eta_\phi - \varrho_\phi \eta_\theta]^2 + \varrho^2[\varrho_\theta^2 + \eta_\theta^2]]^3} \\ & - \frac{[2\varrho_\phi \eta_\theta - 2[\varrho_\theta \eta_\phi - \varrho_\phi \eta_\theta]]\gamma^2 [1 + \gamma \cos \theta]^2}{[[\varrho_\theta \eta_\phi - \varrho_\phi \eta_\theta]^2 + \varrho^2[\varrho_\theta^2 + \eta_\theta^2]]^2}, \end{aligned} \quad (\text{C.30})$$

$$\begin{aligned} I_{2_{\eta_\theta \varrho_\phi}} &= \frac{2\eta_\theta \varrho_\phi - 2[\eta_\phi \varrho_\theta - \varrho_\phi \eta_\theta]}{\gamma^2 [1 + \gamma \cos \theta]^2} + \frac{4\eta_\theta^2[\eta_\phi \varrho_\theta - \varrho_\phi \eta_\theta][1 + \gamma \cos \theta]^2}{[[\varrho_\theta \eta_\phi - \varrho_\phi \eta_\theta]^2 + \varrho^2[\varrho_\theta^2 + \eta_\theta^2]]^2} \\ & - \frac{2\varrho_\phi \gamma^2 [2\varrho^2 \eta_\theta - 2\varrho_\phi[\eta_\phi \varrho_\theta - \varrho_\phi \eta_\theta]]}{[[\varrho_\theta \eta_\phi - \varrho_\phi \eta_\theta]^2 + \varrho^2[\varrho_\theta^2 + \eta_\theta^2]]^2} \\ & - \frac{[2\varrho_\phi \eta_\theta - 2[\eta_\phi \varrho_\theta - \varrho_\phi \eta_\theta]] [[\varrho_\theta^2 + \eta_\theta^2][1 + \gamma \cos \theta]^2 + [\varrho_\phi^2 + \eta_\phi^2 + \varrho^2]\gamma^2]}{[[\varrho_\theta \eta_\phi - \varrho_\phi \eta_\theta]^2 + \varrho^2[\varrho_\theta^2 + \eta_\theta^2]]^2} \\ & - \frac{4\eta_\theta[\eta_\phi \varrho_\theta - \varrho_\phi \eta_\theta] [2\varrho^2 \varrho_\theta - 2\varrho_\phi[\eta_\phi \varrho_\theta - \varrho_\phi \eta_\theta]] [[\varrho_\theta^2 + \eta_\theta^2][1 + \gamma \cos \theta]^2 + [\varrho_\phi^2 + \eta_\phi^2 + \varrho^2]\gamma^2}{[[\varrho_\theta \eta_\phi - \varrho_\phi \eta_\theta]^2 + \varrho^2[\varrho_\theta^2 + \eta_\theta^2]]^3}, \end{aligned} \quad (\text{C.31})$$

$$\beta[\mathbf{C}_{\eta_\theta \varrho_\phi} \mathbf{D}] \cdot \mathbf{D} = -\frac{\Phi_0^2[\varrho_\theta \eta_\theta \eta_\phi - \eta_\theta^2 \varrho_\phi][2\varrho_\phi^2 \eta_\theta - 2\eta_\phi \varrho_\phi \varrho_\theta + 2\varrho^2 \eta_\theta]}{\beta H^2 [[\varrho_\theta \eta_\phi - \varrho_\phi \eta_\theta]^2 + \varrho^2[\varrho_\theta^2 + \eta_\theta^2]] \gamma^2 [1 + \gamma \cos \theta]^2} - \frac{\Phi_0^2[\varrho_\phi \eta_\theta - \varrho_\theta \eta_\phi + \varrho_\phi \eta_\theta]}{2\beta H^2 \gamma^2 [1 + \gamma \cos \theta]^2} \quad (\text{C.32})$$

The second derivative of  $\Omega$  with respect to  $\eta_\theta$  is computed as

$$\Omega_{\eta_\theta \eta_\theta} = C_1[I_{1_{\eta_\theta \eta_\theta}} + \alpha I_{2_{\eta_\theta \eta_\theta}}] + \beta[\mathbf{C}_{\eta_\theta \eta_\theta} \mathbf{D}] \cdot \mathbf{D}, \quad (\text{C.33})$$



where

$$I_{1\eta_\theta\eta_\theta} = \frac{2}{\gamma^2} + \frac{2\gamma^2[1 + \gamma \cos \theta]^2 [2\varrho_\phi^2 \eta_\theta - 2\eta_\phi \varrho_\phi \varrho_\theta + 2\varrho^2 \eta_\theta]^2}{[[\varrho_\theta \eta_\phi - \varrho_\phi \eta_\theta]^2 + \varrho^2[\varrho_\theta^2 + \eta_\theta^2]]^3} - \frac{\gamma^2[1 + \gamma \cos \theta]^2 [2\varrho_\phi^2 + 2\varrho^2]}{[[\varrho_\theta \eta_\phi - \varrho_\phi \eta_\theta]^2 + \varrho^2[\varrho_\theta^2 + \eta_\theta^2]]^2}, \quad (\text{C.34})$$

$$I_{2\eta_\theta\eta_\theta} = \frac{2\varrho^2 + 2\varrho_\phi^2}{\gamma^2[1 + \gamma \cos \theta]^2} - \frac{4\eta_\theta[1 + \gamma \cos \theta]^2 [2\varrho^2 \eta_\theta + 2\varrho_\phi^2 \eta_\theta - 2\varrho_\theta \varrho_\phi \eta_\phi]}{[[\varrho_\theta \eta_\phi - \varrho_\phi \eta_\theta]^2 + \varrho^2[\varrho_\theta^2 + \eta_\theta^2]]^2} + \frac{2[1 + \gamma \cos \theta]^2}{[\varrho_\theta \eta_\phi - \varrho_\phi \eta_\theta]^2 + \varrho^2[\varrho_\theta^2 + \eta_\theta^2]} \\ + \frac{2[[\varrho_\theta^2 + \eta_\theta^2][1 + \gamma \cos \theta]^2 + [\varrho_\phi^2 + \eta_\phi^2 + \varrho^2]\gamma^2] [2\varrho_\phi^2 \eta_\theta - 2\eta_\phi \varrho_\phi \varrho_\theta + 2\varrho^2 \eta_\theta]^2}{[[\varrho_\theta \eta_\phi - \varrho_\phi \eta_\theta]^2 + \varrho^2[\varrho_\theta^2 + \eta_\theta^2]]^3} \\ - \frac{[[\varrho_\theta^2 + \eta_\theta^2][1 + \gamma \cos \theta]^2 + [\varrho_\phi^2 + \eta_\phi^2 + \varrho^2]\gamma^2] [2\varrho_\phi^2 + 2\varrho^2]}{[[\varrho_\theta \eta_\phi - \varrho_\phi \eta_\theta]^2 + \varrho^2[\varrho_\theta^2 + \eta_\theta^2]]^2}, \quad (\text{C.35})$$

$$\beta[\mathbf{C}_{\eta_\theta\eta_\theta} \mathbf{D}] \cdot \mathbf{D} = \frac{2\Phi_0^2[\varrho_\phi^2 \eta_\theta - \eta_\phi \varrho_\phi \varrho_\theta + \varrho^2 \eta_\theta]^2}{\beta H^2 [[\varrho_\theta \eta_\phi - \varrho_\phi \eta_\theta]^2 + \varrho^2[\varrho_\theta^2 + \eta_\theta^2]] \gamma^2 [1 + \gamma \cos \theta]^2} - \frac{\Phi_0^2[\varrho_\phi^2 + \varrho^2]}{2\beta H^2 \gamma^2 [1 + \gamma \cos \theta]^2} \quad (\text{C.36})$$

The second derivative of  $\Omega$  with respect to  $\eta_\theta$  and  $\eta_\phi$  is given by

$$\Omega_{\eta_\theta\eta_\phi} = C_1[I_{1\eta_\theta\eta_\phi} + \alpha I_{2\eta_\theta\eta_\phi}] + \beta[\mathbf{C}_{\eta_\theta\eta_\phi} \mathbf{D}] \cdot \mathbf{D}, \quad (\text{C.37})$$

where

$$I_{1\eta_\theta\eta_\phi} = \frac{4\varrho_\theta[\eta_\phi \varrho_\theta - \varrho_\phi \eta_\theta]\gamma^2[1 + \gamma \cos \theta]^2 [2\varrho_\phi^2 \eta_\theta - 2\varrho_\phi \eta_\phi \varrho_\theta + 2\varrho^2 \eta_\theta]}{[[\varrho_\theta \eta_\phi - \varrho_\phi \eta_\theta]^2 + \varrho^2[\varrho_\theta^2 + \eta_\theta^2]]^3} + \frac{2\varrho_\phi \varrho_\theta \gamma^2 [1 + \gamma \cos \theta]^2}{[[\varrho_\theta \eta_\phi - \varrho_\phi \eta_\theta]^2 + \varrho^2[\varrho_\theta^2 + \eta_\theta^2]]^2}, \quad (\text{C.38})$$

$$I_{2\eta_\theta\eta_\phi} = -\frac{2\varrho_\phi \varrho_\theta}{\gamma^2[1 + \gamma \cos \theta]^2} - \frac{4\varrho_\theta \eta_\theta[\eta_\phi \varrho_\theta - \varrho_\phi \eta_\theta][1 + \gamma \cos \theta]^2}{[[\varrho_\theta \eta_\phi - \varrho_\phi \eta_\theta]^2 + \varrho^2[\varrho_\theta^2 + \eta_\theta^2]]^2} - \frac{2\eta_\phi [2\varrho^2 \eta_\theta - 2\varrho_\phi[\eta_\phi \varrho_\theta - \varrho_\phi \eta_\theta]] \gamma^2}{[[\varrho_\theta \eta_\phi - \varrho_\phi \eta_\theta]^2 + \varrho^2[\varrho_\theta^2 + \eta_\theta^2]]^2} \\ + \frac{2\varrho_\phi \varrho_\theta [[\varrho_\theta^2 + \eta_\theta^2][1 + \gamma \cos \theta]^2 + [\varrho_\phi^2 + \eta_\phi^2 + \varrho^2]\gamma^2]}{[[\varrho_\theta \eta_\phi - \varrho_\phi \eta_\theta]^2 + \varrho^2[\varrho_\theta^2 + \eta_\theta^2]]^2} \\ + \frac{4\varrho_\theta[\eta_\phi \varrho_\theta - \varrho_\phi \eta_\theta] [2\varrho^2 \eta_\theta - 2\varrho_\phi[\eta_\phi \varrho_\theta - \varrho_\phi \eta_\theta]] [[\varrho_\theta^2 + \eta_\theta^2][1 + \gamma \cos \theta]^2 + [\varrho_\phi^2 + \eta_\phi^2 + \varrho^2]\gamma^2]}{[[\varrho_\theta \eta_\phi - \varrho_\phi \eta_\theta]^2 + \varrho^2[\varrho_\theta^2 + \eta_\theta^2]]^3}, \quad (\text{C.39})$$

$$\beta[\mathbf{C}_{\eta_\theta\eta_\phi} \mathbf{D}] \cdot \mathbf{D} = \frac{\Phi_0^2 \varrho_\theta[\eta_\phi \varrho_\theta - \varrho_\phi \eta_\theta] [2\varrho_\phi^2 \eta_\theta - 2\varrho_\phi \eta_\phi \varrho_\theta + 2\varrho^2 \eta_\theta]}{\beta H^2 [[\varrho_\theta \eta_\phi - \varrho_\phi \eta_\theta]^2 + \varrho^2[\varrho_\theta^2 + \eta_\theta^2]] \gamma^2 [1 + \gamma \cos \theta]^2} - \frac{\Phi_0^2 \varrho_\phi \varrho_\theta}{2\beta H^2 \gamma^2 [1 + \gamma \cos \theta]^2}. \quad (\text{C.40})$$

The second derivative of  $\Omega$  with respect to  $\varrho_\phi$  is given by

$$\Omega_{\varrho_\phi \varrho_\phi} = C_1[I_{1\varrho_\phi \varrho_\phi} + \alpha I_{2\varrho_\phi \varrho_\phi}] + \beta[\mathbf{C}_{\varrho_\phi \varrho_\phi} \mathbf{D}] \cdot \mathbf{D}, \quad (\text{C.41})$$

where

$$I_{1\varrho_\phi\varrho_\phi} = \frac{2}{[1 + \gamma \cos \theta]^2} - \frac{2\eta_\theta^2 \gamma^2 [1 + \gamma \cos \theta]^2}{[[\varrho_\theta \eta_\phi - \varrho_\phi \eta_\theta]^2 + \varrho^2 [\varrho_\theta^2 + \eta_\theta^2]]^2} + \frac{8\eta_\theta^2 [\varrho_\theta \eta_\phi - \varrho_\phi \eta_\theta]^2 \gamma^2 [1 + \gamma \cos \theta]^2}{[[\varrho_\theta \eta_\phi - \varrho_\phi \eta_\theta]^2 + \varrho^2 [\varrho_\theta^2 + \eta_\theta^2]]^3}, \quad (\text{C.42})$$

$$\begin{aligned} I_{2\varrho_\phi\varrho_\phi} &= \frac{2\gamma^2}{[\varrho_\theta \eta_\phi - \varrho_\phi \eta_\theta]^2 + \varrho^2 [\varrho_\theta^2 + \eta_\theta^2]} + \frac{8\varrho_\phi \eta_\theta [\varrho_\theta \eta_\phi - \varrho_\phi \eta_\theta] \gamma^2}{[[\varrho_\theta \eta_\phi - \varrho_\phi \eta_\theta]^2 + \varrho^2 [\varrho_\theta^2 + \eta_\theta^2]]^2} + \frac{2\eta_\theta^2}{\gamma^2 [1 + \gamma \cos \theta]^2} \\ &\quad - \frac{2\eta_\theta^2 [[\varrho_\theta^2 + \eta_\theta^2][1 + \gamma \cos \theta]^2 + [\varrho_\phi^2 + \eta_\phi^2 + \varrho^2] \gamma^2]}{[[\varrho_\theta \eta_\phi - \varrho_\phi \eta_\theta]^2 + \varrho^2 [\varrho_\theta^2 + \eta_\theta^2]]^2} \\ &\quad + \frac{8\eta_\theta^2 [\varrho_\theta \eta_\phi - \varrho_\phi \eta_\theta]^2 [[\varrho_\theta^2 + \eta_\theta^2][1 + \gamma \cos \theta]^2 + [\varrho_\phi^2 + \eta_\phi^2 + \varrho^2] \gamma^2]}{[[\varrho_\theta \eta_\phi - \varrho_\phi \eta_\theta]^2 + \varrho^2 [\varrho_\theta^2 + \eta_\theta^2]]^3}, \end{aligned} \quad (\text{C.43})$$

$$\beta[\mathbf{C}_{\varrho_\phi\varrho_\phi} \mathbf{D}] \cdot \mathbf{D} = \frac{\Phi_0^2 \eta_\theta^2}{2\beta H^2 \gamma^2 [1 + \gamma \cos \theta]^2} + \frac{2\Phi_0^2 \eta_\theta^2 [\varrho_\theta \eta_\phi - \varrho_\phi \eta_\theta]^2}{\beta H^2 [[\varrho_\theta \eta_\phi - \varrho_\phi \eta_\theta]^2 + \varrho^2 [\varrho_\theta^2 + \eta_\theta^2]] \gamma^2 [1 + \gamma \cos \theta]^2}. \quad (\text{C.44})$$

The second derivative of  $\Omega$  with respect to  $\eta_\phi$  is given by

$$\Omega_{\eta_\phi \eta_\phi} = C_1 [I_{1\eta_\phi \eta_\phi} + \alpha I_{2\eta_\phi \eta_\phi}] + \beta [\mathbf{C}_{\eta_\phi \eta_\phi} \mathbf{D}] \cdot \mathbf{D}, \quad (\text{C.45})$$

where

$$I_{1\eta_\phi \eta_\phi} = \frac{2}{[1 + \gamma \cos \theta]^2} - \frac{2\varrho_\theta^2 \gamma^2 [1 + \gamma \cos \theta]^2}{[[\varrho_\theta \eta_\phi - \varrho_\phi \eta_\theta]^2 + \varrho^2 [\varrho_\theta^2 + \eta_\theta^2]]^2} + \frac{8\varrho_\theta^2 [\varrho_\theta \eta_\phi - \varrho_\phi \eta_\theta]^2 \gamma^2 [1 + \gamma \cos \theta]^2}{[[\varrho_\theta \eta_\phi - \varrho_\phi \eta_\theta]^2 + \varrho^2 [\varrho_\theta^2 + \eta_\theta^2]]^3}, \quad (\text{C.46})$$

$$\begin{aligned} I_{2\eta_\phi \eta_\phi} &= \frac{2\gamma^2}{[\varrho_\theta \eta_\phi - \varrho_\phi \eta_\theta]^2 + \varrho^2 [\varrho_\theta^2 + \eta_\theta^2]} - \frac{8\eta_\phi \varrho_\theta [\varrho_\theta \eta_\phi - \varrho_\phi \eta_\theta] \gamma^2}{[[\varrho_\theta \eta_\phi - \varrho_\phi \eta_\theta]^2 + \varrho^2 [\varrho_\theta^2 + \eta_\theta^2]]^2} + \frac{2\varrho_\theta^2}{\gamma^2 [1 + \gamma \cos \theta]^2} \\ &\quad - \frac{2\varrho_\theta^2 [[\varrho_\theta^2 + \eta_\theta^2][1 + \gamma \cos \theta]^2 + [\varrho_\phi^2 + \eta_\phi^2 + \varrho^2] \gamma^2]}{[[\varrho_\theta \eta_\phi - \varrho_\phi \eta_\theta]^2 + \varrho^2 [\varrho_\theta^2 + \eta_\theta^2]]^2} \\ &\quad + \frac{8\varrho_\theta^2 [\varrho_\theta \eta_\phi - \varrho_\phi \eta_\theta]^2 [[\varrho_\theta^2 + \eta_\theta^2][1 + \gamma \cos \theta]^2 + [\varrho_\phi^2 + \eta_\phi^2 + \varrho^2] \gamma^2]}{[[\varrho_\theta \eta_\phi - \varrho_\phi \eta_\theta]^2 + \varrho^2 [\varrho_\theta^2 + \eta_\theta^2]]^3}, \end{aligned} \quad (\text{C.47})$$

$$\beta[\mathbf{C}_{\eta_\phi \eta_\phi} \mathbf{D}] \cdot \mathbf{D} = \frac{\Phi_0^2 \varrho_\theta^2}{2\beta H^2 \gamma^2 [1 + \gamma \cos \theta]^2} + \frac{2\Phi_0^2 \varrho_\theta^2 [\varrho_\theta \eta_\phi - \varrho_\phi \eta_\theta]^2}{\beta H^2 [[\varrho_\theta \eta_\phi - \varrho_\phi \eta_\theta]^2 + \varrho^2 [\varrho_\theta^2 + \eta_\theta^2]] \gamma^2 [1 + \gamma \cos \theta]^2}. \quad (\text{C.48})$$

The second derivative of  $\Omega$  with respect to  $\varrho_\phi$  and  $\eta_\phi$  is given by

$$\Omega_{\varrho_\phi \eta_\phi} = C_1 [I_{1\varrho_\phi \eta_\phi} + \alpha I_{2\varrho_\phi \eta_\phi}] + \beta [\mathbf{C}_{\varrho_\phi \eta_\phi} \mathbf{D}] \cdot \mathbf{D}, \quad (\text{C.49})$$

where

$$I_{1\varrho_\phi\eta_\phi} = \frac{2\varrho_\theta\eta_\theta\gamma^2[1+\gamma\cos\theta]^2}{[[\varrho_\theta\eta_\phi - \varrho_\phi\eta_\theta]^2 + \varrho^2[\varrho_\theta^2 + \eta_\theta^2]]^2} - \frac{8\varrho_\theta\eta_\theta[\varrho_\theta\eta_\phi - \varrho_\phi\eta_\theta]^2\gamma^2[1+\gamma\cos\theta]^2}{[[\varrho_\theta\eta_\phi - \varrho_\phi\eta_\theta]^2 + \varrho^2[\varrho_\theta^2 + \eta_\theta^2]]^3}, \quad (\text{C.50})$$

$$\begin{aligned} I_{2\varrho_\phi\eta_\phi} = & -\frac{2\varrho_\theta\eta_\theta}{\gamma^2[1+\gamma\cos\theta]^2} - \frac{4\varrho_\phi\varrho_\theta[\varrho_\theta\eta_\phi - \varrho_\phi\eta_\theta]\gamma^2}{[[\varrho_\theta\eta_\phi - \varrho_\phi\eta_\theta]^2 + \varrho^2[\varrho_\theta^2 + \eta_\theta^2]]^2} + \frac{4\eta_\phi\eta_\theta[\varrho_\theta\eta_\phi - \varrho_\phi\eta_\theta]\gamma^2}{[[\varrho_\theta\eta_\phi - \varrho_\phi\eta_\theta]^2 + \varrho^2[\varrho_\theta^2 + \eta_\theta^2]]^2} \\ & + \frac{8\varrho_\theta\eta_\theta[\varrho_\theta\eta_\phi - \varrho_\phi\eta_\theta]^2[[\varrho_\theta^2 + \eta_\theta^2][1+\gamma\cos\theta]^2 + [\varrho_\phi^2 + \eta_\phi^2 + \varrho^2]\gamma^2]}{[[\varrho_\theta\eta_\phi - \varrho_\phi\eta_\theta]^2 + \varrho^2[\varrho_\theta^2 + \eta_\theta^2]]^3} \\ & + \frac{2\varrho_\theta\eta_\theta[[\varrho_\theta^2 + \eta_\theta^2][1+\gamma\cos\theta]^2 + [\varrho_\phi^2 + \eta_\phi^2 + \varrho^2]\gamma^2]}{[[\varrho_\theta\eta_\phi - \varrho_\phi\eta_\theta]^2 + \varrho^2[\varrho_\theta^2 + \eta_\theta^2]]^2}, \end{aligned} \quad (\text{C.51})$$

$$\beta[\mathbf{C}_{\varrho_\phi\eta_\phi} \mathbf{D}] \cdot \mathbf{D} = \frac{\Phi_0^2\varrho_\theta\eta_\theta}{2\beta H^2\gamma^2[1+\gamma\cos\theta]^2} - \frac{2\Phi_0^2\varrho_\theta\eta_\theta[\varrho_\theta\eta_\phi - \varrho_\phi\eta_\theta]^2}{\beta H^2[[\varrho_\theta\eta_\phi - \varrho_\phi\eta_\theta]^2 + \varrho^2[\varrho_\theta^2 + \eta_\theta^2]]\gamma^2[1+\gamma\cos\theta]^2}. \quad (\text{C.52})$$

Finally, the full derivative of  $\Omega_{\varrho_\phi\eta_\phi}$  with respect to  $\phi$  is expressed as

$$\frac{d\Omega_{\varrho_\phi\eta_\phi}}{d\phi} = C_1\left[\frac{dI_{1\varrho_\phi\eta_\phi}}{d\phi} + \alpha\frac{dI_{2\varrho_\phi\eta_\phi}}{d\phi}\right] + \beta\left[\frac{d\mathbf{C}_{\varrho_\phi\eta_\phi}}{d\phi} \mathbf{D}\right] \cdot \mathbf{D}, \quad (\text{C.53})$$

where

$$\begin{aligned}
\frac{dI_{1\varrho\varrho\phi}}{d\phi} &= -\frac{8\varrho\eta\theta[\eta_{\phi\phi}\varrho_{\theta}-\varrho_{\phi\phi}\eta_{\theta}][\varrho_{\theta}^2+\eta_{\theta}^2]\gamma^2[1+\gamma\cos\theta]^2}{[[\varrho_{\theta}\eta_{\phi}-\varrho_{\phi}\eta_{\theta}]^2+\varrho^2[\varrho_{\theta}^2+\eta_{\theta}^2]]^3}-\frac{8\varrho_{\phi}\eta_{\theta}[\eta_{\phi}\varrho_{\theta}-\varrho_{\phi}\eta_{\theta}][\varrho_{\theta}^2+\eta_{\theta}^2]\gamma^2[1+\gamma\cos\theta]^2}{[[\varrho_{\theta}\eta_{\phi}-\varrho_{\phi}\eta_{\theta}]^2+\varrho^2[\varrho_{\theta}^2+\eta_{\theta}^2]]^3} \\
&+ \frac{24\varrho\eta_{\theta}[\eta_{\phi}\varrho_{\theta}-\varrho_{\phi}\eta_{\theta}][\varrho_{\theta}^2+\eta_{\theta}^2]\gamma^2[1+\gamma\cos\theta]^2}{[[\varrho_{\theta}\eta_{\phi}-\varrho_{\phi}\eta_{\theta}]^2+\varrho^2[\varrho_{\theta}^2+\eta_{\theta}^2]]^4}[2[\eta_{\phi}\varrho_{\theta}-\varrho_{\phi}\eta_{\theta}][\eta_{\phi\phi}\varrho_{\theta}-\varrho_{\phi\phi}\eta_{\theta}]+2\varrho_{\phi}\varrho[\varrho_{\theta}^2+\eta_{\theta}^2]], \\
\frac{dI_{2\varrho\varrho\phi}}{d\phi} &= \frac{4\varrho_{\phi}\gamma^2\eta_{\theta}[\varrho_{\theta}\eta_{\phi}-\varrho_{\phi}\eta_{\theta}]}{[[\varrho_{\theta}\eta_{\phi}-\varrho_{\phi}\eta_{\theta}]^2+\varrho^2[\varrho_{\theta}^2+\eta_{\theta}^2]]^2}+\frac{4\varrho\gamma^2\eta_{\theta}[\varrho_{\theta}\eta_{\phi\phi}-\varrho_{\phi\phi}\eta_{\theta}]}{[[\varrho_{\theta}\eta_{\phi}-\varrho_{\phi}\eta_{\theta}]^2+\varrho^2[\varrho_{\theta}^2+\eta_{\theta}^2]]^2} \\
&- \frac{8\varrho\gamma^2\eta_{\theta}[\varrho_{\theta}\eta_{\phi}-\varrho_{\phi}\eta_{\theta}]}{[[\varrho_{\theta}\eta_{\phi}-\varrho_{\phi}\eta_{\theta}]^2+\varrho^2[\varrho_{\theta}^2+\eta_{\theta}^2]]^3}[2[\varrho_{\theta}\eta_{\phi}-\varrho_{\phi}\eta_{\theta}][\varrho_{\theta}\eta_{\phi\phi}-\varrho_{\phi\phi}\eta_{\theta}]+2\varrho\varrho_{\phi}[\varrho_{\theta}^2+\eta_{\theta}^2]] \\
&- \frac{4\varrho_{\phi\phi}\varrho[\varrho_{\theta}^2+\eta_{\theta}^2]\gamma^2}{[[\varrho_{\theta}\eta_{\phi}-\varrho_{\phi}\eta_{\theta}]^2+\varrho^2[\varrho_{\theta}^2+\eta_{\theta}^2]]^2}-\frac{4\varrho_{\phi}\varrho_{\phi}[\varrho_{\theta}^2+\eta_{\theta}^2]\gamma^2}{[[\varrho_{\theta}\eta_{\phi}-\varrho_{\phi}\eta_{\theta}]^2+\varrho^2[\varrho_{\theta}^2+\eta_{\theta}^2]]^2} \\
&+ \frac{8\varrho_{\phi}\varrho[\varrho_{\theta}^2+\eta_{\theta}^2]\gamma^2}{[[\varrho_{\theta}\eta_{\phi}-\varrho_{\phi}\eta_{\theta}]^2+\varrho^2[\varrho_{\theta}^2+\eta_{\theta}^2]]^3}[2[\varrho_{\theta}\eta_{\phi}-\varrho_{\phi}\eta_{\theta}][\varrho_{\theta}\eta_{\phi\phi}-\varrho_{\phi\phi}\eta_{\theta}]+2\varrho\varrho_{\phi}[\varrho_{\theta}^2+\eta_{\theta}^2]] \\
&- \frac{8\varrho_{\phi}\eta_{\theta}[\varrho_{\theta}\eta_{\phi}-\varrho_{\phi}\eta_{\theta}][\varrho_{\theta}^2+\eta_{\theta}^2][[\varrho_{\theta}^2+\eta_{\theta}^2][1+\gamma\cos\theta]^2+[\varrho_{\phi}^2+\eta_{\phi}^2+\varrho^2]\gamma^2]}{[[\varrho_{\theta}\eta_{\phi}-\varrho_{\phi}\eta_{\theta}]^2+\varrho^2[\varrho_{\theta}^2+\eta_{\theta}^2]]^3} \\
&- \frac{8\varrho\eta_{\theta}[\varrho_{\theta}\eta_{\phi\phi}-\varrho_{\phi\phi}\eta_{\theta}][\varrho_{\theta}^2+\eta_{\theta}^2][[\varrho_{\theta}^2+\eta_{\theta}^2][1+\gamma\cos\theta]^2+[\varrho_{\phi}^2+\eta_{\phi}^2+\varrho^2]\gamma^2]}{[[\varrho_{\theta}\eta_{\phi}-\varrho_{\phi}\eta_{\theta}]^2+\varrho^2[\varrho_{\theta}^2+\eta_{\theta}^2]]^3} \\
&- \frac{8\varrho\eta_{\theta}[\varrho_{\theta}\eta_{\phi}-\varrho_{\phi}\eta_{\theta}][\varrho_{\theta}^2+\eta_{\theta}^2][2\varrho_{\phi}\varrho_{\phi\phi}+2\eta_{\phi}\eta_{\phi\phi}+2\varrho\varrho_{\phi}]\gamma^2}{[[\varrho_{\theta}\eta_{\phi}-\varrho_{\phi}\eta_{\theta}]^2+\varrho^2[\varrho_{\theta}^2+\eta_{\theta}^2]]^3} \\
&+ \frac{24\varrho\eta_{\theta}[\varrho_{\theta}\eta_{\phi}-\varrho_{\phi}\eta_{\theta}][\varrho_{\theta}^2+\eta_{\theta}^2][[\varrho_{\theta}^2+\eta_{\theta}^2][1+\gamma\cos\theta]^2+[\varrho_{\phi}^2+\eta_{\phi}^2+\varrho^2]\gamma^2]}{[[\varrho_{\theta}\eta_{\phi}-\varrho_{\phi}\eta_{\theta}]^2+\varrho^2[\varrho_{\theta}^2+\eta_{\theta}^2]]^4} \\
&\cdot [2[\varrho_{\theta}\eta_{\phi}-\varrho_{\phi}\eta_{\theta}][\varrho_{\theta}\eta_{\phi\phi}-\varrho_{\phi\phi}\eta_{\theta}]+2\varrho\varrho_{\phi}[\varrho_{\theta}^2+\eta_{\theta}^2]] \\
&+ \frac{24\varrho\eta_{\theta}[\eta_{\phi}\varrho_{\theta}-\varrho_{\phi}\eta_{\theta}][\varrho_{\theta}^2+\eta_{\theta}^2]\gamma^2[1+\gamma\cos\theta]^2}{[[\varrho_{\theta}\eta_{\phi}-\varrho_{\phi}\eta_{\theta}]^2+\varrho^2[\varrho_{\theta}^2+\eta_{\theta}^2]]^4}[2[\eta_{\phi}\varrho_{\theta}-\varrho_{\phi}\eta_{\theta}][\eta_{\phi\phi}\varrho_{\theta}-\varrho_{\phi\phi}\eta_{\theta}]+2\varrho_{\phi}\varrho[\varrho_{\theta}^2+\eta_{\theta}^2]], \\
\beta\left[\frac{d\mathbf{C}_{\varrho\varrho\phi}}{d\phi}\cdot\mathbf{D}\right]\cdot\mathbf{D} &= -\frac{2\Phi_0^2\varrho\eta_{\theta}[\eta_{\phi\phi}\varrho_{\theta}-\varrho_{\phi\phi}\eta_{\theta}][\varrho_{\theta}^2+\eta_{\theta}^2]}{\beta H^2[[\varrho_{\theta}\eta_{\phi}-\varrho_{\phi}\eta_{\theta}]^2+\varrho^2[\varrho_{\theta}^2+\eta_{\theta}^2]]\gamma^2[1+\gamma\cos\theta]^2} \\
&- \frac{2\Phi_0^2\varrho_{\phi}\eta_{\theta}[\eta_{\phi}\varrho_{\theta}-\varrho_{\phi}\eta_{\theta}][\varrho_{\theta}^2+\eta_{\theta}^2]}{\beta H^2[[\varrho_{\theta}\eta_{\phi}-\varrho_{\phi}\eta_{\theta}]^2+\varrho^2[\varrho_{\theta}^2+\eta_{\theta}^2]]\gamma^2[1+\gamma\cos\theta]^2} \\
&+ \frac{6\Phi_0^2\varrho\eta_{\theta}[\eta_{\phi}\varrho_{\theta}-\varrho_{\phi}\eta_{\theta}][\varrho_{\theta}^2+\eta_{\theta}^2]}{\beta H^2[[\varrho_{\theta}\eta_{\phi}-\varrho_{\phi}\eta_{\theta}]^2+\varrho^2[\varrho_{\theta}^2+\eta_{\theta}^2]]^2\gamma^2[1+\gamma\cos\theta]^2}[2[\eta_{\phi}\varrho_{\theta}-\varrho_{\phi}\eta_{\theta}][\eta_{\phi\phi}\varrho_{\theta}-\varrho_{\phi\phi}\eta_{\theta}]+2\varrho_{\phi}\varrho[\varrho_{\theta}^2+\eta_{\theta}^2]].
\end{aligned} \tag{C.54}$$

## 567 Appendix D. Reformulation of the coupled ODEs

The derivatives of the stretches in equations (9) with respect to  $\theta$  are expressed as

$$\lambda_{1\theta} = \frac{\varrho_{\theta}\varrho_{\theta\theta}+\eta_{\theta}\eta_{\theta\theta}}{\gamma[\varrho_{\theta}^2+\eta_{\theta}^2]^{1/2}} = \frac{\varrho_{\theta}\varrho_{\theta\theta}+\eta_{\theta}\eta_{\theta\theta}}{\gamma^2\lambda_1}, \quad \lambda_{2\theta} = \frac{\varrho_{\theta}}{1+\gamma\cos\theta} + \frac{\varrho\gamma\sin\theta}{[1+\gamma\cos\theta]^2}. \tag{D.1}$$

The equations (31a) and (31b) can be rewritten as

$$\begin{aligned}
& -\gamma \sin \theta \left[ \frac{2\rho\theta}{\gamma^2} [1 + \alpha\lambda_2^2] \left[ 1 - \frac{1}{\lambda_1^4\lambda_2^2} \right] - \frac{\rho\theta \mathcal{E}\lambda_2^2}{2\gamma^2} \right] \\
& + [1 + \gamma \cos \theta] \left[ \frac{2\rho\theta\theta}{\gamma^2} [1 + \alpha\lambda_2^2] \left[ 1 - \frac{1}{\lambda_1^4\lambda_2^2} \right] + \frac{2\rho\theta}{\gamma^2} [2\alpha\lambda_2\lambda_{2\theta}] \left[ 1 - \frac{1}{\lambda_1^4\lambda_2^2} \right] \right. \\
& \left. + \frac{2\rho\theta}{\gamma^2} [1 + \alpha\lambda_2^2] \left[ \frac{2\lambda_{2\theta}}{\lambda_2^3\lambda_1^4} + \frac{4\lambda_{1\theta}}{\lambda_2^2\lambda_1^5} \right] - \frac{\mathcal{E}\lambda_2^2}{2\gamma^2}\rho_{\theta\theta} - \frac{2\rho\theta\mathcal{E}}{\gamma^2}\lambda_2\lambda_{2\theta} \right] \\
& - 2\lambda_2 [1 + \alpha\lambda_1^2] \left[ 1 - \frac{1}{\lambda_1^2\lambda_2^4} \right] + \frac{\mathcal{E}\lambda_2\lambda_1^2}{2} + \frac{P\rho\eta\theta}{\gamma} = 0, \tag{D.2}
\end{aligned}$$

$$\begin{aligned}
& -\gamma \sin \theta \left[ \frac{2\eta\theta}{\gamma^2} [1 + \alpha\lambda_2^2] \left[ 1 - \frac{1}{\lambda_1^4\lambda_2^2} \right] - \frac{\mathcal{E}\eta\theta\lambda_2^2}{2\gamma^2} \right] \\
& + [1 + \gamma \cos \theta] \left[ \frac{2\eta\theta\theta}{\gamma^2} [1 + \alpha\lambda_2^2] \left[ 1 - \frac{1}{\lambda_1^4\lambda_2^2} \right] + \frac{2\eta\theta}{\gamma^2} [2\alpha\lambda_2\lambda_{2\theta}] \left[ 1 - \frac{1}{\lambda_1^4\lambda_2^2} \right] \right. \\
& \left. + \frac{2\eta\theta}{\gamma^2} [1 + \alpha\lambda_2^2] \left[ \frac{2\lambda_{2\theta}}{\lambda_2^3\lambda_1^4} + \frac{4\lambda_{1\theta}}{\lambda_2^2\lambda_1^5} \right] - \frac{\mathcal{E}\lambda_2^2}{2\gamma^2}\eta_{\theta\theta} - \frac{2\eta\theta\mathcal{E}}{\gamma^2}\lambda_2\lambda_{2\theta} \right] - \frac{P\rho\theta\theta}{\gamma} = 0. \tag{D.3}
\end{aligned}$$

From the first equation, the coefficient of  $\rho_{\theta\theta}$  is

$$A_1 = [1 + \gamma \cos \theta] \left[ \frac{2}{\gamma^2} [1 + \alpha\lambda_2^2] \left[ 1 - \frac{1}{\lambda_1^4\lambda_2^2} \right] + \frac{8\rho_{\theta\theta}^2}{\gamma^4\lambda_1^6\lambda_2^2} [1 + \alpha\lambda_2^2] - \frac{\mathcal{E}\lambda_2^2}{2\gamma^2} \right]. \tag{D.4}$$

The coefficient of  $\eta_{\theta\theta}$  is given by

$$A_2 = [1 + \gamma \cos \theta] \frac{8\rho\theta\eta\theta}{\gamma^4\lambda_1^6\lambda_2^2} [1 + \alpha\lambda_2^2], \tag{D.5}$$

and the remaining term is

$$\begin{aligned}
A_3 = & -\gamma \sin \theta \left[ \frac{2\rho\theta}{\gamma^2} [1 + \alpha\lambda_2^2] \left[ 1 - \frac{1}{\lambda_1^4\lambda_2^2} \right] - \frac{\mathcal{E}\rho\theta\lambda_2^2}{2\gamma^2} \right] \\
& + [1 + \gamma \cos \theta] \left[ \frac{2\rho\theta}{\gamma^2} [2\alpha\lambda_2\lambda_{2\theta}] \left[ 1 - \frac{1}{\lambda_1^4\lambda_2^2} \right] + \frac{4\rho\theta\lambda_{2\theta}}{\gamma^2\lambda_2^3\lambda_1^4} [1 + \alpha\lambda_2^2] - \frac{2\rho\theta\mathcal{E}}{\gamma^2}\lambda_2\lambda_{2\theta} \right] \\
& - 2\lambda_2 [1 + \alpha\lambda_1^2] \left[ 1 - \frac{1}{\lambda_1^2\lambda_2^4} \right] + \frac{\mathcal{E}\lambda_2\lambda_1^2}{2} + \frac{P\rho\eta\theta}{\gamma} \tag{D.6}
\end{aligned}$$

From the second equation, the coefficient of  $\rho''$  is

$$B_1 = [1 + \gamma \cos \theta] \frac{8\rho\theta\eta\theta}{\gamma^4\lambda_1^6\lambda_2^2} [1 + \alpha\lambda_2^2] \tag{D.7}$$

and the coefficient of  $\eta''$  is

$$B_2 = [1 + \gamma \cos \theta] \left[ \frac{2}{\gamma^2} [1 + \alpha\lambda_2^2] \left[ 1 - \frac{1}{\lambda_1^2\lambda_2^4} \right] + \frac{8\eta_{\theta\theta}^2}{\gamma^4\lambda_1^6\lambda_2^2} [1 + \alpha\lambda_2^2] - \frac{\mathcal{E}\lambda_2^2}{2\gamma^2} \right] \tag{D.8}$$

and the remaining term is

$$B_3 = -\gamma \sin \theta \left[ \frac{2\eta_\theta}{\gamma^2} [1 + \alpha\lambda_2^2] \left[ 1 - \frac{1}{\lambda_1^4 \lambda_2^2} \right] - \frac{\mathcal{E} \lambda_2^2 \eta_\theta}{2\gamma^2} \right] \\ + [1 + \gamma \cos \theta] \left[ \frac{2\eta'}{\gamma^2} [2\alpha\lambda_2 \lambda_{2\theta}] \left[ 1 - \frac{1}{\lambda_1^4 \lambda_2^2} \right] + [1 + \alpha\lambda_2^2] \frac{4\eta_\theta \lambda_{2\theta}}{\gamma^2 \lambda_1^4 \lambda_2^3} - \frac{2\eta_\theta \mathcal{E}}{\gamma^2} \lambda_2 \lambda_{2\theta} \right] - \frac{P \varrho \varrho_\theta}{\gamma}. \quad (\text{D.9})$$

Therefore the above set of coupled ODEs can be rewritten as

$$A_1 \varrho_{\theta\theta} + A_2 \eta_{\theta\theta} + A_3 = 0, \quad (\text{D.10})$$

$$B_1 \varrho_{\theta\theta} + B_2 \eta_{\theta\theta} + B_3 = 0. \quad (\text{D.11})$$

## 568 Appendix E. Reformulation of the ODEs arising from the relaxed energy

The governing equations (31) are now modified as in equations (50) where the modified energy density function is expressed as:

$$\Omega^*(\lambda_1, \mathcal{E}) = C_1 [I_1^* - 3] + C_2 [I_2^* - 3] + \beta [\mathbf{C} \mathbf{D}] \cdot \mathbf{D}. \quad (\text{E.1})$$

As  $\Omega^*$  is not a function of  $\lambda_2$ ,  $\frac{\partial \Omega^*}{\partial \varrho}$  is vanished. We first use the chain rule to compute the derivatives of  $\Omega^*$  with respect to  $\varrho_\theta$  and  $\eta_\theta$  as

$$\frac{\partial \Omega^*}{\partial \varrho_\theta} = \frac{\partial \Omega^*}{\partial \lambda_1} \frac{\partial \lambda_1}{\partial \varrho_\theta}, \quad \frac{\partial \Omega^*}{\partial \eta_\theta} = \frac{\partial \Omega^*}{\partial \lambda_1} \frac{\partial \lambda_1}{\partial \eta_\theta}. \quad (\text{E.2})$$

The derivatives of  $\lambda_1$  with respect to  $\varrho_\theta$  and  $\eta_\theta$  are easy to be computed as

$$\frac{\partial \lambda_1}{\partial \varrho_\theta} = \frac{\varrho_\theta}{\gamma} [\varrho_\theta^2 + \eta_\theta^2]^{-\frac{1}{2}}, \quad \frac{\partial \lambda_1}{\partial \eta_\theta} = \frac{\eta_\theta}{\gamma} [\varrho_\theta^2 + \eta_\theta^2]^{-\frac{1}{2}}. \quad (\text{E.3})$$

The derivative of  $\Omega^*$  with respect to  $\lambda_1$  can be decomposed as follows

$$\frac{\partial \Omega^*}{\partial \lambda_1} = C_1 \frac{\partial I_1^*}{\partial \lambda_1} + C_2 \frac{\partial I_2^*}{\partial \lambda_1} + \frac{\partial (\beta [\mathbf{C} \mathbf{D}] \cdot \mathbf{D})}{\partial \lambda_1}, \quad (\text{E.4})$$

where

$$\frac{\partial I_1^*}{\partial \lambda_1} = 2\lambda_1 + \frac{\partial(\lambda_2^{*2})}{\partial \lambda_1} - \frac{2}{\lambda_1^3 \lambda_2^{*2}} - \frac{1}{\lambda_1^2 \lambda_2^{*4}} \frac{\partial(\lambda_2^{*2})}{\partial \lambda_1}, \quad (\text{E.5})$$

$$\frac{\partial I_2^*}{\partial \lambda_1} = -\frac{2}{\lambda_1^3} - \frac{\partial(\lambda_2^{*2})}{\lambda_2^{*4} \partial \lambda_1} + \lambda_1^2 \frac{\partial(\lambda_2^{*2})}{\partial \lambda_1} + 2\lambda_1 \lambda_2^{*2} \quad (\text{E.6})$$

and

$$\frac{\partial (\beta [\mathbf{C} \mathbf{D}] \cdot \mathbf{D})}{\partial \lambda_1} = \frac{C_1 \mathcal{E}}{4} \left[ 2\lambda_1 \lambda_2^{*2} + \lambda_1^2 \frac{\partial(\lambda_2^{*2})}{\partial \lambda_1} \right], \quad (\text{E.7})$$

where

$$\begin{aligned} \frac{\partial(\lambda_2^{*2})}{\partial\lambda_1} = & -\frac{PH[8\alpha\lambda_1 - 2\mathcal{E}\lambda_1]}{R_b[4\lambda_1 + 4\alpha\lambda_1^2 - \mathcal{E}\lambda_1^2]^2} \\ & + \frac{\frac{P^2H^2}{R_b^2}\lambda_1 + 32\alpha^2\lambda_1^3 - 8\mathcal{E}\alpha\lambda_1^3 + 32\alpha\lambda_1 - 4\mathcal{E}\lambda_1}{\left[\sqrt{\frac{P^2H^2}{R_b^2}\lambda_1^2 - 4\alpha\mathcal{E}\lambda_1^4 + 16\alpha^2\lambda_1^4 + 32\alpha\lambda_1^2 - 4\mathcal{E}\lambda_1^2 + 16}\right] [4\lambda_1 + 4\alpha\lambda_1^3 - \mathcal{E}\lambda_1^3]} \\ & - \frac{\left[\frac{PH}{R_b}\lambda_1 + \sqrt{\frac{P^2H^2}{R_b^2}\lambda_1^2 - 4\alpha\mathcal{E}\lambda_1^4 + 16\alpha^2\lambda_1^4 + 32\alpha\lambda_1^2 - 4\mathcal{E}\lambda_1^2 + 16}\right] [12\alpha\lambda_1^2 - 3\mathcal{E}\lambda_1^2 + 4]}{[4\lambda_1 + 4\alpha\lambda_1^3 - \mathcal{E}\lambda_1^3]^2}. \end{aligned} \quad (\text{E.8})$$

Then, the total derivatives of the two terms with respect to  $\theta$  are calculated as

$$\frac{d}{d\theta} \left( \frac{\partial\Omega^*}{\partial\varrho_\theta} \right) = \frac{d}{d\theta} \left( \frac{\varrho_\theta}{\gamma} [\varrho_\theta^2 + \eta_\theta^2]^{-\frac{1}{2}} \right) \frac{\partial\Omega^*}{\partial\lambda_1} + \frac{d}{d\theta} \left( \frac{\partial\Omega^*}{\partial\lambda_1} \right) \underbrace{\left[ \frac{\varrho_\theta}{\gamma} [\varrho_\theta^2 + \eta_\theta^2]^{-\frac{1}{2}} \right]}_{\mathcal{W}_1}, \quad (\text{E.9})$$

$$\frac{d}{d\theta} \left( \frac{\partial\Omega^*}{\partial\eta_\theta} \right) = \frac{d}{d\theta} \left( \frac{\eta_\theta}{\gamma} [\varrho_\theta^2 + \eta_\theta^2]^{-\frac{1}{2}} \right) \frac{\partial\Omega^*}{\partial\lambda_1} + \frac{d}{d\theta} \left( \frac{\partial\Omega^*}{\partial\lambda_1} \right) \underbrace{\left[ \frac{\eta_\theta}{\gamma} [\varrho_\theta^2 + \eta_\theta^2]^{-\frac{1}{2}} \right]}_{\mathcal{W}_2}. \quad (\text{E.10})$$

Upon explicitly computing the first full derivative terms in both equations and separating the coefficients of  $\varrho_{\theta\theta}$  and  $\eta_{\theta\theta}$  yields

$$\begin{aligned} \frac{d}{d\theta} \left( \frac{\varrho_\theta}{\gamma} [\varrho_\theta^2 + \eta_\theta^2]^{-\frac{1}{2}} \right) &= \frac{\varrho_{\theta\theta}}{\gamma} [\varrho_\theta^2 + \eta_\theta^2]^{-\frac{1}{2}} - \frac{\varrho_\theta}{\gamma} [\varrho_\theta \varrho_{\theta\theta} + \eta_\theta \eta_{\theta\theta}] [\varrho_\theta^2 + \eta_\theta^2]^{-\frac{3}{2}} \\ &= \underbrace{\left[ \frac{1}{\gamma[\varrho_\theta^2 + \eta_\theta^2]^{\frac{1}{2}}} - \frac{\varrho_\theta^2}{\gamma[\varrho_\theta^2 + \eta_\theta^2]^{\frac{3}{2}}} \right]}_{\mathcal{U}_1} \varrho_{\theta\theta} - \underbrace{\frac{\varrho_\theta \eta_\theta}{\gamma[\varrho_\theta^2 + \eta_\theta^2]^{\frac{3}{2}}}}_{\mathcal{U}_2} \eta_{\theta\theta}, \end{aligned} \quad (\text{E.11})$$

and

$$\begin{aligned} \frac{d}{d\theta} \left( \frac{\eta_\theta}{\gamma} [\varrho_\theta^2 + \eta_\theta^2]^{-\frac{1}{2}} \right) &= \frac{\eta_{\theta\theta}}{\gamma} [\varrho_\theta^2 + \eta_\theta^2]^{-\frac{1}{2}} - \frac{\eta_\theta}{\gamma} [\varrho_\theta \varrho_{\theta\theta} + \eta_\theta \eta_{\theta\theta}] [\varrho_\theta^2 + \eta_\theta^2]^{-\frac{3}{2}} \\ &= \underbrace{\left[ \frac{1}{\gamma[\varrho_\theta^2 + \eta_\theta^2]^{\frac{1}{2}}} - \frac{\eta_\theta^2}{\gamma[\varrho_\theta^2 + \eta_\theta^2]^{\frac{3}{2}}} \right]}_{\mathcal{V}_2} \eta_{\theta\theta} - \underbrace{\frac{\varrho_\theta \eta_\theta}{\gamma[\varrho_\theta^2 + \eta_\theta^2]^{\frac{3}{2}}}}_{\mathcal{V}_1} \varrho_{\theta\theta}. \end{aligned} \quad (\text{E.12})$$

The remaining full derivative term  $\frac{d}{d\theta} \left( \frac{\partial\Omega^*}{\partial\lambda_1} \right)$  is expressed as

$$\frac{d}{d\theta} \left( \frac{\partial\Omega^*}{\partial\lambda_1} \right) = C_1 \frac{d}{d\theta} \left( \frac{\partial I_1^*}{\partial\lambda_1} \right) + C_2 \frac{d}{d\theta} \left( \frac{\partial I_2^*}{\partial\lambda_1} \right) + \frac{d}{d\theta} \left( \frac{C_1 \mathcal{E}}{4} \left[ 2\lambda_1 \lambda_2^{*2} + \lambda_1^2 \frac{\partial(\lambda_2^{*2})}{\partial\lambda_1} \right] \right), \quad (\text{E.13})$$

where

$$\begin{aligned}
C_1 \frac{d}{d\theta} \left( \frac{\partial I_1^*}{\partial \lambda_1} \right) &= C_1 \frac{d}{d\theta} \left( \left[ 2\lambda_1 + \frac{\partial(\lambda_2^{*2})}{\partial \lambda_1} - \frac{2}{\lambda_1^3 \lambda_2^{*2}} - \frac{1}{\lambda_1^2 \lambda_2^{*4}} \frac{\partial(\lambda_2^{*2})}{\partial \lambda_1} \right] \right) \\
&= 2C_1 \lambda_{1\theta} + C_1 \left( \frac{\partial(\lambda_2^{*2})}{\partial \lambda_1} \right)_\theta + C_1 \left[ \frac{6\lambda_{1\theta}}{\lambda_1^4 \lambda_2^{*2}} + \frac{2(\lambda_2^{*2})_\theta}{\lambda_1^3 \lambda_2^{*4}} \right] \\
&\quad - C_1 \left[ \frac{1}{\lambda_1^2 \lambda_2^{*4}} \left( \frac{\partial(\lambda_2^{*2})}{\partial \lambda_1} \right)_\theta - \frac{2\lambda_{1\theta}}{\lambda_1^3 \lambda_2^{*4}} \frac{\partial(\lambda_2^{*2})}{\partial \lambda_1} - \frac{2(\lambda_2^{*2})_\theta}{\lambda_1^2 \lambda_2^{*6}} \frac{\partial(\lambda_2^{*2})}{\partial \lambda_1} \right] \\
&= C_1 \left[ \left[ 2 + \frac{6}{\lambda_1^4 \lambda_2^{*2}} + \frac{2}{\lambda_1^3 \lambda_1^{*4}} \frac{\partial(\lambda_2^{*2})}{\partial \lambda_1} \right] + \left[ \frac{2}{\lambda_1^3 \lambda_1^{*4}} + \frac{2}{\lambda_1^2 \lambda_1^{*6}} \frac{\partial(\lambda_2^{*2})}{\partial \lambda_1} \right] \frac{\partial(\lambda_2^{*2})}{\partial \lambda_1} \right. \\
&\quad \left. + \left[ 1 - \frac{1}{\lambda_1^2 \lambda_2^{*4}} \right] \frac{\partial^2(\lambda_2^{*2})}{\partial \lambda_1^2} \right] \lambda_{1\theta}, \tag{E.14}
\end{aligned}$$

$$\begin{aligned}
C_2 \frac{d}{d\theta} \left( \frac{\partial I_2^*}{\partial \lambda_1} \right) &= \frac{d}{d\theta} \left( C_2 \left[ -\frac{2}{\lambda_1^3} - \frac{1}{\lambda_2^{*4}} \frac{\partial(\lambda_2^{*2})}{\partial \lambda_1} + \lambda_1^2 \frac{\partial(\lambda_2^{*2})}{\partial \lambda_1} + 2\lambda_1 \lambda_2^{*2} \right] \right) \\
&= C_2 \frac{6}{\lambda_1^4} \lambda_{1\theta} - C_2 \left[ \frac{1}{\lambda_2^{*4}} \left( \frac{\partial(\lambda_2^{*2})}{\partial \lambda_1} \right)_\theta - \frac{2(\lambda_2^{*2})_\theta}{\lambda_2^{*6}} \frac{\partial(\lambda_2^{*2})}{\partial \lambda_1} \right] \\
&\quad + C_2 \left[ \lambda_1^2 \left( \frac{\partial(\lambda_2^{*2})}{\partial \lambda_1} \right)_\theta + 2\lambda_1 \lambda_{1\theta} \frac{\partial(\lambda_2^{*2})}{\partial \lambda_1} \right] + C_2 [2\lambda_1 (\lambda_2^{*2})_\theta + 2\lambda_2^{*2} \lambda_{1\theta}] \\
&= C_2 \left[ \left[ \frac{6}{\lambda_1^4} + 2\lambda_1 \frac{\partial(\lambda_2^{*2})}{\partial \lambda_1} + 2\lambda_2^{*2} \right] + \left[ \frac{2}{\lambda_2^{*6}} \frac{\partial(\lambda_2^{*2})}{\partial \lambda_1} + 2\lambda_1 \right] \frac{\partial(\lambda_2^{*2})}{\partial \lambda_1} \right. \\
&\quad \left. + \left[ \lambda_1^2 - \frac{1}{\lambda_2^{*4}} \right] \frac{\partial^2(\lambda_2^{*2})}{\partial \lambda_1^2} \right] \lambda_{1\theta}, \tag{E.15}
\end{aligned}$$

and

$$\begin{aligned}
&\frac{d}{d\theta} \left( \frac{C_1 \mathcal{E}}{4} \left[ 2\lambda_1 \lambda_2^{*2} + \lambda_1^2 \frac{\partial(\lambda_2^{*2})}{\partial \lambda_1} \right] \right) \\
&= \frac{C_1 \mathcal{E}}{4} \left[ 2\lambda_2^{*2} \lambda_{1\theta} + 2\lambda_1 (\lambda_2^{*2})_\theta + 2\lambda_1 \frac{\partial(\lambda_2^{*2})}{\partial \lambda_1} \lambda_{1\theta} + \lambda_1^2 \left( \frac{\partial(\lambda_2^{*2})}{\partial \lambda_1} \right)_\theta \right] \\
&= \frac{C_1 \mathcal{E}}{4} \left[ 2\lambda_2^{*2} + 4\lambda_1 \frac{\partial(\lambda_2^{*2})}{\partial \lambda_1} + \lambda_1^2 \frac{\partial^2(\lambda_2^{*2})}{\partial \lambda_1^2} \right] \lambda_{1\theta}. \tag{E.16}
\end{aligned}$$

The term

$$\begin{aligned}
\frac{\partial(\lambda_2^{*2})}{\partial \lambda_1} &= -\frac{PH[8\alpha\lambda_1 - 2\mathcal{E}\lambda_1]}{R_b[4\lambda_1 + 4\alpha\lambda_1^3 - \mathcal{E}\lambda_1^3]^2} \\
&\quad + \frac{\frac{P^2 H^2}{R_b^2} \lambda_1 + 32\alpha^2 \lambda_1^3 - 8\mathcal{E}\alpha \lambda_1^3 + 32\alpha \lambda_1 - 4\mathcal{E}\lambda_1}{\underbrace{\left[ \sqrt{\frac{P^2 H^2}{R_b^2} \lambda_1^2 - 4\alpha \mathcal{E} \lambda_1^4 + 16\alpha^2 \lambda_1^4 + 32\alpha \lambda_1^2 - 4\mathcal{E} \lambda_1^2 + 16} \right]}_c [4\lambda_1 + 4\alpha\lambda_1^3 - \mathcal{E}\lambda_1^3]} \\
&\quad - \frac{\left[ \frac{PH}{R_b} \lambda_1 + \sqrt{\frac{P^2 H^2}{R_b^2} \lambda_1^2 - 4\alpha \mathcal{E} \lambda_1^4 + 16\alpha^2 \lambda_1^4 + 32\alpha \lambda_1^2 - 4\mathcal{E} \lambda_1^2 + 16} \right] [12\alpha \lambda_1^2 - 3\mathcal{E} \lambda_1^2 + 4]}{\underbrace{[4\lambda_1 + 4\alpha\lambda_1^3 - \mathcal{E}\lambda_1^3]^2}_D}, \tag{E.17}
\end{aligned}$$



and hence

$$\frac{\partial^2(\lambda_2^{*2})}{\partial\lambda_1^2} = \frac{\partial}{\partial\lambda_1} \left( -\frac{PH[8\alpha\lambda_1 - 2\mathcal{E}\lambda_1]}{R_b[4\lambda_1 + 4\alpha\lambda_1^3 - \mathcal{E}\lambda_1^3]^2} \right) + \frac{\partial\mathcal{A}}{\partial\lambda_1} + \frac{\partial\mathcal{B}}{\partial\lambda_1}, \quad (\text{E.18})$$

where

$$\frac{\partial}{\partial\lambda_1} \left( -\frac{PH[8\alpha\lambda_1 - 2\mathcal{E}\lambda_1]}{R_b[4\lambda_1 + 4\alpha\lambda_1^2 - \mathcal{E}\lambda_1^2]^2} \right) = -\frac{PH}{R_b} \left[ \frac{8\alpha - 2\mathcal{E}}{[4\lambda_1 + 4\alpha\lambda_1^2 - \mathcal{E}\lambda_1^2]^2} - \frac{2[8\alpha\lambda_1 - 2\mathcal{E}\lambda_1]^2}{[4\lambda_1 + 4\alpha\lambda_1^2 - \mathcal{E}\lambda_1^2]^3} \right], \quad (\text{E.19})$$

$$\begin{aligned} \frac{\partial\mathcal{C}}{\partial\lambda_1} = & \frac{\frac{P^2H^2}{R_b^2} + 96\alpha^2\lambda_1^2 - 24\mathcal{E}\alpha\lambda_1^2 + 32\alpha - 4\mathcal{E}}{\left[ \sqrt{\frac{P^2H^2}{R_b^2}\lambda_1^2 - 4\alpha\mathcal{E}\lambda_1^4 + 16\alpha^2\lambda_1^4 + 32\alpha\lambda_1^2 - 4\mathcal{E}\lambda_1^2 + 16} \right] [4\lambda_1 + 4\alpha\lambda_1^3 - \mathcal{E}\lambda_1^3]} \\ & - \frac{\left[ \frac{P^2H^2}{R_b^2}\lambda_1 + 32\alpha^2\lambda_1^3 - 8\mathcal{E}\alpha\lambda_1^3 + 32\alpha\lambda_1 - 4\mathcal{E}\lambda_1 \right]^2}{\left[ \sqrt{\frac{P^2H^2}{R_b^2}\lambda_1^2 - 4\alpha\mathcal{E}\lambda_1^4 + 16\alpha^2\lambda_1^4 + 32\alpha\lambda_1^2 - 4\mathcal{E}\lambda_1^2 + 16} \right]^3 [4\lambda_1 + 4\alpha\lambda_1^3 - \mathcal{E}\lambda_1^3]} \\ & - \frac{\left[ \frac{P^2H^2}{R_b^2}\lambda_1 + 32\alpha^2\lambda_1^3 - 8\mathcal{E}\alpha\lambda_1^3 + 32\alpha\lambda_1 - 4\mathcal{E}\lambda_1 \right] [12\alpha\lambda_1^2 - 3\mathcal{E}\lambda_1^2 + 4]}{\left[ \sqrt{\frac{P^2H^2}{R_b^2}\lambda_1^2 - 4\alpha\mathcal{E}\lambda_1^4 + 16\alpha^2\lambda_1^4 + 32\alpha\lambda_1^2 - 4\mathcal{E}\lambda_1^2 + 16} \right] [4\lambda_1 + 4\alpha\lambda_1^3 - \mathcal{E}\lambda_1^3]^2}, \end{aligned} \quad (\text{E.20})$$

and

$$\begin{aligned} \frac{\partial\mathcal{D}}{\partial\lambda_1} = & \frac{\left[ \frac{PH}{R_b}\lambda_1 + \sqrt{\frac{P^2H^2}{R_b^2}\lambda_1^2 - 4\alpha\mathcal{E}\lambda_1^4 + 16\alpha^2\lambda_1^4 + 32\alpha\lambda_1^2 - 4\mathcal{E}\lambda_1^2 + 16} \right] [(24\alpha - 6\mathcal{E})\lambda_1]}{[4\lambda_1 + 4\alpha\lambda_1^3 - \mathcal{E}\lambda_1^3]^2} \\ & + \frac{\left[ \frac{PH}{R_b} + \frac{\frac{P^2H^2}{R_b^2}\lambda_1 + 32\alpha^2\lambda_1^3 - 8\mathcal{E}\alpha\lambda_1^3 + 32\alpha\lambda_1 - 4\mathcal{E}\lambda_1}{\sqrt{\frac{P^2H^2}{R_b^2}\lambda_1^2 - 4\alpha\mathcal{E}\lambda_1^4 + 16\alpha^2\lambda_1^4 + 32\alpha\lambda_1^2 - 4\mathcal{E}\lambda_1^2 + 16}} \right] [12\alpha\lambda_1^2 - 3\mathcal{E}\lambda_1^2 + 4]}{[4\lambda_1 + 4\alpha\lambda_1^3 - \mathcal{E}\lambda_1^3]^2} \\ & - 2 \frac{\left[ \frac{PH}{R_b}\lambda_1 + \sqrt{\frac{P^2H^2}{R_b^2}\lambda_1^2 - 4\alpha\mathcal{E}\lambda_1^4 + 16\alpha^2\lambda_1^4 + 32\alpha\lambda_1^2 - 4\mathcal{E}\lambda_1^2 + 16} \right] [12\alpha\lambda_1^2 - 3\mathcal{E}\lambda_1^2 + 4]^2}{[4\lambda_1 + 4\alpha\lambda_1^3 - \mathcal{E}\lambda_1^3]^3}. \end{aligned} \quad (\text{E.21})$$

$$\frac{d}{d\theta} \left( \frac{\partial\Omega^*}{\partial\lambda_1} \right) = C_1\mathcal{Z}\mathcal{W}_1\varrho_{\theta\theta} + C_1\mathcal{Z}\mathcal{W}_2\eta_{\theta\theta} \quad (\text{E.22})$$

where

$$\begin{aligned} \mathcal{Z} = & \left[ \left[ 2 + \frac{6}{\lambda_1^4\lambda_1^{*2}} + \frac{2}{\lambda_1^3\lambda_1^{*4}} \frac{\partial(\lambda_2^{*2})}{\partial\lambda_1} \right] + \left[ \frac{2}{\lambda_1^3\lambda_1^{*4}} + \frac{2}{\lambda_1^2\lambda_1^{*6}} \frac{\partial(\lambda_2^{*2})}{\partial\lambda_1} \right] \frac{\partial(\lambda_2^{*2})}{\partial\lambda_1} + \left[ 1 - \frac{1}{\lambda_1^2\lambda_2^{*4}} \right] \frac{\partial^2(\lambda_2^{*2})}{\partial\lambda_1^2} \right] \\ & + \alpha \left[ \left[ \frac{6}{\lambda_1^4} + 2\lambda_1 \frac{\partial(\lambda_2^{*2})}{\partial\lambda_1} + 2\lambda_2^{*2} \right] + \left[ \frac{2}{\lambda_2^{*6}} \frac{\partial(\lambda_2^{*2})}{\partial\lambda_1} + 2\lambda_1 \right] \frac{\partial(\lambda_2^{*2})}{\partial\lambda_1} + \left[ \lambda_1^2 - \frac{1}{\lambda_2^{*4}} \right] \frac{\partial^2(\lambda_2^{*2})}{\partial\lambda_1^2} \right] \\ & + \frac{\mathcal{E}}{4} \left[ 2\lambda_2^{*2} + 4\lambda_1 \frac{\partial(\lambda_2^{*2})}{\partial\lambda_1} + \lambda_1^2 \frac{\partial^2(\lambda_2^{*2})}{\partial\lambda_1^2} \right]. \end{aligned} \quad (\text{E.23})$$

Thus

$$\frac{d}{d\theta} \left( \frac{\partial\Omega^*}{\partial\varrho_\theta} \right) = \left[ \mathcal{U}_1 \frac{\partial\Omega^*}{\partial\lambda_1} + C_1\mathcal{Z}\mathcal{W}_1^2 \right] \varrho_{\theta\theta} + \left[ \mathcal{U}_2 \frac{\partial\Omega^*}{\partial\lambda_1} + C_1\mathcal{Z}\mathcal{W}_2\mathcal{W}_1 \right] \eta_{\theta\theta} \quad (\text{E.24})$$

$$\frac{d}{d\theta} \left( \frac{\partial\Omega^*}{\partial\eta_\theta} \right) = \left[ \mathcal{V}_1 \frac{\partial\Omega^*}{\partial\lambda_1} + C_1\mathcal{Z}\mathcal{W}_1\mathcal{W}_2 \right] \varrho_{\theta\theta} + \left[ \mathcal{V}_2 \frac{\partial\Omega^*}{\partial\lambda_1} + C_1\mathcal{Z}\mathcal{W}_2^2 \right] \eta_{\theta\theta} \quad (\text{E.25})$$

One introduces a term  $\mathcal{Y}$  to cancel out the material property  $C_1$ :

$$\mathcal{Y} = \frac{\partial \Omega^*}{\partial \lambda_1} / C_1. \quad (\text{E.26})$$

The governing equations are now written as ODEs:

$$[1 + \gamma \cos \theta] \left[ [\mathcal{U}_1 \mathcal{Y} + \mathcal{Z} \mathcal{W}_1^2] \varrho_{\theta\theta} + [\mathcal{U}_2 \mathcal{Y} + \mathcal{Z} \mathcal{W}_2 \mathcal{W}_1] \eta_{\theta\theta} \right] - \sin \theta \varrho_{\theta} [\varrho_{\theta}^2 + \eta_{\theta}^2]^{-\frac{1}{2}} \mathcal{Y} + \frac{P \varrho \eta_{\theta}}{\gamma} = 0 \quad (\text{E.27})$$

$$[1 + \gamma \cos \theta] \left[ [\mathcal{V}_1 \mathcal{Y} + \mathcal{Z} \mathcal{W}_1 \mathcal{W}_2] \varrho_{\theta\theta} + [\mathcal{V}_2 \mathcal{Y} + \mathcal{Z} \mathcal{W}_2^2] \eta_{\theta\theta} \right] - \sin \theta \eta_{\theta} [\varrho_{\theta}^2 + \eta_{\theta}^2]^{-\frac{1}{2}} \mathcal{Y} - \frac{P \varrho \varrho_{\theta}}{\gamma} = 0. \quad (\text{E.28})$$

The coefficients in ODEs system (34) are modified as

$$\begin{aligned} A_1^* &= [1 + \gamma \cos \theta] [\mathcal{U}_1 \mathcal{Y} + \mathcal{Z} \mathcal{W}_1^2], \\ A_2^* &= [1 + \gamma \cos \theta] [\mathcal{U}_2 \mathcal{Y} + \mathcal{Z} \mathcal{W}_1 \mathcal{W}_2], \\ A_3^* &= -\sin \theta \varrho_{\theta} [\varrho_{\theta}^2 + \eta_{\theta}^2]^{-\frac{1}{2}} \mathcal{Y} + \frac{P \varrho \eta_{\theta}}{\gamma}, \end{aligned} \quad (\text{E.29})$$

and

$$\begin{aligned} B_1^* &= [1 + \gamma \cos \theta] [\mathcal{V}_1 \mathcal{Y} + \mathcal{Z} \mathcal{W}_1 \mathcal{W}_2], \\ B_2^* &= [1 + \gamma \cos \theta] [\mathcal{V}_2 \mathcal{Y} + \mathcal{Z} \mathcal{W}_2^2], \\ B_3^* &= -\sin \theta \eta_{\theta} [\varrho_{\theta}^2 + \eta_{\theta}^2]^{-\frac{1}{2}} \mathcal{Y} - \frac{P \varrho \varrho_{\theta}}{\gamma}. \end{aligned} \quad (\text{E.30})$$